The Effects of Obesity, Weight Loss, and Weight Cycling on the Immunometabolic Properties of Mouse Adipose Tissue

By

Emily Kathleen Anderson

Dissertation

Submitted to the Faculty of the

Graduate School of Vanderbilt University

in partial fulfillment of the requirements

for the degree of

DOCTOR of PHILOSOPHY

In

Molecular Physiology and Biophysics

May, 2013

Nashville, Tennessee

Approved:

Owen McGuinness, PhD

Roger Cone, PhD

John Stafford, MD, PhD

Amy Major, PhD

Peggy Kendall, MD

MOLECULAR PHYSIOLOGY AND BIOPHYSICS

The Effects of Obesity, Weight Loss, and Weight Cycling on the Immunometabolic Properties of Mouse Adipose Tissue

Emily Kathleen Anderson

Dissertation under the direction of Professor Alyssa Herweyer Hasty

Obesity is a prevalent disorder that increases the risk of developing many metabolic diseases, including insulin resistance (IR) and type 2 diabetes. Research conducted in the past decade has shown that accumulation of immune cells in obese adipose tissue (AT) contributes to inflammation and IR both locally and systemically. As a result of these novel findings, the immune system has come to the forefront of obesity research. However, many questions remain in this emerging field of immunometabolism. The studies in this dissertation have contributed to the understanding of: 1) the factors within the local milieu of obese AT that influence the phenotype and activation status of AT macrophages (ATMs), 2) the mechanisms regulating macrophage accumulation in AT during obesity and weight loss, and 3) the role of adaptive immune cells in the AT during weight cycling. First, I have shown *in vitro* that free fatty acid accumulation in macrophages activates inflammatory signaling, leading to endoplasmic reticulum (ER) stress-mediated apoptosis. However, pharmacological activation of lipolysis in obese AT does not result in ATM lipotoxicity. Second, I have demonstrated

that ATM apoptosis occurs in lean AT, is decreased during obesity, and is “re-activated” after weight loss. These findings suggest that ATM apoptosis is a novel mechanism by which ATM number is maintained. Interestingly, ATM ER stress signaling was regulated in a similar manner, but did not play a role in the activation of macrophage apoptosis. Third, I have shown that weight cycling increases the accumulation of pro-inflammatory T cell subsets in AT, suggesting that a nutritionally regulated local secondary adaptive immune response may occur. Overall, the studies in this dissertation have made important contributions to the field of immunometabolism by increasing our understanding of the dynamic regulation of AT immune cell composition and activation status in various nutritional states including obesity, weight loss, and weight cycling.

Approved: Professor Alyssa H. Hasty:_____.

For my Mom and Dad,

who have always emphasized the importance of

education, creative thinking, and pursuing my passions.

I would not be where I am today without your love and encouragement.

ACKNOWLEDGEMENTS

First, I would like to thank my mentor, Alyssa Hasty. I truly cannot imagine a better person or mentor to have experienced the past four years with. Alyssa has encouraged me to develop and test my own hypotheses and has allowed me to grow as an independent scientist. Her excellent mentorship has inspired me to pursue my goal of becoming a PI. Personally, Alyssa has become a great friend and I know that we will remain close for years to come.

Second, I would like to thank the members of my dissertation committee: Drs. Owen McGuinness, Roger Cone, John Stafford, Amy Major, and Peggy Kendall. I am continually amazed by Owen's ability to interpret data in novel ways and challenge me to think outside of the box. His suggestions and questions have greatly influenced my dissertation research and my way of thinking. Roger's unique perspective on metabolic regulation and weight loss, as well as John's knowledge of whole-body glucose and lipid metabolism have been essential for the completion of these projects. Without the immunology expertise of Amy and Peggy, many of these experiments would not have been possible.

I would also like to thank the members of the Hasty lab, both past and present, for their invaluable scientific expertise and continual willingness to help. The collaborative environment of our lab has helped me personally and professionally in so many ways. I know that I have made friends that I will value for a lifetime.

Additionally, I would like to thank the Molecular Physiology and Biophysics administrative staff, especially Angie Pernell, Nancy Cobb, and Beth Cyr, for their patience and assistance throughout my time in the department.

Lastly, I would like to thank my fiancé, AJ Baucum. Words cannot express how much I value your constant love and support. Throughout the ups and downs of graduate school, you have always known exactly what to say to encourage me and keep me optimistic. Wherever life takes us next, I cannot wait to experience it with you.

Support for this dissertation research was provided by an NIH grant (HL089466), the Cellular, Biochemical, and Molecular Sciences Training Program at Vanderbilt (NIH T32GM008554), and an American Heart Association Pre-doctoral Fellowship (12PRE11910047).

TABLE OF CONTENTS

Page

LIST OF FIGURES

Figure Page

LIST OF TABLES

Table **Page**

List of Abbreviations

ACSL: long-chain acyl-CoA synthetase

AT: adipose tissue

ATF-6: activating transcription factor 6

ATM: adipose tissue macrophage

BiP: immunoglobulin heavy chain-binding protein

CCR2: C-C chemokine receptor type 2

CHOP: CCAAT/enhancer binding protein (CEBP)-homologous protein

CLS: crown-like structure

CVD: cardiovascular disease

ER: endoplasmic reticulum

FFA: free fatty acid

GTT: glucose tolerance test

HF: high fat

IFN-γ: interferon-gamma

IKK-β: inhibitor of κB kinase

IL: interleukin

iNKT: invariant natural killer T cells

InsR: insulin receptor

IRE-1α: inositol-requiring enzyme 1α

IR: insulin resistance

IRS: insulin receptor substrate

JNK: jun N-terminal kinase

KO: knockout

LF: low fat

LPS: lipopolysaccharide

MCP: monocyte-chemoattractant protein

MGL1: macrophage galactose-type C-type lectin 1

MPM: mouse peritoneal macrophage

PBA: 4-phenyl butyric acid

PERK: double-stranded RNA-dependent protein kinase-like ER kinase

PI3K: phosphatidylinositol 3-kinase

PIP_3: phosphatidylinositol (3,4,5)-trisphosphate

PKB: protein kinase B

SS: sodium salicylate

SVF: stromal vascular fraction

T2D: type 2 diabetes

TC: triacsin C

TCR: T cell receptor

T_H: T helper cell

TLR: toll-like receptor

TNF-α: tumor necrosis factor-α

T_{reg}: regulatory T cell

TUNEL: Terminal deoxynucleotidyl transferase dUTP nick end labeling

TZD: thiazolidinediones

UPR: unfolded protein response

WT: wild-type

CHAPTER I

INTRODUCTION

Portions of this Introduction have been published in a review article in *Current Opinion in Lipidology* written by Anderson, Gutierrez, and Hasty (1).

Obesity epidemic

Obesity, defined as a body mass index of greater than 30 kg/m^2, has become a worldwide epidemic that affects individuals of all socioeconomic status (2). Currently, it is estimated that two-thirds of adults in the United States are either overweight or obese (2). In addition, childhood obesity rates have tripled in the past 30 years to nearly 17% of school-aged American children (3). If current trends hold, close to 90% of American adults will be overweight by the year 2030 (4). These statistics are especially alarming as obese individuals are predisposed to various metabolic disorders.

Obesity significantly increases the risk of developing many diseases including type 2 diabetes (T2D), atherosclerosis, cardiovascular disease (CVD), stroke, osteoarthritis, and multiple forms of cancer (4). In fact, obesity decreases the average lifespan by greater than 10 years (5). In addition to having a tremendous impact upon the health of individuals, obesity and associated pathologies have significant economic consequences for the nation. A 2008 study by the Center for Disease Control and Prevention estimated that the

annual health care cost associated with treating obesity-related health complications, primarily T2D and CVD, was a staggering $147 billion (6).

Insulin signaling, insulin resistance, and T2D

Obesity increases the risk for the development of T2D and a pre-diabetic condition known as insulin resistance (IR) (7). It is estimated that nearly 30% of American adults are pre-diabetic, with a subset of these patients progressing to overt diabetes (8). Recent findings have contributed substantially to the understanding of mechanisms leading to IR and T2D.

Insulin signaling: In healthy non-diabetic individuals, ingestion of glucose and free fatty acids (FFAs) stimulates insulin release from the β-cells of the pancreas. As shown in Figure 1.1A, insulin binding to the insulin receptor (InsR) initiates a signaling cascade to promote glucose uptake in the liver and muscle, storage of lipids in the adipose tissue (AT), and suppression of appetite in the hypothalamus. Specifically, insulin stimulates the intrinsic tyrosine kinase activity of the InsR, resulting in autophosphorylation of the receptor as well as tyrosine phosphorylation of several insulin receptor substrate (IRS) proteins. Phosphorylation of IRS-1/2 allows for the recruitment of another kinase, phosphatidylinositol 3-kinase (PI3K), to the plasma membrane. PI3K catalyzes the formation of phosphatidylinositol (3,4,5)-trisphosphate (PIP_3), a potent lipid second messenger. PIP_3, in conjunction with 3-phosphoinositide-dependent protein kinase-1 (PDK-1), phosphorylates and activates AKT/protein kinase B

(PKB), a serine-theronine kinase responsible for many of the effects of insulin. Signaling downstream of AKT increases glycogen synthesis in the liver and muscle, augments glucose uptake in the muscle via translocation of the glucose transporter, GLUT-4, and increases storage of FFA as triglyceride in the AT (9).

IR and T2D: Inflammatory signaling in metabolic tissues during obesity (discussed in detail below) directly interferes with insulin signaling pathways, leading to IR (10; 11). Tumor necrosis factor-α (TNF-α) and other pro-inflammatory cytokines activate serine kinases including c-jun N-terminal kinase (JNK), inhibitor of κB kinase (IKK-β), and atypical protein kinase C isoforms. As shown in Figure 1.1B, these serine kinases phosphorylate and inhibit multiple proteins involved in the insulin signaling cascade, including the InsR and IRS-1/2 (12-14). As a result of this insulin resistant state, peripheral glucose uptake is decreased and inhibition of hepatic glucose output is impaired, leading to hyperglycemia. Additionally, IR in AT causes dysregulated lipolysis leading to ectopic storage of lipids in tissues including the muscle, liver, and pancreas. During IR, pancreatic β-cells increase in mass and secrete elevated levels of insulin in an attempt to compensate for the inhibition of insulin signaling pathways. However, chronic nutrient overload can lead to β-cell death due to lipotoxicity, oxidative stress, or endoplasmic reticulum (ER) stress (15). The failure of β-cells to properly compensate for the insulin resistant state results in progression to overt T2D (15). See Figure 1.1 for a diagram of insulin signaling and IR.

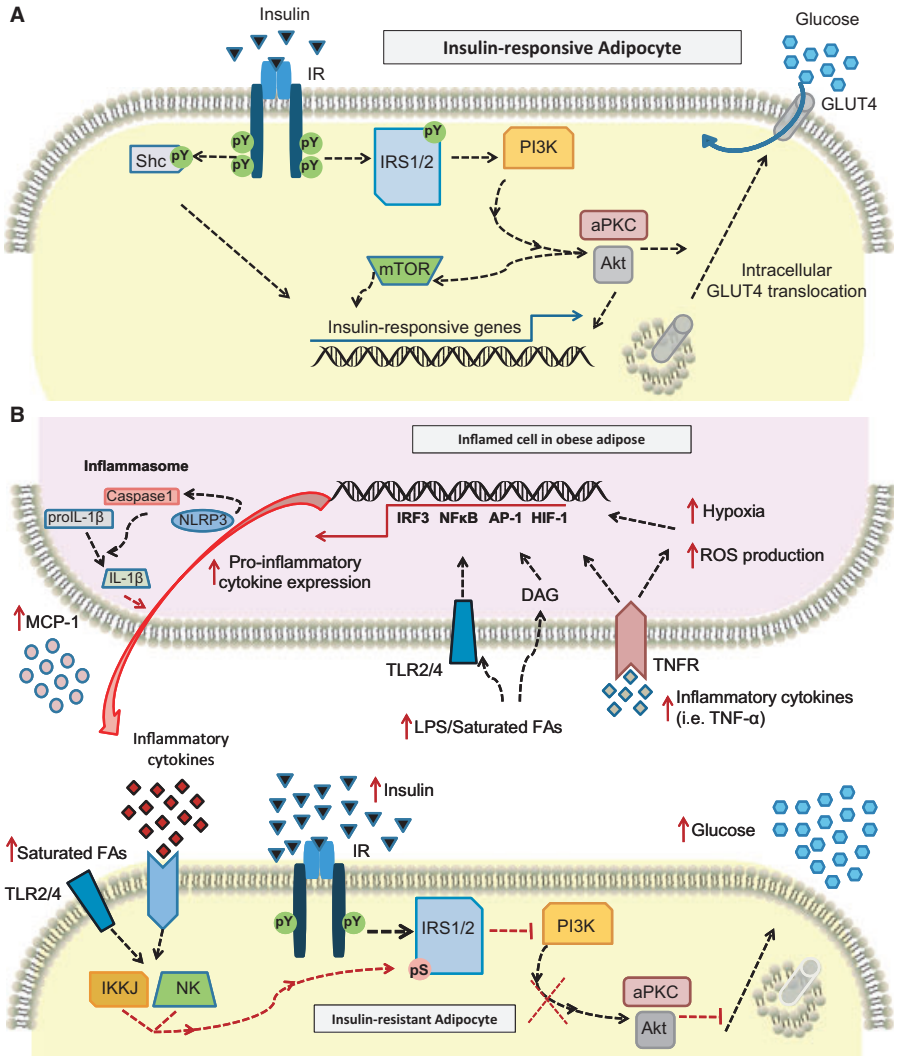

Figure 1.1: Pathways of insulin signaling and IR. From Johnson, *et al.* Immunological Reviews. 249 (2012) 218-238 (9). A) Insulin binding to the InsR initiates a tyrosine kinase cascade, resulting in glucose uptake in liver and muscle, and lipid storage in AT. B) During obesity, inflammatory cytokine signaling directly inhibits the InsR and IRS-1/2 via serine phosphorylation, leading to a state of IR.

AT as an active endocrine organ

It has long been recognized that AT plays a key role in the regulation of systemic energy balance (16). During caloric excess, lipids are stored as triglyceride in AT. In periods of food shortage, FFAs are lipolyzed from AT and oxidized to provide energy for peripheral tissues including liver and muscle (16). Over the past several decades it has become increasingly clear that AT is not simply an inert energy storage depot, but is also an active endocrine organ. AT secretes more than 50 hormones and cytokines, collectively known as adipokines (17). These adipokines act in an autocrine, paracrine, or endocrine fashion to modulate AT insulin sensitivity and whole-body glucose and FFA utilization (17). The first adipokine discovered was leptin, an adipocyte-derived hormone that circulates in proportion to fat mass (18; 19). Leptin primarily acts in the hypothalamus to decrease food intake (20-22). Another well-studied adipokine is the insulin-sensitizing hormone, adiponectin. In contrast to leptin, circulating adiponectin levels are inversely correlated with body weight (23). Adiponectin acts in the liver to decrease hepatic glucose production (24) and in the muscle and AT to increase glucose uptake and promote FFA oxidation (25-27).

In addition to producing hormones involved in the regulation of glucose and energy homeostasis, recent findings have demonstrated that obese AT also secretes pro-inflammatory cytokines, including TNF-α. Hotamisligil and colleagues have shown that protein and mRNA levels of TNF-α are dramatically increased in the AT of obese mice (28) and humans (29). Additionally, antibody-

mediated depletion of TNF-α greatly improved insulin sensitivity in a mouse model of obesity (30). These groundbreaking studies were the first to demonstrate a link between obesity, inflammation, and IR. Subsequent findings have shown that obese AT secretes many additional pro-inflammatory molecules, including interleukin-6 (IL-6), IL-1β, monocyte chemoattractant protein-1 (MCP-1), plasminogen activator inhibitor-1, and complement factors (31). As described above, these AT-derived inflammatory cytokines directly inhibit insulin signaling in the liver, muscle, and AT leading to IR, hyperglycemia, and hyperlipidemia (10; 11). Thus, it is now well established that obesity results in chronic low-grade inflammation, also known as “metainflammation” (32), that is a primary driver of obesity-associated IR in both mice and humans.

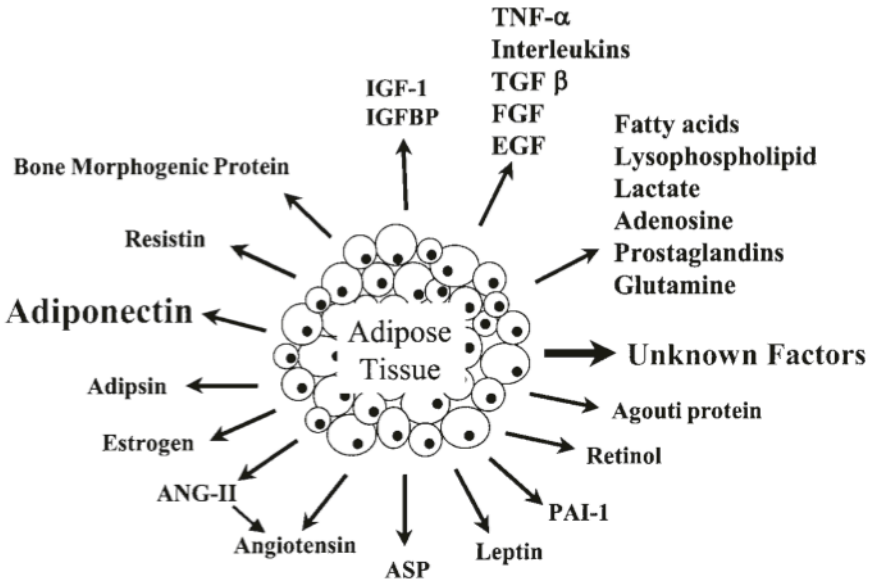

Figure 1.2: AT as an active endocrine organ. From Ravussin, The Pharmacogenomics Journal (2002), 4-7 (33). It is becoming increasing clear that AT is an active endocrine organ that secretes over 50 different peptides, hormones, and cytokines, including the ones listed above.

Macrophage accumulation in obese AT

In 2003, two independent studies demonstrated that macrophages, cells of the innate immune system, accumulate in AT during obesity (34; 35). AT macrophage (ATM) content is positively correlated with increasing adiposity and IR in multiple mouse models of diet- and genetic-induced obesity (34; 35). Additionally, macrophages accumulate in the AT of obese humans (34). The above findings suggest that these immune cells play an essential role in the pathogenesis of obesity. Indeed, macrophages are the major source of pro-inflammatory cytokines secreted from AT during obesity (34-36). Interestingly, macrophages have also been found to accumulate in the liver and muscle during obesity (36). As a result of these novel discoveries, the immune system has come to the forefront of obesity research. Ongoing research in this new field of "immunometabolism" has focused on determining the phenotype of macrophages in obese AT, defining mechanisms by which macrophages accumulate in AT, and understanding whether other immune cell subsets play a role in AT inflammation and IR. These topics will be reviewed below.

Macrophage phenotype in AT

Macrophages and their monocyte precursors are highly heterogeneous cell populations. Subtypes of macrophages were originally defined *in vitro* as "classically activated" (M1) or "alternatively activated" (M2) (37). Treatment of macrophages with lipopolysaccharide (LPS) and interferon-gamma (IFN-γ) resulted in an M1 pro-inflammatory phenotype, whereas treatment with IL-4 or IL-

13 induced an M2 anti-inflammatory phenotype (37). M1 macrophages participate in the resolution of bacterial infections, while M2 macrophages are thought to be involved in tissue homeostasis and repair.

In 2007, Lumeng, *et al.* extended this M1/M2 paradigm to macrophages residing in AT (38). In lean AT, the majority of ATMs are macrophage galactose-type C-type lectin 1 (MGL1)-expressing M2 macrophages (38). However, during obesity there is an increase in a unique population of CD11c-expressing pro-inflammatory M1 macrophages (38; 39). The increase in M1 ATM number may be due to recruitment of these immune cells specifically to “crown-like structures” (CLS) surrounding what are assumed to be dead or dying adipocytes (40). Additionally, there is evidence that a “phenotypic switch” from an M2 to an M1 polarization state may occur in ATMs during obesity (41). Below, I will review the known roles of M1 and M2 macrophages in the AT.

M1 “classically activated” ATMs: $CD11c^+$ M1 macrophages in obese AT express high levels of inflammatory cytokines when compared to $CD11c^-$ M2 macrophages (39). These findings suggest that M1 macrophages contribute to AT inflammation and IR. In support of this hypothesis, ablation of CD11c-expressing cells during high fat (HF) diet feeding decreased CLS formation and AT inflammation, leading to improved systemic glucose tolerance and increased insulin sensitivity (42). Although it is recognized that M1 macrophages contribute to obesity-associated AT dysfunction, the factors determining the phenotype and activation status of these cells are not completely understood. However, it is

believed that toll-like receptors (TLRs), FFAs, and inflammatory kinases play a role in M1 macrophage polarization.

TLRs and FFAs: TLRs are pattern recognition receptors expressed on many cell types, including macrophages (43). Binding of pathogen-associated molecules, such as LPS, to TLRs initiates an inflammatory signaling cascade, leading to the activation of JNK and NF-kB (44). Recent evidence suggests that TLR2 and 4 may also be activated by nutritional cues, including saturated FFAs (39; 45-47); however, others dispute this claim (48). Nonetheless, these pattern recognition receptors have been hypothesized to contribute to M1 polarization of macrophages during obesity.

In support of this concept, inhibition or deletion of TLR2 decreased obesity-associated AT inflammation and systemic IR (45; 49). Additionally, several groups have reported that mutation or deletion of TLR4 moderately reduced AT inflammation (47; 50-52). Olefsky and colleagues demonstrated that hematopoietic deletion of TLR4 decreased macrophage number and inflammatory cytokine expression in obese AT (53). Recent findings from our laboratory show that ATM number is not modulated by immune cell-specific deletion of TLR4 (54). However, in this study, TLR4 deficiency promoted M2 polarization of macrophages, leading to decreased AT inflammation (54). Taken together, the above data indicate that activation of TLR2/4 may contribute to increased M1 polarization of ATMs during obesity. In Chapter III of this dissertation, we will describe our findings that saturated FFAs activate

macrophages in a TLR2/4-independent manner *in vitro*, and that a transient increase in FFA flux *in vivo* does not result in ATM inflammation or lipotoxicity.

Inflammatory kinases: Increased cytokine expression and elevated FFA flux during obesity activates pro-inflammatory kinases, including JNK and IKK-β, in the AT (36). As previously mentioned, both of these kinases directly interfere with insulin signaling, leading to IR. Additionally, JNK and IKK-β activate transcription factors (AP-1 and NF-κB, respectively) capable of stimulating the expression of many inflammatory cytokines (36). Therefore, it is probable that activation of inflammatory kinases increases M1 polarization in ATMs. In fact, hematopoietic- or macrophage-specific deletion of JNK was shown to decrease ATM number and M1 polarization, resulting in increased systemic insulin sensitivity (55; 56). Additionally, macrophage-specific deletion of IKK-β improved obesity-associated glucose intolerance (57); however, macrophage phenotype was not determined in this study.

M2 "alternatively activated" ATMs: While many studies have attempted to determine the detrimental role of M1 ATMs during obesity (38; 40; 42), very little is known about the control of M2 polarization or the role of resident M2 macrophages in lean AT. The determinants of M2 macrophage polarization are just beginning to be investigated and include peroxisome proliferator-activated receptor (58; 59) and adiponectin (60). Although the exact role of M2 ATMs is not known, it is believed that M2 macrophages participate in AT repair and

remodeling (61). In addition, recent findings have established a role for M2 macrophages in the post-natal development of mouse epididymal AT (62). In this study, macrophages were present in "primitive" AT depots before the appearance of adipocytes, and depletion of macrophages decreased angiogenesis and impaired the development of mature AT (62). Additionally, ongoing studies in our laboratory suggest that M2 macrophages may be involved in the maintenance of AT iron homeostasis (Orr, *et al*., unpublished). However, the role of M2 ATMs remains incompletely understood. In Chapters IV and V of this dissertation, we present our data demonstrating that ER stress and apoptosis are increased preferential in interstitially spaced M2 macrophages in lean AT. Understanding the signaling pathways that are activated in M2 macrophages will give insight into the function of these immune cells.

Mechanisms of macrophage accumulation in AT during obesity

Accumulation of macrophages in AT is now recognized as a key event in the pathogenesis of obesity (36). However, mechanisms by which macrophage accumulation is initiated and propagated are incompletely understood. Current hypotheses (reviewed below) include adipocyte cell death, increased FFA flux, and chemokine-mediated recruitment of macrophage precursors to AT (63).

Adipocyte cell death: In order to store excess nutrients during obesity, AT expands by both adipocyte hypertrophy and hyperplasia (64). The inability of the AT vasculature to accommodate this rapidly expanding tissue, as well as the

increased size of individual adipocytes, is thought to result in local hypoxia in AT (65). Hypoxia, along with oxidative and ER stress, may promote adipocyte cell death either through necrosis (66) or apoptosis (67). Indeed, multiple studies have demonstrated that adipocyte death is dramatically increased during the progression of obesity (66; 67). Interestingly, 90% of macrophages that accumulate in AT during obesity are localized to CLS surrounding dead or dying adipocytes (68). Additionally, transgenic activation of massive adipocyte apoptosis led to macrophage accumulation in AT (69), suggesting that adipocyte death is involved in the initiation of macrophage accumulation in AT. However, a recent study has shown that inhibition of adipocyte apoptosis during HF diet feeding does not decrease ATM accumulation (70). Therefore, these findings call into question whether adipocyte cell death is the initiating factor for macrophage recruitment to obese AT.

FFAs: During obesity, dysregulated lipolysis in insulin resistant adipocytes increases serum FFA concentrations (71). Epidemiological studies have established that elevated serum FFA levels increase the risk of developing both T2D and CVD (72; 73); however, mechanisms explaining this correlation are incompletely understood. A recent study by Kosteli and colleagues (74) has shown that activation of AT lipolysis due to fasting or pharmacological manipulation leads to a transient increase in the number of lipid-laden macrophages in the AT. Our laboratory and others have also demonstrated that obesity increases the lipid content of ATMs (75; 76). Although the hypothesis

remains to be tested, these findings indicate that elevated basal lipolysis during obesity may contribute to macrophage accumulation in AT. In turn, lipid accumulation in ATMs may modulate the activation status of these immune cells, promoting further adipocyte IR. In Chapter III of this dissertation, we will demonstrate that FFA accumulation in macrophages activates inflammatory signaling and ER stress-mediated apoptosis. However, pharmacological activation of AT lipolysis *in vivo* does not appear to result in ATM lipotoxicity.

Chemokines: Chemokines are small proteins involved in the chemotaxis of immune cells to sites of inflammation (77). Multiple chemokines and chemokine receptors are highly expressed in mouse and human AT during obesity (78-81). In addition, labeling studies have shown that bone marrow-derived monocytes are recruited to the AT during obesity (40). Therefore, many in the field have sought to determine whether reducing the chemoattractant potential of AT can inhibit ATM accumulation during obesity. However, these studies have yielded controversial results, suggesting that recruitment-independent mechanisms may also regulate ATM number.

MCP-1 and CCR2: To date, the potent chemokine, MCP-1, and its receptor, C-C chemokine receptor type 2 (CCR2), are the most well studied chemokine/chemokine receptor pair in regards to the regulation of ATM number. Additionally, CCR2 is the functional receptor for many other chemokines including MCP-2, 3, 4, and 5 (82). Multiple groups have demonstrated that

transgenic over-expression of MCP-1 from AT increased ATM number and worsened glucose tolerance and insulin sensitivity (80; 83). Conversely, deficiency of MCP-1 reduced ATM accumulation and protected from IR (40; 80; 81). These studies suggest that MCP-1 contributes to metabolic dysfunction during obesity. However, two conflicting reports by Kirk *et al*. and Inoeye *et al*., showed that MCP-1 deficiency does not decrease macrophage number in AT or improve insulin sensitivity (84; 85). In fact, in these studies, absence of MCP-1 actually slightly *increased* ATM number and systemic IR. Therefore, while it has been demonstrated that over-expression of MCP-1 increases ATM number, it is not clear whether MCP-1 deficiency modulates AT immune cell content.

With regards to CCR2, deficiency or pharmacological inhibition of this chemokine receptor during HF diet feeding resulted in a small decrease (~20-30%) in ATM number and glucose intolerance in all reported studies (81; 86-88). However, in these studies, ATM number was never normalized to levels observed in lean AT. Interestingly, our laboratory has recently shown that the protective effects of CCR2 deficiency are only observed after long periods of HF diet feeding (>20 weeks) (88).

Taken together, what is consistently demonstrated is that over-expression of MCP-1 increases macrophage accumulation in AT, and that CCR2 deficiency decreases macrophage number. However, it is not clear whether MCP-1 deficiency modulates AT immune cell content. The reasons for these inconsistencies are not clear, but may include differences in the length of the diet regimen (88) and the genetic background of the mouse model utilized (89).

Additional chemokines: In addition to MCP-1/CCR2, multiple other chemokines and chemokines receptors have been studied. CXCL14 (90), CXCR2 (91; 92), and CCR5 (93) were noted to play a role in macrophage accumulation in AT. In contrast, CXCR1 (94) and MIP-1α (95) did not modulate ATM number during obesity. See Table 1.1 for a comprehensive overview of the role of chemokines and chemokine receptors in ATM number and metabolic phenotype.

Molecule	Model	Change in ATM	Insulin Sensitivity	Reference
CHEMOKINES				
MCP-1	Knockout	↓	Improved	(80)
MCP-1	Knockout	↑	No change or worsened	(84; 85)
MCP-1	AT overexpression	↑	Worsened	(80; 83)
CXCL14	Knockout	↓	Improved (females only)	(90)
MIP-1α	Knockout	↔	Not determined	(95)
CHEMOKINE RECEPTORS				
CCR2	Knockout	↓	Improved	(40; 81; 87)
CCR2	Pharmacologic antagonist	↓	Improved	(81; 86; 87)
CCR5	Knockout	↓	Improved	(93)
CXCR2	Bone marrow transplant of CXCR2-/- into wild type mice	↓	Improved	(91)
CX3CR1	Deficiency	↔	No change	(94)

Table 1.1: Role of chemokines and chemokine receptors in ATM accumulation during obesity.

Monocyte trafficking: Preferential trafficking of certain monocyte subpopulations to AT may also contribute to obesity-induced inflammation. In fact, obesity has been shown to increase the number of Ly6C^{hi} monocytes in the blood (96). Circulating Ly6C^{hi} monocytes are believed to be recruited to sites of inflammation and to differentiate into pro-inflammatory M1 macrophages (97), whereas Ly6C^{lo} monocytes are thought to differentiate into anti-inflammatory M2 macrophages (98). Deletion of CCR2 in obese mice resulted in an almost complete loss of circulating Ly6C^{hi} monocytes (88; 99), indicating that this chemokine receptor is essential for the proper mobilization of inflammatory monocyte population. Additionally, Lumeng and colleagues have identified MGL1 as a critical factor regulating the survival and migration of Ly6C^{hi} monocytes (100). Animals deficient in MGL1 do not mobilize Ly6C^{hi} monocytes from the bone marrow to the blood in response to HF diet feeding (100). Interestingly, despite the near absence of circulating pro-inflammatory monocyte populations, deletion of either CCR2 or MGL1 does not normalize ATM number to levels observed in lean AT (81; 100). These findings suggest that recruitment-independent mechanism may contribute to ATM accumulation in obese AT in these mouse models.

Potential recruitment-independent mechanisms contributing to ATM accumulation in obese AT: The contribution of different chemokines to the recruitment of ATMs is complex. Furthermore, even in studies showing that deficiency of chemokines, chemokine receptors, or monocyte precursors

decreases obesity-induced ATM accumulation, macrophage number is never completely normalized to levels seen in lean AT. These findings suggest that recruitment-independent mechanisms may also contribute to the regulation of ATM number during obesity. It is possible that increased ATM proliferation, decreased egress of macrophages out of the AT, or decreased apoptosis of ATM may also play a role in macrophage accumulation in obese AT (Figure 1.3). In Chapter IV, we will demonstrate that ATM apoptosis is modulated during obesity and weight loss. Alterations in ATM apoptosis may contribute to the accumulation of macrophages in the AT during obesity, as well as the decrease in ATM content after weight loss.

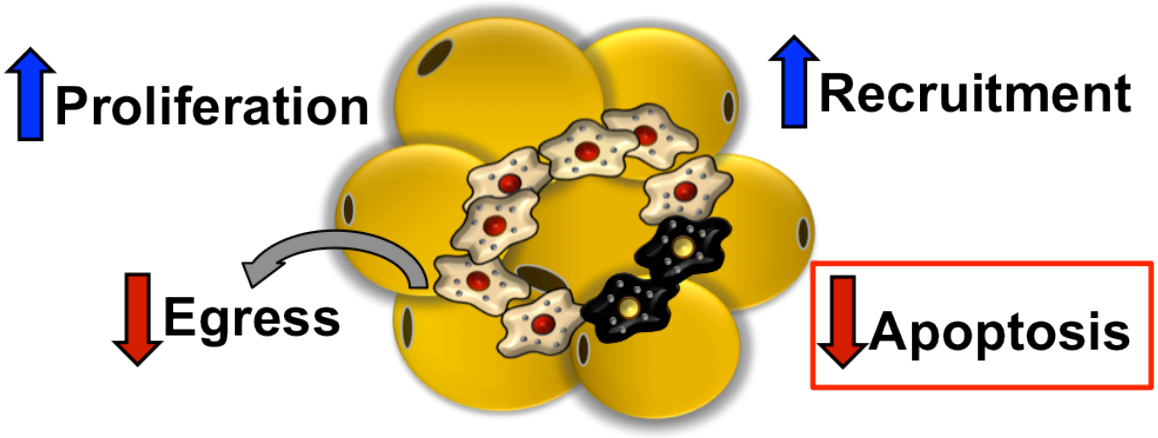

Figure 1.3: Potential mechanisms contributing to ATM accumulation in obese AT. Increased recruitment of monocytes may increase ATM number. However, additional recruitment-independent mechanisms could contribute to the accumulation of macrophages in obese AT. Potential mechanisms include increased proliferation, decreased egress, or decreased apoptosis of ATMs.

Accumulation of other innate immune cells in AT

Macrophages were the first immune cell to be described in AT. Although these cells are the most well studied and most abundant cell type in the AT (representing up to 40% of AT cells during obesity (34)), recent reports also describe the presence of other innate leukocyte populations in AT. The innate immune system is the first line of defense against infection. Pattern recognition receptors on innate immune cells recognize pathogen-associated molecular patterns and orchestrate the removal of invading microbes. Innate immunity is not characterized by the development of long-term memory towards specific pathogens (101). See Table 1.2 for characteristics of an innate immune response, and Figure 1.4 for a comprehensive review of AT immune cell composition.

Eosinophils: Eosinophils are granulocytic innate immune cells that are involved in allergic reactions as well as protection from helminth infection (102). In contrast to macrophages, AT eosinophil number is inversely correlated with body weight (103), suggesting that eosinophils promote an anti-inflammatory AT phenotype. Indeed, mouse models of eosinophil depletion and eosinophilia demonstrated that eosinophils induced M2 polarization of ATMs and improved glucose tolerance in an IL-4/13-dependent manner (103). These findings indicate that eosinophils promote M2 polarization in lean AT; however, loss of eosinophils during obesity leads to a progressive skewing of macrophages towards an M1 phenotype.

Mast cells: Mast cells are traditionally thought of as mediators of allergic responses. However, recent studies have shown mast cell involvement in metabolic diseases, including obesity and T2D. Liu, *et al*. demonstrated that mast cells accumulated in obese AT before the appearance of macrophages (104). An additional study has suggested a role for mast cells in obesity-associated AT fibrosis in humans (105). Depletion of mast cells in mice resulted in decreased weight gain and reduced ATM content during obesity, suggesting that mast cells may be involved in the regulation of energy expenditure and body weight. In addition, mast cell-derived IL-6 and IFN-γ increased protease expression in AT. These proteases promoted angiogenesis by degrading anti-angiogenic molecules (104). Thus, mast cell-induced angiogenesis may allow for further recruitment of leukocytes to the AT.

Neutrophils: Granulocytic neutrophils are often the first leukocytes to arrive at sites of inflammation (106). Consistent with these reports, HF diet feeding increased the accumulation of neutrophils in AT within 3 days (107; 108). A recent publication has shown that the neutrophil-derived serine protease, neutrophil elastase, contributes to diet-induced glucose intolerance, IR, and M1 macrophage accumulation in AT (108). Neutrophil elastase was shown to impair insulin signaling in the AT and liver through degradation of multiple proteins including IRS-1 (108).

Role of adaptive immune cells in AT inflammation during obesity

Recent exciting findings demonstrate that, in addition to cells of the innate immune system, adaptive immune cells are also modulated by obesity and play a key role in HF diet-induced AT inflammation and IR (109). In contrast to innate immunity, the adaptive immune response is characterized by an antigen-specific response directed against invading pathogens or infected cells. Additionally, an adaptive immune response results in the development of immunological memory against specific antigens. Therefore, subsequent exposure to the same pathogen activates a more rapid and potent secondary adaptive immune response (Table 1.2) (101).

	Innate Immunity	Adaptive Immunity
Response Time	Rapid	Delayed
Specificity	Recognition of pathogen-associated molecular patterns	Antigen specific
Diversity	Limited	Highly diverse due to genetic recombination of receptors
Self/Non-Self Discrimination	Perfect	Good, but occasional autoimmunity
Major Cell Types	Monocytes, macrophages, dendritic cells, neutrophils, eosinophils, mast cells, NK cells	B and T lymphocytes
Memory Response	None	Initial antigen exposure results in formation of memory cells capable of mounting a more potent and rapid secondary immune response

Table 1.2: Characteristics of the innate and adaptive immune systems. Adapted from Kindt, Goldsby, and Osborne. Kuby Immunology. 2007. p61 (101). Innate immunity is characterized by the rapid recognition and elimination of a limited number of pathogen-associated molecular patterns. In contrast, cells of the adaptive immune system recognize a large number of specific antigens. Additionally, adaptive immunity can result in the formation of memory cells and activation of a more rapid and potent secondary immune response.

T lymphocytes: Obesity results in a striking increase in $CD8^+$ cytotoxic T cells and $CD4^+$ T helper 1 (T_H1) cells, while both $CD4^+$ T_H2 and regulatory T (T_{reg}) cells are decreased in epididymal AT (110-112).

$CD8^+$ cytotoxic T cells: Nishimura, *et al.* demonstrated that $CD8^+$ T cells accumulate in AT after 6 weeks of HF diet feeding (113). Genetic or pharmacological depletion of $CD8^+$ cells reduced obesity-associated AT inflammation, IR, and systemic glucose tolerance, while adoptive transfer of these cells from obese mice increased metabolic dysfunction (113). In this study, $CD8^+$ T cell accumulation in AT preceded and was required for increased ATM number during HF diet feeding (113); however, another study did not reproduce this finding (114). Interestingly, co-culture experiments demonstrated that $CD8^+$ T cells isolated from obese AT induced peripheral blood monocyte differentiation into TNF-α^{high} inflammatory macrophages (113). These findings suggest a role for $CD8^+$ T cells in the accumulation of macrophages in AT and, therefore, increased systemic metabolic dysfunction during obesity.

$CD4^+$ T_H1 and T_H2 cells: $CD4^+$ T_H cells are a sub-set of lymphocytes involved in the orchestration of adaptive immune responses through the secretion of immunomodulatory cytokines (115). T_H cells are classically divided into two subsets: IFN-γ producing T_H1 cells and IL-4/13 producing T_H2 cells. T_H1 cells are pro-inflammatory and enhance macrophage secretion of inflammatory cytokines, while T_H2 cells induce an anti-inflammatory M2

macrophage phenotype (115). Winer, *et al.* have shown that obesity leads to a T_H1 bias among the fat-associated T_H cells in mice and humans: T_H2 cell populations are decreased while T_H1 cell number is increased (116). Elevation in the T_H1/T_H2 ratio leads to AT inflammation, accumulation of M1 macrophages, and IR (116).

Of interest, lymphocyte-deficient Rag knockout (KO) mice exhibit increased body weight and decreased insulin sensitivity when placed on a HF diet (116; 117), indicating a protective role for a subset of lymphocytes in obesity-associated pathologies. Adoptive transfer of $CD4^+$, but not $CD8^+$, T cells to Rag KO mice restored insulin sensitivity (116). Interestingly, the improved metabolic phenotype of these mice was dependent upon the presence of adoptively transferred T_H2 cells, suggesting that these cells may protect from HF diet-induced AT inflammation. However, further studies are necessary to confirm this hypothesis.

<u>$CD4^+$ T_{reg} cells:</u> T_{reg} cells are involved in the appropriate control of immune responses. Decreased T_{reg} cell number has been reported in the AT of obese mice (113; 116; 118). Feuerer, *et al*. demonstrated that ablation of T_{reg} cells, mimicking the reduction observed during obesity, leads to decreased insulin sensitivity in AT and liver, as well as increased inflammatory cytokine expression (118). In contrast, pharmacological activation of T_{reg} cells resulted in decreased fasting glucose levels and increased IL-10 secretion from AT. In addition, transcriptional profiling of T_{reg} cells revealed a unique phenotype: AT-

associated T_{reg} cells over-expressed many genes involved in leukocyte migration and extravasation when compared to other tissue-resident T_{reg} cell populations (118). This profile suggests a critical role for AT-associated T_{reg} cells in the control of AT inflammation.

iNKT cells: Invariant natural killer T (iNKT) cells are innate-like T lymphocytes that recognize lipid antigens (119). The role of these cells in the AT during obesity remains controversial. Multiple studies have demonstrated that AT-resident iNKT cells are depleted during the progression of obesity in mice and humans (119-121). In contrast, another study found increased markers of iNKT cells in obese AT (122). Additionally, controversy remains regarding whether AT iNKT cells protect from (123-125), exacerbate (122), or do not contribute to IR during obesity (126).

Potential antigen-specific T cell response in obese AT: Perhaps one of the most interesting and surprising aspects related to T cell involvement in obesity is the finding that T cells in obese AT express a restricted T cell receptor (TCR) repertoire (113; 116; 118) reminiscent of an immune response to a viral pathogen. TCR restriction in obese AT suggests that T cells may recognize self-antigen within this tissue. Indeed, recent publications indicate the antigen presented by adipocytes (127) or macrophages (128) in complex with major histocompatibility complex II molecules contributes to the proliferation of AT T cells during obesity. As mentioned above, adaptive immune responses are

characterized by the formation of long-lived antigen-specific memory lymphocytes (Table 1.2). Interestingly, memory T cells are found in the AT of obese mice and humans (129; 130), supporting the idea that obese AT antigens exist. In chapter VI of this dissertation, we describe our findings that weight cycling modulates the antigen-driven T cell response within AT.

B lymphocytes: B cells also accumulate in AT during HF diet feeding (117). A recent study has established a pathogenic role for B cells in the progression of obesity (131). When placed on a HF diet, mice lacking B cells were protected from obesity-associated glucose intolerance and IR. Furthermore, genetic or antibody-mediated depletion of B cells significantly decreased AT inflammation, but did not modulate the number of macrophages or T cells in the tissue (131). Studies utilizing lymphocyte-deficient Rag KO mice demonstrated that B cells must interact with other lymphocytes to promote metabolic defects. In fact, expression of both major histocompatibility complex I and II was required for the pathogenic effects of B cells (131), indicating that B cell-mediated antigen presentation to T cells is a critical event in the propagation of AT inflammation during obesity.

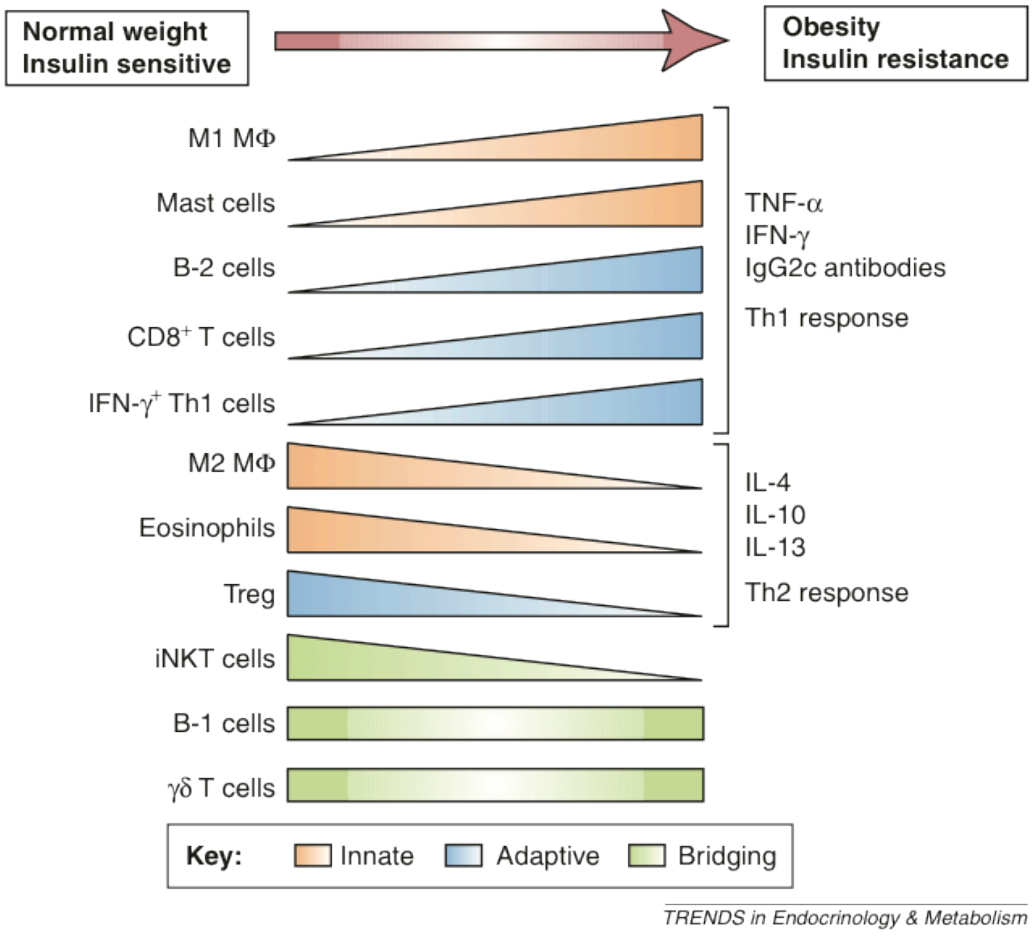

Figure 1.4: Modulation of AT immune cell populations during obesity. From Schipper, *et al*. Trends in Endocrinology and Metabolism. 2012: 23-12 (109). During the progression of obesity, pro-inflammatory immune cell subsets including M1 macrophages, mast cells, B cells, $CD8^+$ T cells, and IFN-γ secreting T_H1 cells accumulate in AT. Additionally, obesity decreased the number of AT-resident anti-inflammatory immune cell populations, including M2 macrophages, eosinophils, T_{regs}, and potentially iNKT cells.

Weight loss restores metabolic control and decreases ATM number

Research conducted in the past decade has defined the time-course of immune cell accumulation during weight gain and has established a causative role for macrophages, T cells, and B cells in IR (36). In contrast, very little is known about the events occurring in AT during weight loss. However, it is accepted that weight loss, when possible, is the ideal method to counteract the negative metabolic consequences of obesity. In fact, insulin resistant individuals who lose 5-7% of body weight decrease their risk of developing T2D by a shocking 58% (5).

The reduction of metabolic dysfunction after sustained weight loss is due in part to decreased systemic inflammation and reduced ATM number (41; 74; 132); however, mechanisms leading to decreased macrophage number are not known. A recent paper has shed light on the impact of weight loss on the AT (74). During weight loss, there was a transient increase in ATM content, followed by a gradual decrease in macrophage numbers (74). These findings suggest that weight loss stimulates an active response within the AT that ultimately reduces macrophage number. In Chapters IV and V, we demonstrate that weight loss increases apoptotic and ER stress signaling in ATMs, potentially contributing to decreased ATM content and inflammation.

Weight cycling may increase metabolic dysfunction

Although weight loss significantly decreases obesity-associated complications, losses are rarely maintained (133). Weight re-gain leads to weight

cycling, commonly known as “yo-yo dieting.” Interestingly, multiple epidemiological studies suggest that weight cycling may increase the risk of developing T2D or CVD, even compared to individuals who maintain an elevated weight (134-138). Although the potentially harmful consequences of weight cycling are recognized, the molecular mechanisms explaining this correlation remain unknown. In Chapter VI, we demonstrate that weight cycling increases pro-inflammatory AT T cell populations. Increased AT inflammation may contribute to the negative metabolic consequences associated with weight cycling.

Signaling pathways studied in this dissertation

ER stress (Figure 1.5) and apoptotic (Figure 1.6) signaling pathways will be investigated in this dissertation. In Chapter III, we describe our findings that intracellular accumulation of saturated FFAs induces ER stress-mediated apoptosis in primary mouse macrophages. Additionally, we show that a transient increase in FFA flux *in vivo* does not lead to ATM lipotoxicity. In Chapters IV and V, we will demonstrate the metabolic regulation of ATM ER stress and apoptosis during weight gain and weight loss. Below, I will provide a brief summary of these signaling pathways.

ER stress signaling pathways: Environmental or cellular stressors that disrupt proper protein folding result in ER stress and activation of the unfolded protein response (UPR, Figure 1.5). The UPR is controlled by three ER-localized

receptors: IRE-1α (inositol-requiring enzyme 1α), PERK (double-stranded RNA-dependent protein kinase-like ER kinase), and ATF-6 (activating transcription factor 6). During ER stress, chaperone proteins such as BiP (immunoglobulin heavy chain-binding protein) dissociate from all three receptors, resulting in proteolytic cleavage of ATF-6 and dimerization and auto-phosphorylation of IRE-1α and PERK (139).

The activated receptors initiate a signaling cascade that decreases the protein load entering the ER and increases the folding capacity of the organelle through up-regulation of a sub-set of genes, including BiP (139). The UPR is initially adaptive. However, if the cellular stressor is too great, apoptotic cell death is initiated to clear dysfunctional cells and allow for survival of the organism. The control of cell fate decision during the progression of ER stress is not well understood (140). However, it is known that all three transmembrane receptors are capable of activating pro-apoptotic proteins, including CEBP-homologous protein (CHOP) (141). In Chapter V of this dissertation, we define the metabolic regulation of ER stress activation in ATMs and determine whether ER stress-mediated apoptosis occurs in macrophages residing in lean AT.

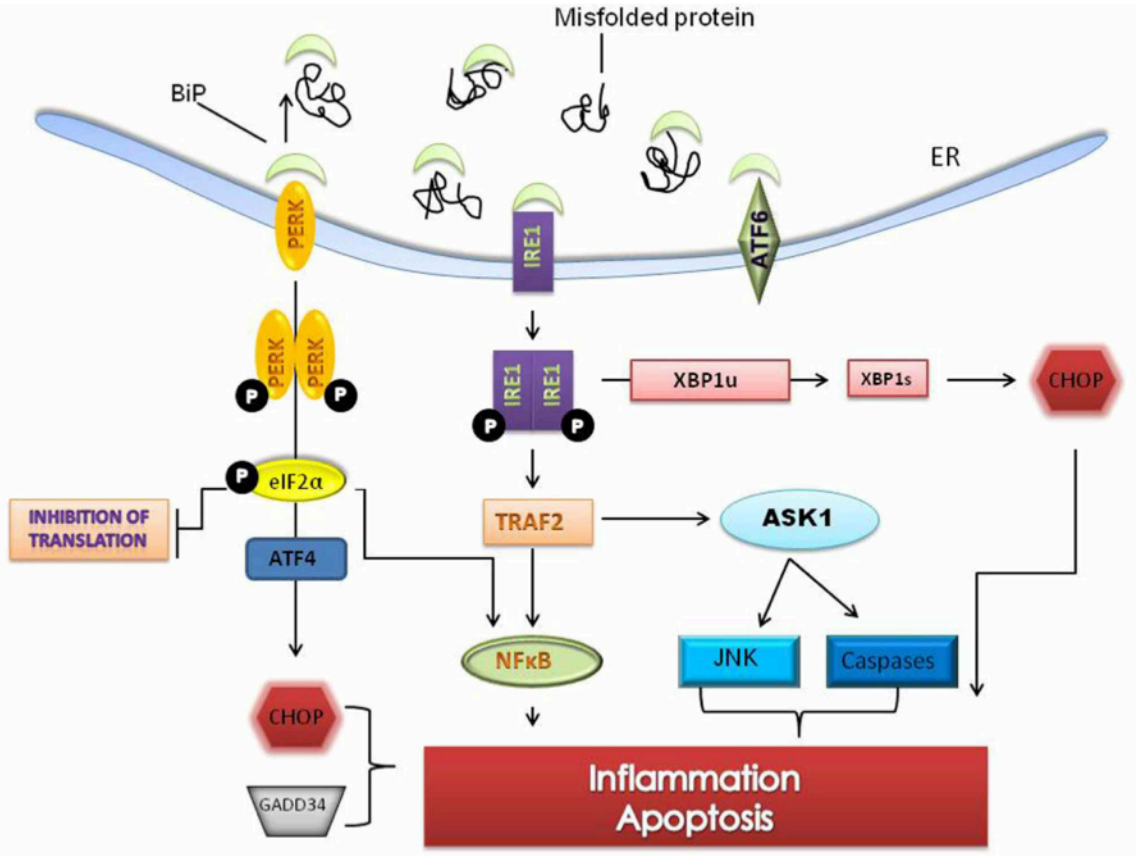

Figure 1.5: ER stress signaling. From Brown and Naidoo. Frontiers in Integrative Physiology. 2012 (142). Accumulation of unfolded proteins in the ER results in dissociation of chaperone proteins including BiP from three receptors in the ER membrane, PERK, IRE-1α, and ATF-6. Activation of these receptors results in inhibition of protein translation and the induction of a subset of genes involved in protein folding and degradation. The ER stress response is initially adaptive; however, long-term activation of this pathway can lead to apoptosis, primarily due to up-regulation of CHOP. Additionally, ER stress signaling can increase the activity of pro-inflammatory factors, such as NF-κB and JNK.

Apoptotic signaling pathways: Apoptosis was first defined over 40 years ago as a set of morphological parameters that differentiated this type of programmed cell death from necrotic death (143). Over the next several decades, it became clear that apoptosis is essential during every stage of development in order to maintain tissue homeostasis and to remove damaged or extraneous cells without evoking an inflammatory response (144). Dysregulation of apoptosis was found to result in multiple disease states, including cancer, neurodegeneration, and autoimmunity (144). However, it was not until the 1990s that biochemical signaling pathways responsible for the initiation and execution of apoptosis were defined (Figure 1.6) (144).

Apoptosis can occur in response to either intrinsic or extrinsic stimuli (145). Intrinsic apoptotic signaling, including DNA damage or ER stress, allows the BCL-2 family members, Bax and Bak, to oligomerize in the outer mitochondrial membrane. Mitochondrial permeabilization results in the release of apoptogenic proteins, including cytochrome c, into the cytosol. Cytochrome c then associates with the adaptor protein, apoptosis protease activating factor-1, and caspase-9. The resulting “apoptosome” cleaves and activates executioner caspases such as capsase-3 and 7. These cysteine proteases then cleave multiple protein substrates, leading to apoptotic cell death (145).

Extrinsic apoptotic stimuli, including TNF-α, bind to extracellular death receptors and initiate the formation of the death-inducing signaling complex. This complex consists of an adaptor protein, Fas-associated death domain, and caspase-8 and 10. Once activated, these initiator caspases can directly cleave

and activate caspase-3 and 7, resulting in apoptosis (145). Caspase-8 is also able to cleave t-Bid to engage the intrinsic apoptotic pathway (145). Regardless of the initiating stimulus, apoptotic death results in the non-inflammatory removal of unneeded, old, or dysfunctional cells, thus maintaining tissue homeostasis. In Chapter IV of this dissertation, we will explore the regulation of ATM apoptosis during obesity and weight loss and determine whether alterations in apoptotic cell death could regulate ATM number.

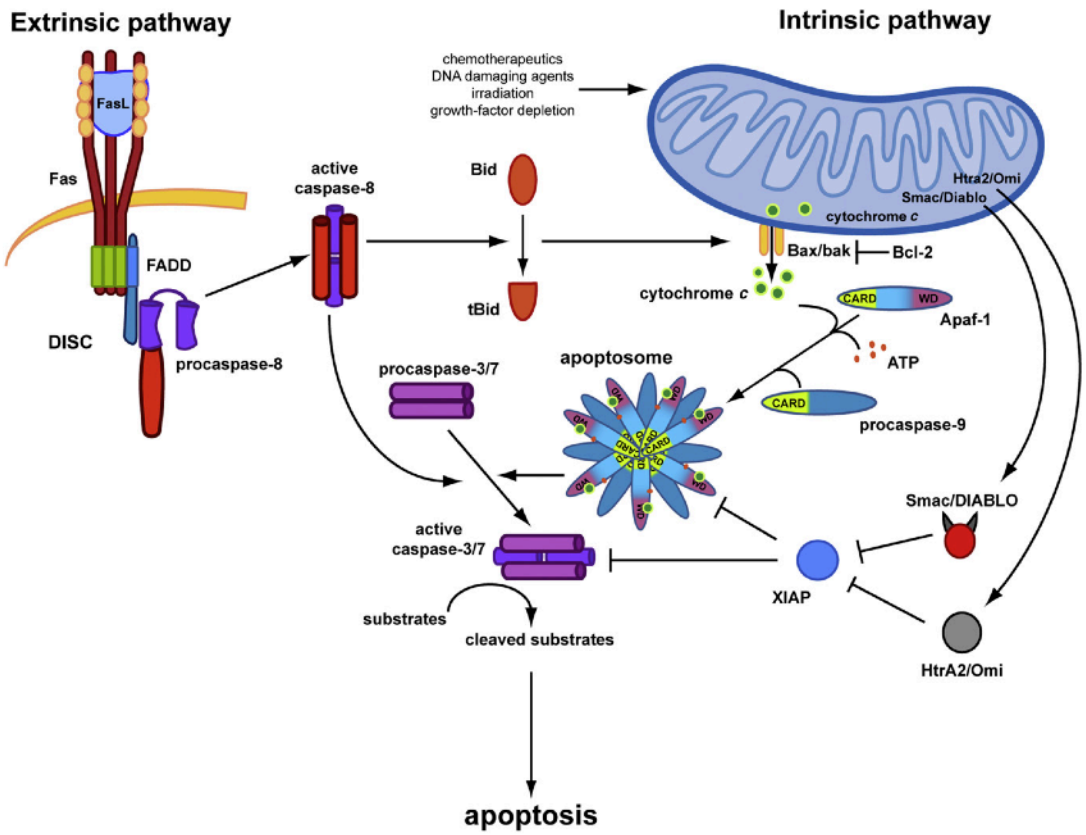

Figure 1.6: Apoptotic signaling. From Lamkanfi and Dixit. Cell Host and Microbe. 2012. 8. 44-54 (145). Extrinsic or intrinsic apoptotic stimuli result in the activation of initiator caspases that then cleave the executioner proteins, caspase-3 and 7. During extrinsic apoptosis, this activation occurs through the formation of the death-inducing signaling complex, while intrinsic apoptosis results in the activation of the apoptosome.

Significance

Currently, two-thirds of adults in the United States are overweight or obese (2). Obesity increases the risk of developing multiple diseases, including IR, T2D, and CVD (4). In the past decade, it has been established that accumulation of pro-inflammatory immune cells in AT contributes to the negative metabolic consequence associated with obesity (36). However, significant gaps remain regarding our understanding of the signaling pathways that are activated in macrophages residing in obese AT and the mechanisms regulating immune cell accumulation in AT during obesity, weight loss, and weight cycling. During obesity, dysregulated lipolysis in insulin resistant adipocytes increases local FFA concentrations. In Chapter III, we detail our *in vitro* and *in vivo* studies used to define signaling pathways that are activated in macrophages during FFA accumulation. In Chapters IV and V, recruitment-independent mechanisms regulating ATM content during obesity and weight loss are described. Lastly, Chapter VI will focus on our finding that weight cycling modulates AT immune cell composition and decreases systemic glucose tolerance. Overall, the studies performed in this dissertation have furthered the scientific community's understanding of mechanisms by which immune cell number and activation state are regulated under various metabolic conditions, including obesity, weight loss, and weight cycling (Figure 1.7). These findings could inform the development of novel therapeutics to modulate AT immune cell content and inflammation, thus limiting the negative metabolic effects associated with obesity.

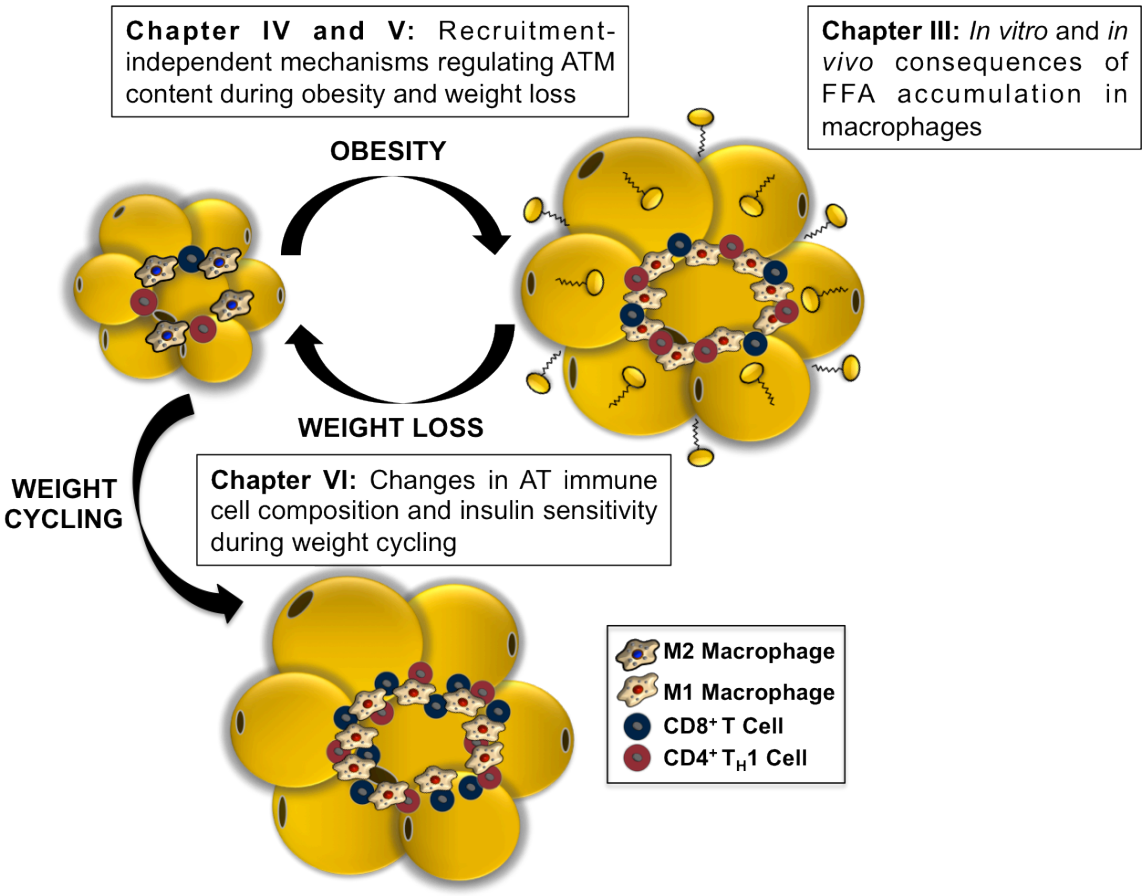

Figure 1.7: Model of questions addressed in this dissertation. Recent studies have established a role for pro-inflammatory ATMs and AT T cells in the pathogenesis of obesity. The studies in this dissertation will further the field's understanding of mechanisms regulating AT immune cell number and activation state.

CHAPTER II

MATERIALS AND METHODS

Animal care and usage

Ethics statement: All animal procedures were performed with approval from the Institutional Animal Care and Usage Committee of Vanderbilt University.

Diets: Unless otherwise indicated, mice were maintained on a standard rodent chow diet (LabDiet 5001) containing 12% of kcal from fat, 28% from protein, and 60% kcal from carbohydrates. When specified, mice were placed on a 10% kcal from fat (low fat diet, D12450B) or 60% kcal from fat diet (high fat diet, D12492) at 8-weeks of age. Both diet were purchased from Research Diets, Inc. (New Brunswick, NJ). The composition of the low fat (LF) and high fat (HF) diets is provided in Table 2.1. All mice were fed ad libitum and given free access to water.

Diet	LF (D12450B)	HF (D12492)
	g/kg	g/kg
Protein Sources	***20% kcal***	***20% kcal***
Casein	200	200
L-Cystine	3	3
Carbohydrate Sources	***20% kcal***	***20% kcal***
Corn Starch	315	0
Maltodextrin 10	35	125
Sucrose	350	68.8
Fat Sources	***10% kcal***	***60% kcal***
Soybean Oil	25	25
Lard	20	245
Other		
Cellulose	50	50
Mineral Mix	10	10
DiCalcium Phosphate	13	13
Calcium Carbonate	5.5	5.5
Potassium Citrate	16.5	16.5
Vitamin Mix	10	10
Choline Bitartrate	2	2
Cholesterol	.018	0.300

Table 2.1: Composition of diets used in Chapters III-VI

Mice used in Chapter III: Mice for macrophage collection: Wild-type (WT) C57Bl/6 mice (stock number: 000664) were originally purchased from Jackson Laboratories (Bar Harbor, ME). TLR4-KO mice on a C57Bl/6 background were a gift from Drs. Satoshi Uematsu and Shizuo Akira at the University of Osaka, Japan. Mice were bred in our colony at Vanderbilt University. TLR2-KO mice on a C57Bl/6 background (stock number: 004650) were purchased from Jackson Laboratories and sacrificed after a two-week acclimatization period. Mice for CL316243 study: WT mice were purchased from Jackson Laboratories at 7-weeks of age. One week later, mice were started on 60% HF for a total of 9 weeks. Five hours before sacrifice, mice were intraperitoneally injected with 0.4 mg/kg CL316243.

Mice used in Chapter IV-V: Male C57Bl/6 mice were purchased from Jackson Laboratories. At 8-weeks of age, mice were placed on one of three diet regiments: 1) LF diet for 9 weeks, 2) HF diet for 9 weeks, or 3) HF diet for 9 weeks, followed by LF diet for 1 week. Ob/ob mice (stock number: 000632) and littermate controls were purchased from Jackson Laboratories at 7 weeks of age and maintained on a standard chow diet until 9-10 weeks of age. CHOP deficient mice on a C57Bl/6 background were originally purchased from Jackson Laboratories and bred in our colony.

Mice used in Chapter VI: Eight-week old male C57Bl/6 mice purchased from Jackson Laboratories were placed on one of three diet regiments: 1) LF diet

for 27 weeks, 2) LF diet for 9 weeks, followed by HF diet for 18 weeks, 3) HF diet for 9 weeks, LF diet for 9 weeks, then HF diet for 9 weeks.

Body weight and composition

In all studies, body weight was measured once weekly. When indicated, total fat and lean mass was quantified by nuclear magnetic resonance using a Bruker Minispec instrument (Woodlands, TX) in the Vanderbilt Mouse Metabolic Phenotyping Center.

Plasma collection and measurements

Mice were fasted for 5 h and bled from the retro-orbital venous plexus using heparinized collection tubes. Plasma was separated via centrifugation. Insulin levels were measured using a Rat/Mouse Insulin ELISA kit (Millipore, Billerica, MA), according to manufacturer's instructions.

Glucose tolerance tests (GTT)

Five-hour fasted mice were bled by the tail vein and baseline blood glucose levels were measured. Mice were then injected intraperitoneally with 2 g/kg lean mass of dextrose (Hospira, Inc, Lake Forest, IL). Blood glucose levels were assessed via the tail vein at 15, 30, 45, 60, 90, and 150 minutes post-injection using a LifeScan One Touch Ultra glucometer (Johnson & Johnson, Northridge, CA).

Mouse peritoneal macrophage collection

Three mL of 3% thioglycollate medium was injected into the peritoneal cavity of WT, TLR4-KO, or TLR2-KO mice on a C57BL/6 background. Three days later, macrophages were collected in serum-free DMEM and washed. Cells were then plated at a density of 1.5 x 10^6 cells per well of a 12-well plate or 3.0 x 10^6 cells per well of a 6-well plate in DMEM containing 10% FBS and incubated at 37 °C for 4 h. At this point, non-adherent cells were removed and the remaining cells were incubated for an additional 48 h at 37 °C before treatment.

Stearic acid treatment

Mouse peritoneal macrophages (MPMs) were treated with stearic acid at a final concentration of 90 μM. Stearic acid was dissolved in ethanol and then added to DMEM supplemented with 5% FBS to achieve a fatty acid to albumin ratio of 3:1. MPMs were treated with 90, 250, or 500 μM stearic acid in the presence or absence of 2.5 μM triascin C (TC). Cells treated with TC were pre-treated for 30 min prior to stearic acid exposure. For time-course treatments, cells were exposed to stearic acid and TC for 2, 4, 8, 16, or 24 h. All controls [vehicle-treated control, TC alone, tunicamycin (1 μM), and stearic acid alone] were treated for 24 h in media containing 5% FBS. For all other studies, macrophages were treated with stearic acid and TC for 16 h. An endpoint chromogenic LAL assay was used to confirm that there was no endotoxin contamination in media used for cell treatments. For co-treatments with 4-phenyl butyric acid (PBA) or sodium salicylate (SS): macrophages were treated with

stearic acid and TC for 16 h, as describe above, in the presence of PBA (6 mM) or SS (1 mM or 5 mM). For TLR4-KO experiments: as a control, macrophages were stimulated with LPS (10 μM), the known ligand for TLR4, and inflammatory cytokine expression was assessed. For all genes analyzed, WT macrophages responded to LPS treatment while TLR4-KO cells failed to respond (data not shown).

Macrophage polarization

MPMs were plated in DMEM containing 10% FBS, as described above. Cells were then washed with PBS and serum-free media was added to the cells 4 h prior to polarization. All macrophages were grown in serum free media. MΘ macrophages were left untreated, M1 macrophages were treated with 10 ng/ml of LPS, and M2 macrophages were treated with 4 ng/ml of IL-13. All polarization treatments were for 24 h. After polarization, cells were washed with PBS and treated with stearic acid and TC for 16 h in the presence of respective polarization agents. Thus, cells were treated with LPS or IL-13 for a total of 40 h by the end of the study. Additionally, control cells were treated with polarization agents for the duration of the studies. These cells were washed with PBS after 24 h of polarization (as treated cells were) and then re-exposed to the polarization agent in the absence of stearic acid and TC for the remaining 16 h.

Stromal vascular fraction (SVF) isolation

Mice were euthanized and perfused through the left ventricle with 20 mL of PBS. Epididymal AT was removed and 0.25-0.5 g of tissue was minced in 3 mL PBS with 0.5% BSA (PBS-B). Subsequently, 3 mL of 0.2 mg/mL collagenase (Sigma-Aldrich, St. Louis, MO) was added to achieve a final concentration of 0.1 mg/mL collagenase. Tissue was incubated at 37° C for 20-30 minutes while shaking at 200 RPM. The cell suspension was then filtered through a 100-μM cell strainer. Cells were spun at 500 x g for 10 minutes to separate adipocytes from the SVF cells. The SVF was re-suspended in 3 mL ACK buffer to lyse red blood cells. Cells were washed 2X with PBS and then counted using a Cellometer Auto T4.

Isolation of hepatocyte and F4/80-enriched fractions from the liver

Mice were euthanized and perfused as described above. The liver was removed and minced in 3 mL RPMI with 5% FBS. Next, 3 mL of 0.2 mg/mL collagenase was added and tissue was incubated at 37° C for 30 minutes while shaking at 200 RPM. The cell suspension was filtered through a 100-μM cell strainer and spun at 300 RPM for 3 minutes. The hepatocyte fraction (pellet) was collected, while the supernatant (non-parenchymal fraction) was spun at 1500 RPM for 10 minutes. The non-parenchymal fraction was re-suspended in ACK buffer to lyse red blood cells and washed twice. Cells were then re-suspended in a 33% normo-osmotic Percol solution containing 10 U/mL heparin and spun at 500 x g with the centrifuge break off. The pellet was washed and cells were

counted. Subsequently, cells were incubated with Fc block for 10 minutes and then stained with anti-mouse F4/80-APC (eBioscience, San Diego, CA) at a concentration of 5 x 10^6 cells/mL for 30 minutes at 4° C. After washing, cells were incubated with anti-APC magnetic beads for 15 minutes at 4° C, washed once, and re-suspended in FACS buffer. Cells were sorted using a Miltenyi AutoMACs magnetic cell sorter in the Vanderbilt Flow Cytometry Core, and the F4/80-enriched fraction was collected.

Western blot analysis

MPMs, SVF cells, and an F4/80-enriched fraction isolated from the liver were collected in lysis buffer containing 20 mM Tris-HCL (pH 8.0), 150 nM NaCl, 1 mM EDTA, 1 mM EGTA, 0.1% Nonidet P-40, 2.5 mM sodium pyrophosphate, 1 mM sodium orthovanadate, and 0.5 mM PMSF. A modified Lowry protocol was used to quantify protein concentration. Whole AT, liver, and muscle (~0.05 g), and the hepatocyte fraction were sonicated in 500-700 µL of 2% SDS containing 2.5 mM sodium pyrophosphate and 0.5 mM PMSF. Protein was quantified using a bicinchoninic acid (BCA) assay (Thermo Scientific). Subsequently, 10-15 µg of protein was electrophoresed through a 4-12% Bis-Tris gel (Invitrogen), transferred to a nitrocellulose membrane, and immunoblotted with the following antibodies:

Chapter III: phospho-PERK, BiP, IRE-1α, phospho-JNK 1/2, phospho-eIF2α, cleaved caspase-3, Bax, and Bak. **Chapter IV:** cleaved caspase-3. Bax, and Bak. **Chapter V:** phospho-PERK, BiP, phospho-JNK 1/2, and phospho-

eIF2α. **Chapter VI:** phospho-AKT and total AKT. All antibodies were obtained from Cell Signaling Technology (Boston, MA). Blots were developed using Western Lightning enhanced chemiluminescence substrate (Perkin Elmer, Waltham, MA). Band intensity was quantified using ImageJ64 software.

RNA isolation, cDNA synthesis, and real-time RT-PCR

MPMs or SVF cells were collected in TRIzol reagent (Invitrogen, Carlsbad, CA). Total RNA was isolated using a phenol-chloroform extraction, according to the manufacturer's instructions. RNA extraction from whole AT (0.05 g) was performed with an RNeasy kit (Qiagen, Valencia, CA) according to the manufacturer's instructions. An iScript cDNA synthesis kit (BioRad, Hercules, CA) was used for reverse transcriptase reactions. Real-time RT-PCR analysis was performed using an iQ5 multicolor real-time PCR detection system (Bio-Rad, Hercules, CA). Primer-probe sets (Assays-on-Demand) were purchased from Applied Biosystems (Foster City, CA). All genes were analyzed using the Pfaffl method (146) and normalized to 18s ribosomal RNA or glyceraldehyde-3-phosphate dehydrogenase (GAPDH). The expression of the following genes was assessed:

Chapter III: *18S* (4352930E), *Ccl2* (Mm00441242_m1), *Tnf* (Mm00443258_m1), *Il6* (Mm00446190_m1), *Chop/Ddit3* (Mm00492097_m1), *Il1b* (Mm01336189_m1). Data are presented as relative to the vehicle-treated control group.

Chapter IV: *Emr1* (Mm00802530_m1) and *Gapdh* (Mm99999915_g1). Data is presented as relative to the 9W HF group.

Chapter VI: *Emr1* (Mm00802530_m1) *Cd68* (Mm00839636_g1), *Itgam* (Mm00434455_m1), *Itgax* (Mm00498698_m1), *Tnf* (Mm00443258_m1), *Ccr2* (Mm99999051_gH), *Arg1* (Mm01190441_g1), *Clec10a* (Mm00546125_g1), *Cd3e* (Mm00599683_m1), *Cd4* (Mm00442754_m1), *Cd8* (Mm01182108_m1), *Ifng* (Mm01168434_m1), *Il12a* (Mm00434165_m1), *Il2* (Mm00434256_m1), *Il2ra* (Mm00434261_m1), *Il2rb* (Mm00434268_m1), *Ccl5* (Mm01302428_m1), *Il4* (Mm00445259_m1), *Il10* (Mm00439614_m1), *Il13* (Mm00434204_m1), and *Gapdh* (Mm99999915_g1). Data are presented as relative to the LF/LF/LF group.

Analysis of XBP-1 splicing

cDNA was generated from treated MPMs, as described above. The *Xbp1* gene was amplified using the following primers: forward: 5'-TGA GAA CCA GGA GTT AAG AAC C-3'; reverse: 5'-TTC TGG GTA GAC CTC TGG GAG TTC C-3'. The resulting PCR product was electrophoresed on a 1.8% agarose gel for 1 h. Expression of the spliced form of *Xbp-1* was normalized to an internal β-actin standard (forward primer: 5'-TGA CCC AGA TCA TGT TTG AGA CC-3'; reverse primer: 5'-CCA TAG CCA AGA AGG AAG GC-3').

Histology

Staining of MPMs (Chapter III): Cells were plated at 250,000 cells/well in an 8-well chamber slide in DMEM containing 10% FBS and treated with stearic

acid and TC, as described above. TUNEL staining was performed using the In Situ Cell Death Detection Kit (Roche-Applied Science) according to manufacturer's instructions. After TUNEL staining, cells were counterstained with DAPI (0.2 mg/mL, Vector Laboratories, Burlingame, CA) and imaged at 20X magnification using an inverted Leica Conventional fluorescent microscope (Vanderbilt Shared Imaging Resource). One or two fields of view (at least 300 cells) were counted for each well of the chamber slide using Histometrix 6 software. Experiments were repeated at least 3 separate times.

Staining of whole AT (Chapter IV): Epididymal AT was harvested and immediately fixed in 1% paraformaldehyde for 1 h. Tissue was blocked in 5% goat serum in PBS for 1 h and stained with an rat anti-mouse F4/80 antibody (Abcam, Cambridge, MA) overnight at 4° C. After washing with PBS, tissue was incubated with an Alexa 488-conjugated anti-rat secondary antibody (Cell Signaling Technology) for 1 h at room temperature. TUNEL staining was performed, again using the In Situ Cell Death Detection Kit (Roche-Applied Science). Tissue was then counter-stained with DAPI (0.2 mg/mL) and imaged at 40X magnification using an Olympus FV-1000 Inverted Confocal Microscope. At least 3 images were captured per mouse.

Flow cytometry

One million SVF cells were incubated in Fc block for 10 minutes, followed by a 30 minute incubation at 4° C with fluorophore-conjugated antibodies: F4/80-

APC (eBioscience, San Diego, CA), CD11b-APC-Cy7 (BD Biosciences, San Jose, CA), CD11c-PE (eBioscience), TCR-β-APC (BD Biosciences), CD4-A700 (BD Biosciences), CD8-PE-Cy7 (BD Biosciences), CD62L-PE (BD Biosciences), and CD44-FITC (BD Biosciences). DAPI (0.2 mg/mL) was added as a viability stain before flow cytometry was performed. Samples were processed on a 5-laser LSRII flow cytometer in the Vanderbilt University Flow Cytometry Core. Data was analyzed using FlowJo software.

Statistical analysis

GraphPad Prism 5.0 software was used for all statistical analyses. Data was analyzed using a two-tailed unpaired t-test to determine differences between two groups, a one-way ANOVA when more than two treatment groups were compared, or a two-way ANOVA to compare measurements with two different variables. Outliers were excluded from the data for each individual parameter using the Grubbs outlier test (147). A p of ≤ 0.05 was considered significant.

CHAPTER III

Stearic acid accumulation in macrophages induces TLR4/2-independent inflammation leading to ER stress-mediated apoptosis

(Adapted from Anderson, *et al*. (2011). *ATVB*. Jul: 32 (7): 1687-95).

INTRODUCTION

During obesity, dysregulated lipolysis in insulin resistant adipocytes leads to increased FFA concentrations and hyperlipidemia (72). Elevated serum FFA levels are independently associated with an increased risk for both CVD and T2D (72; 73); however mechanisms explaining this correlation have not been fully defined. Importantly, systemic FFA toxicity may be mediated, in part, by activation of inflammatory pathways in macrophages residing in metabolic tissues, including AT (34; 35; 40; 148) and liver (149), or in atherosclerotic plaques (150; 151). The majority of the studies regarding macrophage lipotoxicity have sought to identify extracellular receptors that are responsible for mediating the inflammatory affects of saturated FFAs. Several groups have suggested that saturated FFAs may act through TLR4 to generate macrophage inflammation and lipotoxicity (152); however, others dispute this claim (48). An additional study has demonstrated that saturated FFAs activate a TLR2-dependent apoptotic pathway in macrophages undergoing ER stress (153).

Interestingly, recent studies suggest that intracellular accumulation of FFAs within macrophages may play a pathogenic role in the progression of both T2D and atherosclerosis. Treatment of human macrophages with dyslipidemic

serum from diabetic patients increases intracellular FFA concentrations (154; 155), suggesting that macrophages in metabolic tissues of these patients may encounter high levels of FFAs. In addition, multiple FFA species are present in macrophage-rich regions of human atherosclerotic lesions, and increased FFA concentrations are observed in inflammatory plaques from diabetic individuals (156). Therefore, it is critically important to determine the *in vitro* consequences of intracellular FFA accumulation within macrophages and to understand the affects of increased FFA concentrations on macrophages residing in metabolic tissues. Our lab has previously shown that accumulation of the saturated FFA, stearic acid, in macrophages results in apoptotic cell death (75); however, the mechanism of lipotoxicity remains unknown.

The ER is not simply a site of protein synthesis and maturation, but also functions as a nutrient sensor to regulate the energy needs of the cell. Therefore, changes in nutrient availability or inflammatory status can cause ER stress and activation of the UPR. In fact, increased levels of free cholesterol in macrophages (induced by inhibition of ACAT activity) (157) or exposure of pancreatic β-cells (158), hepatocytes (159), or adipocytes (160) to saturated FFAs results in UPR activation. The UPR is controlled by three ER-localized receptors: IRE-1α, PERK, and ATF-6. ER stress initiates a signaling cascade that decreases the protein load entering the ER and increases the folding capacity of the organelle by up-regulating genes including BiP (139). ER stress can also activate inflammatory signaling through JNK (161) and NF-κB (162) and initiate apoptosis (163). Interestingly, ER stress is increased in atherosclerotic plaques,

whole AT, and liver of obese, dyslipidemic mice and humans (164-166). Decreasing ER stress through treatment with the chemical chaperone, PBA, reduces systemic inflammation and IR in response to a high-fat diet (167) and decreases macrophage apoptosis in atherosclerotic plaques during conditions of hyperlipidemia (168).

The above data suggest that the systemic elevation of FFAs observed in obese individuals may result in ER stress activation, inflammation, and apoptosis in macrophages residing in metabolic tissues. In addition, recent data indicate that macrophages in atherosclerotic plaques accumulate FFAs (154-156); however, the molecular consequences of FFA accumulation in these immune cells remain ill defined. We have previously demonstrated that triascin C (TC)-mediated inhibition of long-chain acyl-CoA synthetases (ACSL) during stearic acid treatment of MPMs increases intracellular stearic acid concentrations and results in apoptotic cell death (75). Using this model, we now show that stearic acid accumulation in macrophages results in TLR4/2-independent induction of inflammation, leading to ER stress-mediated apoptosis. Polarization of macrophages to a pro-inflammatory M1 phenotype increases the susceptibility of these cells to inflammation and ER stress, but not apoptosis. These findings advance our understanding of the molecular changes that occur in macrophages upon FFA accumulation, and demonstrate that intracellular FFAs induce macrophage ER stress, inflammation, and apoptosis. Activation of these signaling pathways, specifically in macrophages, may play a key role in the progression of IR and atherosclerosis.

RESULTS

Intracellular accumulation of stearic acid induces ER stress in MPMs

Previous studies from our lab have shown that incubation of MPMs with low-level stearic acid and TC inhibits ACSL activity, leading to a 4-fold increase in intracellular stearic acid content when compared to control cells or cells treated with stearic acid alone (169). To determine if intracellular stearic acid accumulation within macrophages induces ER stress, MPMs were co-treated with 90 μM stearic acid (identified as 18:0 in figures) and 2.5 μM TC for 2 to 24 h. In addition, cells were treated with either TC or stearic acid alone for 24 h. Tunicamycin (1 μM for 24 h) was used as a positive control for ER stress induction. Co-treatment with stearic acid and TC significantly increased the phosphorylation of PERK after 8 ($p<0.001$) and 16 h ($p<0.001$) compared to vehicle-treated control cells (Figure 3.1A). Treatment with stearic acid or TC alone did not increase PERK phosphorylation, indicating that ER stress activation is due to intracellular stearic acid accumulation as opposed to FFA exposure without accumulation (Figure 3.1A). During the time-course of stearic acid accumulation, BiP and IRE-1α protein levels were increased at 16 ($p<0.001$) and 24 h ($p<0.01$) of co-treatment (Figure 3.1B-C). PCR amplification of the IRE-1α target gene, *Xbp1*, revealed an increase in the spliced form of *Xbp1* after 8 ($p<0.01$), 16 ($p<0.001$), and 24 h ($p<0.01$, Figure 3.1D).

Intracellular accumulation of stearic acid increases inflammation in MPMs

ER stress signaling can result in the activation of pro-inflammatory kinases, including JNK and NF-κB (161). A significant increase in the phosphorylation of JNK 1/2 was observed after 8 ($p<0.05$) and 16 h ($p<0.05$) of stearic acid and TC co-treatment (Figure 3.1E). Additionally, intracellular stearic acid accumulation increased the expression of the NF-κB target genes, TNF-α (*Tnf*), IL-6 (*Il6*), and IL-1β (*Il1b*, $p<0.05$, Figure 3.2A-C). These data indicate that intracellular accumulation of stearic acid induces both JNK- and NF-κB-mediated inflammatory pathways. In addition, gene expression of the chemokine, MCP-1 (*Ccl2*), was also increased by stearic acid and TC co-treatment ($p<0.05$, Figure 3.2D). MIP-1α (*Ccl3*) expression was not modulated by FFA accumulation (Figure 3.2E).

Intracellular accumulation of stearic acid induces apoptosis in MPMs

Cleavage of caspase-3, a key executioner caspase, was significantly increased after 8 ($p<0.05$) and 24 h ($p<0.001$) of treatment, with maximal cleavage observed at 16 h ($p<0.001$, Figure 1F). TUNEL staining was performed on macrophages at the peak of apoptosis (16 h). Approximately 17.9 ± 4.1% of cells co-treated with stearic acid and TC were TUNEL positive, while only 0.10 ± 0.10% of control cells stained positive for TUNEL ($p<0.01$, Figure 3.1G). Gene expression of *Chop*, the primary mediator of apoptosis following ER stress, was increased after 16 h ($p<0.05$) of co-treatment with stearic acid and TC (Figure 1H). Additionally, higher concentrations of stearic acid (250 μM and 500 μM) in

the absence of TC resulted in ER stress, inflammation, and apoptosis (Figure 3.3), indicating that inhibition of ACSL activity accelerates, but is not required for, the lipotoxic effects of stearic acid.

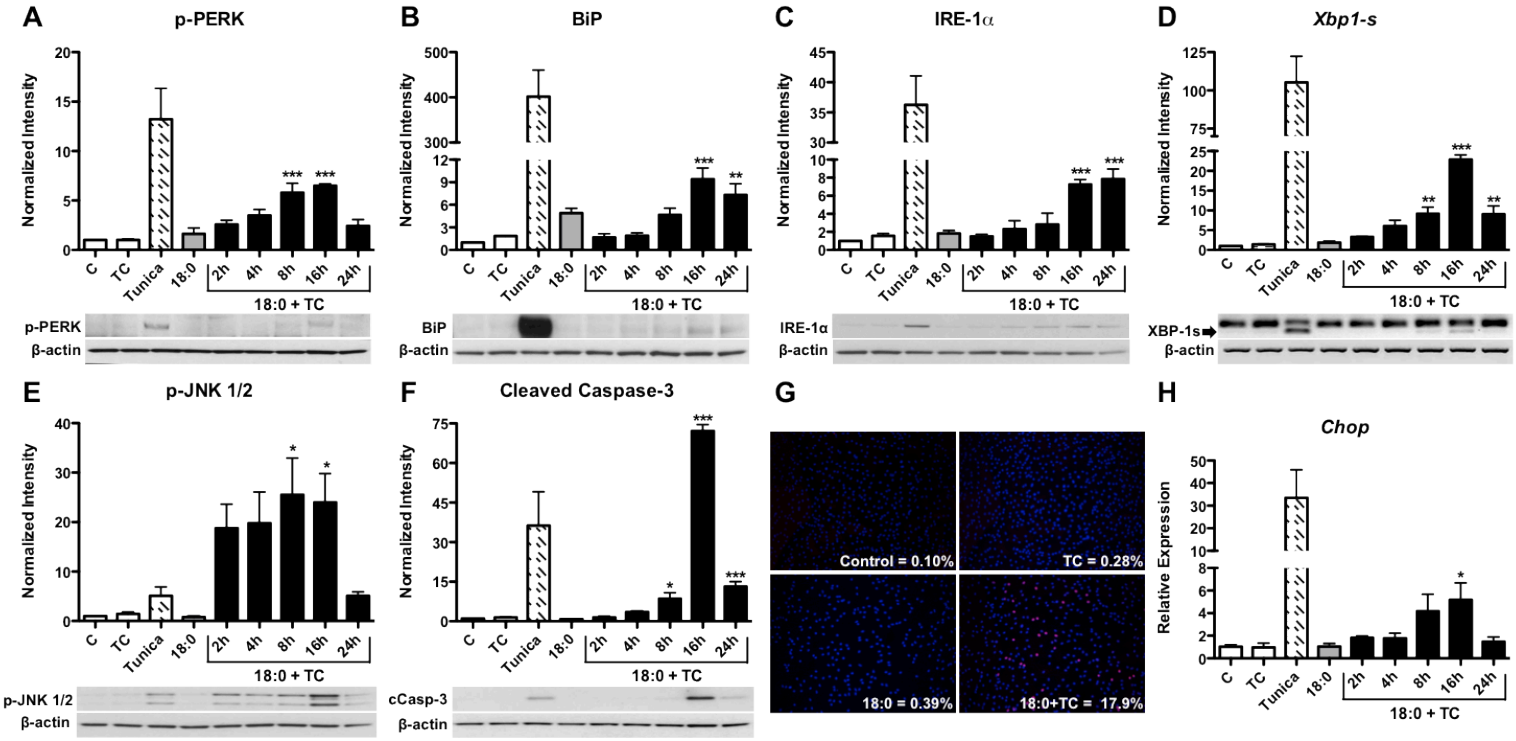
A
p-PERK
Normalized Intensity
C
TC
Tunica
18:0
2h
4h
8h
16h
24h
18:0 + TC
p-PERK
β-actin
B
BiP
Normalized Intensity
BiP
β-actin
C
IRE-1α
Normalized Intensity
IRE-1α
β-actin
D
Xbp1-s
Normalized Intensity
XBP-1s
β-actin
E
p-JNK 1/2
Normalized Intensity
p-JNK 1/2
β-actin
F
Cleaved Caspase-3
Normalized Intensity
cCasp-3
β-actin
G
Control = 0.10%
TC = 0.28%
18:0 = 0.39%
18:0+TC = 17.9%
H
Chop
Relative Expression

Figure 3.1: Intracellular stearic acid accumulation induces ER stress, inflammation, and apoptosis. MPMs were co-treated with stearic acid (18:0, 90 μM) and TC (2.5 μM) for 2 to 24 h in DMEM containing 5% FBS. All controls [vehicle-treated (C), TC, tunicamycin (1 μM), and 18:0 alone] were treated for 24 h. A-C) Western blot analysis for markers of ER stress: A) phospho-PERK, B) BiP, C) IRE-1α. D) RT-PCR analysis of *Xbp1* mRNA splicing. E-F) Western blot analysis of: E) phospho-JNK1/2 and F) cleaved caspase-3. G) Detection of apoptotic cells by TUNEL (red) and DAPI (blue) staining of MPMs treated for 16 h. Magnification: 20X. H) Gene expression analysis of *Chop* mRNA by real-time RT-PCR. Data are presented as mean ± SEM, n = 3/group. * $p<0.05$, ** $p<0.01$, *** $p<0.001$ compared to control. Tunicamycin treatment was used as a positive control for Western blotting and is not included in statistical analysis.

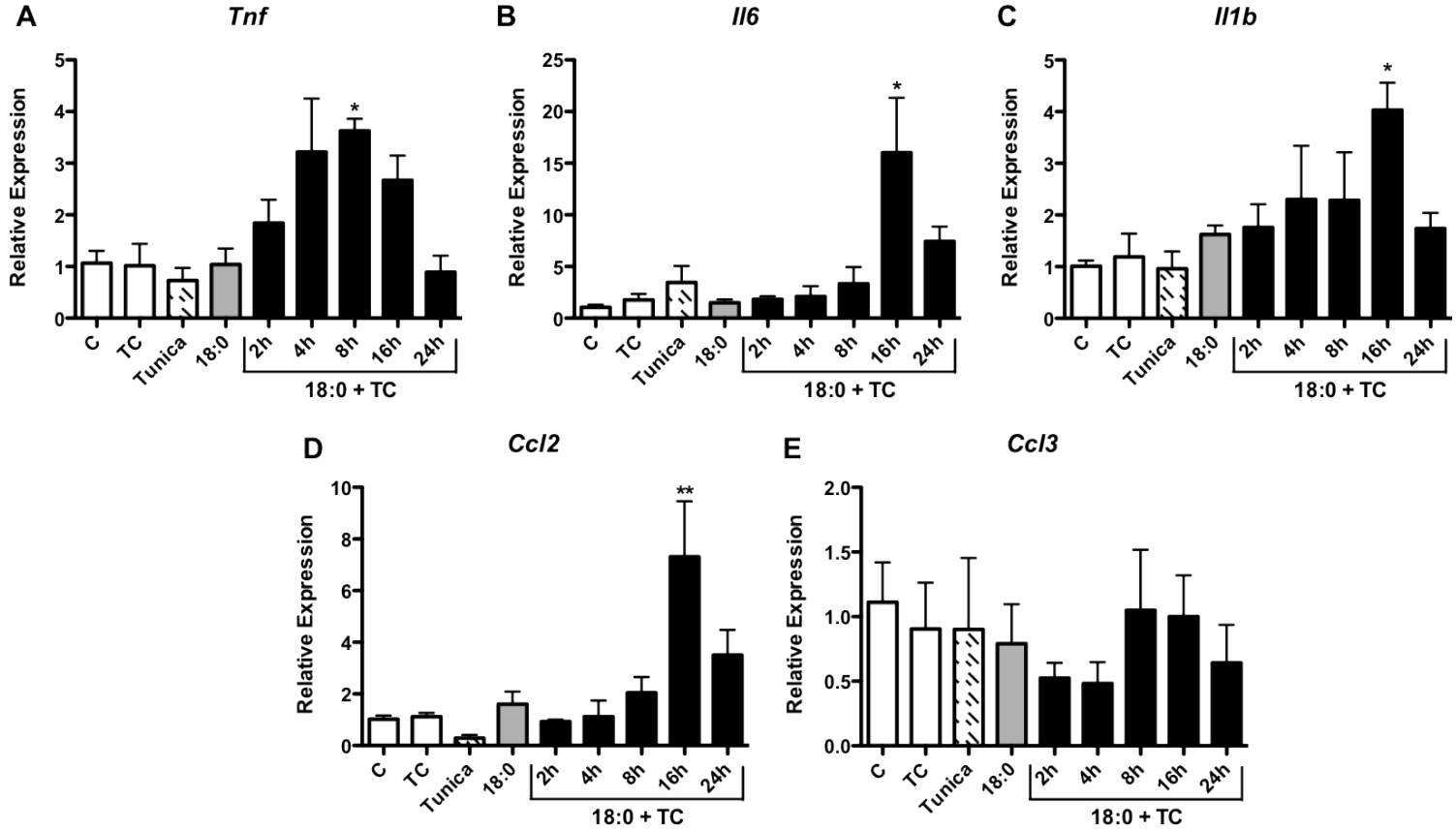
A
Tnf
B
Il6
C
Il1b
D
Ccl2
E
Ccl3
Relative Expression
C
TC
Tunica
18:0
2h
4h
8h
16h
24h
18:0 + TC
*
**

Figure 3.2: Intracellular stearic acid accumulation increases inflammatory cytokine gene expression in MPMs. MPMs were co-treated with stearic acid (18:0, 90 μM) and TC (2.5 μM) for 2 to 24 h in DMEM containing 5% FBS. All controls [vehicle-treated control, TC alone, tunicamycin (1 μM), and 18:0 alone] were treated for 24 h. Analysis of A) *Tnf*, B) *Il6*, C) *Il1b*, D) *Ccl2*, and E) *Ccl3* gene expression by real-time RT-PCR. Data are presented as mean ± SEM, n = 3/group. * $p<0.05$, ** $p<0.01$ compared to control.

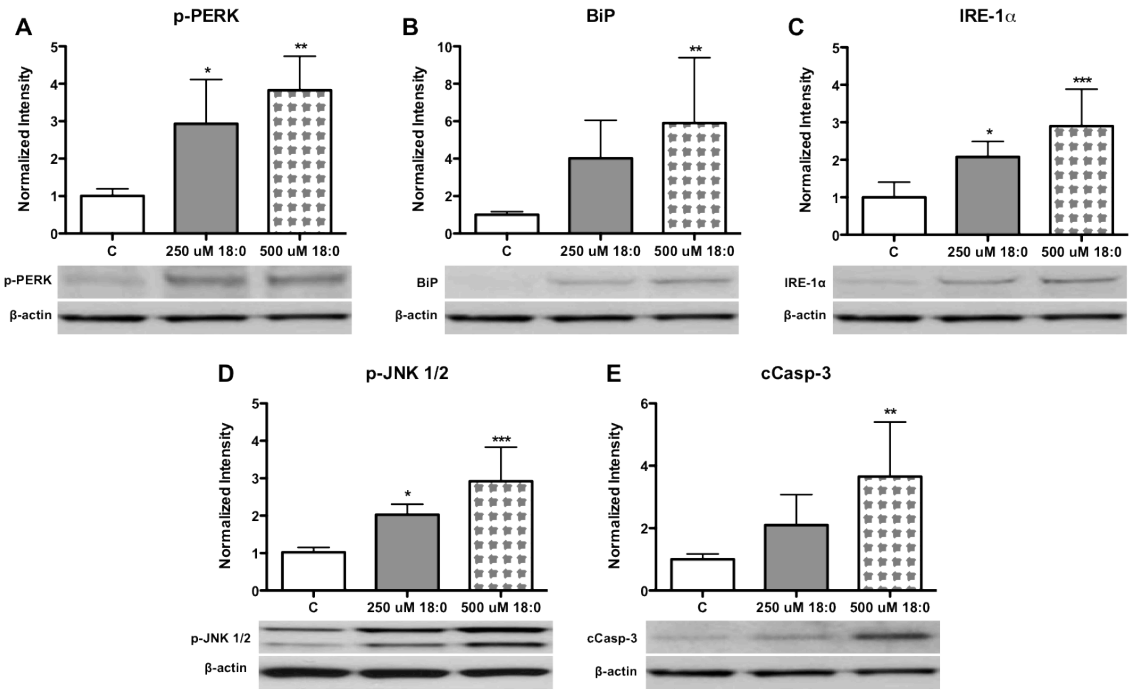

Figure 3.3: Higher levels of stearic acid, in the absence of TC, are sufficient to induce MPM ER stress, inflammation, and apoptosis. MPMs were treated with stearic acid (18:0, 250 or 500 μM) for 16 h in DMEM containing 5% FBS. A-E) Western blot analysis of: A) phospho-PERK, B) BiP, C) IRE-1α, D) phospho-JNK1/2, and E) cleaved caspase-3. Data are presented as mean ± SEM, n = 3-5/group. * $p<0.05$, ** $p<0.01$ compared to control.

Inhibition of ER stress during stearic acid loading of MPMs decreases apoptosis

To determine if ER stress induced by intracellular stearic acid accumulation is upstream of inflammation and apoptosis, MPMs were treated with stearic acid and TC in the presence of the chemical chaperone, PBA. Co-treatment with PBA during stearic acid accumulation resulted in a 60% decrease in PERK phosphorylation ($p<0.05$ compared to stearic acid and TC, Figure 3.4A). Additionally, co-treatment with stearic acid, TC, and PBA decreased BiP and IRE-1α protein levels by approximately 50% ($p<0.05$ compared to stearic acid and TC, Figure 3.4B-C). Activation of ER stress can result in inflammation and secretion of chemokines (161; 162). However, phosphorylation of JNK1/2 was not decreased in the presence of PBA (Figure 3.4D). Gene expression of *Il6* and *Il1b* was also not modulated by PBA co-treatment (Figure 3.5A-B). In contrast, PBA co-treatment significantly decreased gene expression of the chemokine, *Ccl2* ($p<0.05$ compared to stearic acid and TC, Figure 3.4E). In regards to apoptosis, PBA co-treatment decreased caspase-3 cleavage, TUNEL staining, and *Chop* gene expression ($p<0.05$ compared to stearic acid and TC, Figure 3.4F-H).

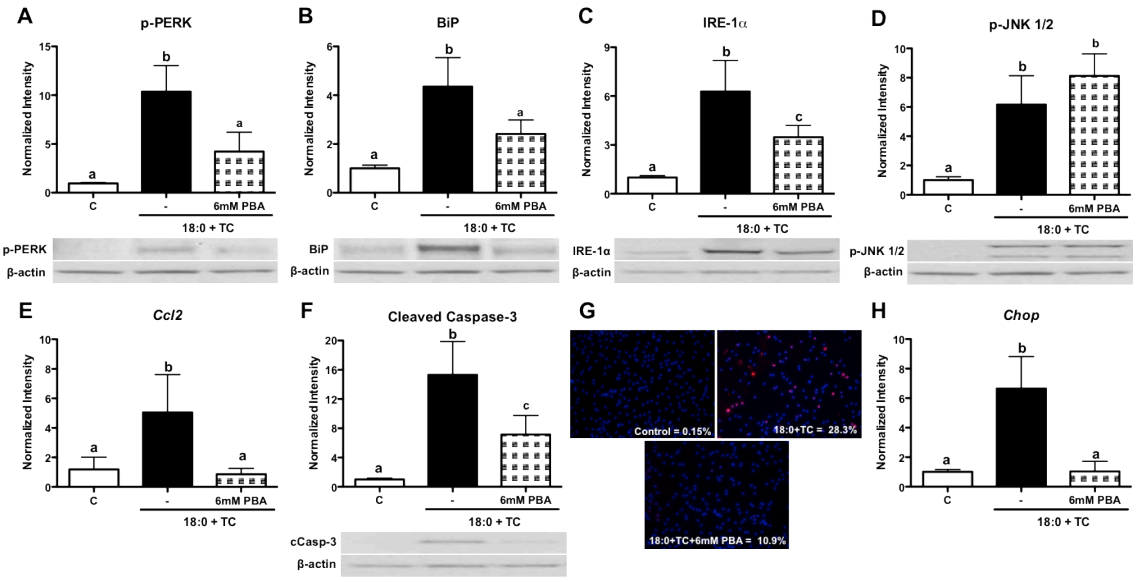

Figure 3.4: PBA attenuates ER stress, chemokine secretion, and apoptosis, but not inflammation, induced by stearic acid accumulation. MPMs were co-treated with stearic acid (18:0, 90 μM) and TC (2.5 μM) in the presence or absence of PBA (6 mM) for 16 h in DMEM containing 5% FBS. A-D) Western blot analysis for: A) phospho-PERK, B) BiP, C) IRE-1α, D) phospho-JNK1/2. E) Real-time RT-PCR analysis of *Ccl2* gene expression. F) Western blot analysis for cleaved caspase-3. G) TUNEL (red) and DAPI (blue) staining to detect apoptotic cells. Magnification: 20X. H) Gene expression analysis of *Chop* mRNA by real-time RT-PCR. Data are presented as mean ± SEM, n = 4-5/group. Groups not connected by the same letter are significantly different, $p<0.05$.

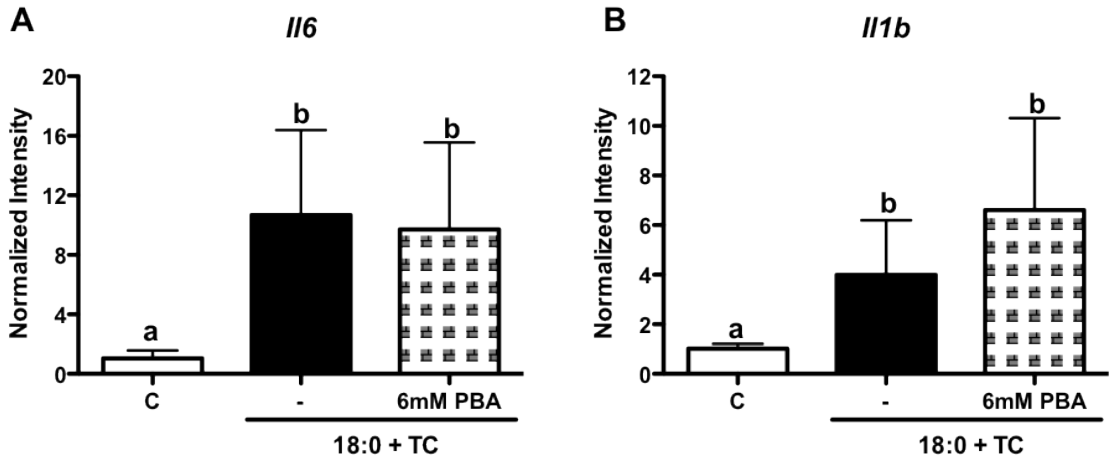

Figure 3.5: PBA co-treatment does not attenuate inflammatory cytokine expression in response to intracellular stearic acid accumulation in MPMs. MPMs were co-treated with stearic acid (18:0, 90 μM) and TC (2.5 μM) in the presence or absence of PBA (6 mM) for 16 h in DMEM containing 5% FBS. Analysis of A) *Il6* and B) *Il1b* gene expression by real-time RT-PCR. Data are presented as mean ± SEM, n = 7/group. Groups not connected by the same letter are significantly different, $p<0.05$.

Inhibition of inflammation during stearic acid loading of MPMs decreases ER stress and apoptosis

Sodium salicylate (SS), a derivative of aspirin (170; 171), was utilized to further assess the role of inflammation during stearic acid accumulation in MPMs. Cells were co-treated with stearic acid and TC in the presence of 1 or 5 mM SS for 16 h. JNK 1/2 phosphorylation (Figure 3.6A) and gene expression of the NF-κB target genes, *Il6* (Figure 3.6B) and *Ccl2* (data not shown), were decreased by either 1 or 5 mM SS ($p<0.05$ compared to stearic acid and TC). Inhibition of inflammation by SS during stearic acid accumulation significantly decreased PERK phosphorylation (Figure 3.6C) and reduced BiP (Figure 3.6D) and IRE-1α (Figure 3.6E) protein levels ($p<0.05$ compared to stearic acid and TC). Additionally, co-treatment with stearic acid, TC, and either 1 or 5 mM SS decreased caspase-3 cleavage, TUNEL staining, and *Chop* gene expression ($p<0.05$ compared to stearic acid and TC, Figure 3.6F-H). These data indicate that inflammation is responsible for the activation of ER stress-mediated apoptosis during stearic acid accumulation.

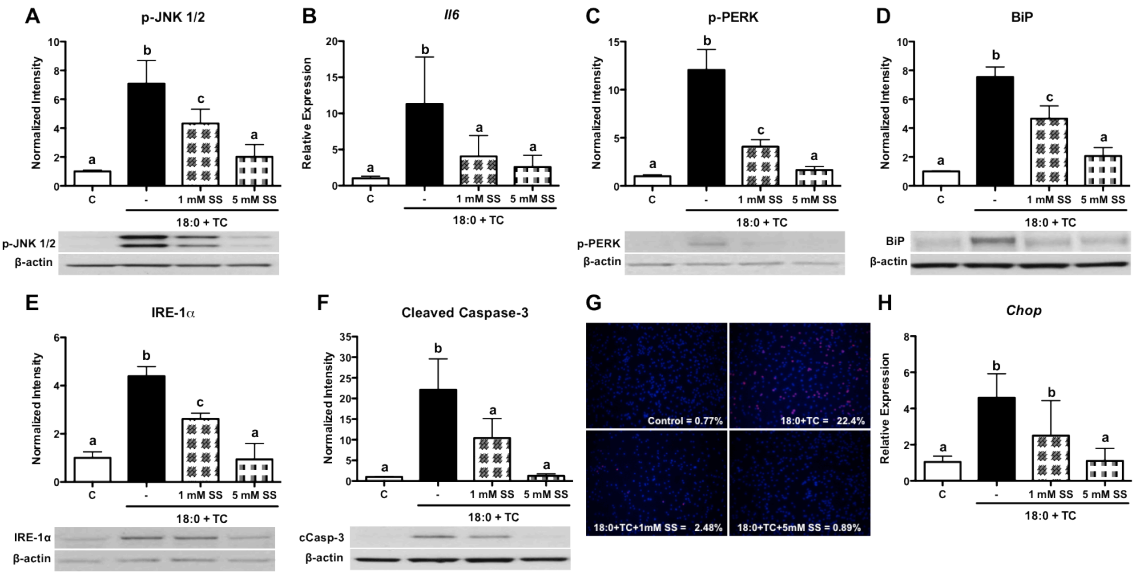

Figure 3.6: Inhibition of inflammation by sodium salicylate decreases MPM ER stress and apoptosis during stearic acid accumulation. MPMs were co-treated with stearic acid (18:0, 90 μM) and TC (2.5 μM) in the presence or absence of 1 or 5 mM SS for 16 h in DMEM containing 5% FBS. A) Western blot analysis of phospho-JNK1/2, B) Real-time RT-PCR analysis of *Il6* gene expression. C-F) Western blot analysis for: C) phospho-PERK, D) BiP, E) IRE-1α, and F) cleaved caspase-3. G) TUNEL (red) and DAPI (blue) staining to detect apoptotic cells. Magnification: 20X. H) Gene expression analysis of *Chop* mRNA by real-time RT-PCR. Treatment with 5 mM SS alone resulted in a significant increase in cleaved caspase-3 protein levels (data not shown, $p<0.01$). Data are presented as mean ± SEM, n = 3/group. Groups not connected by the same letter are significantly different, $p<0.05$.

Intracellular stearic acid accumulation in MPMs increases inflammation, ER stress, and apoptosis independent of TLR4 and TLR2

To determine if the inflammation, ER stress, and apoptosis generated by intracellular stearic acid accumulation in MPMs is dependent upon TLR4 or TLR2 signaling, WT, TLR4-KO, and TLR2-KO macrophages were treated with stearic acid and TC for 16 h (Figure 3.7). Intracellular accumulation of stearic acid increased the phosphorylation of JNK 1/2 to the same extent in WT, TLR4-KO, and TLR2-KO macrophages (genotype effect = ns, Figure 3.7A and E). Deficiency of either TLR4 or TLR2 resulted in a significant decrease in *Il6* gene expression during intracellular FFA accumulation (genotype effect = $p<0.05$, Figure 3.7B and F). However, gene expression of *Il1b* and *Ccl2* was not decreased by TLR4 or TLR2 deficiency (Figure 3.7C-D, G-H). In fact, *Il1b* gene expression was higher in TLR2-KO macrophages co-treated with stearic acid and TC (genotype effect = $p<0.05$, Figure 3.7G). Stearic acid accumulation increased phospho-PERK and BiP protein levels to a similar extent in WT, TLR4-KO, and TLR2-KO macrophages (genotype effect = ns, Figure 3.8A-B, E-F). Stearic acid accumulation resulted in a significant increase in the cleaved form of caspase-3 in WT, TLR4-KO, and TLR2-KO macrophages (genotype effect = ns, Figure 3.8C and G). Additionally, gene expression of *Chop* was also increased upon stearic acid accumulation, regardless of genotype (genotype effect = ns, Figure 3.8D and H). Together, these data indicate that TLR4 and TLR2 signaling are not necessary for the induction of macrophage inflammation, ER stress, or apoptosis in response to intracellular accumulation of stearic acid.

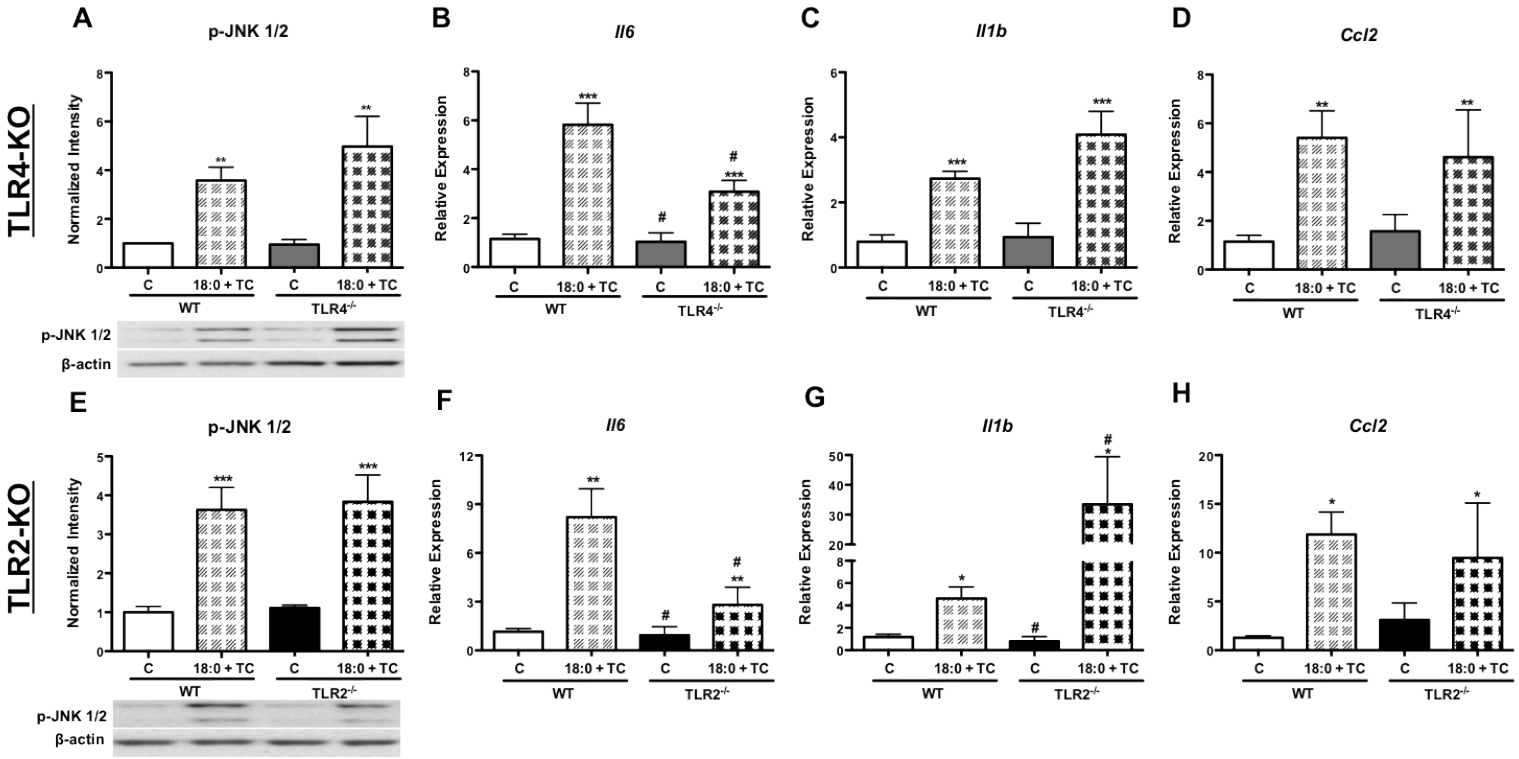
A
p-JNK 1/2
TLR4-KO
Normalized Intensity
C
18:0 + TC
WT
TLR4-/-
p-JNK 1/2
β-actin
B
Il6
Relative Expression
C
D
Il1b
Ccl2
E
TLR2-KO
TLR2-/-
F
G
H

Figure 3.7: Absence of TLR4 or TLR2 does not protect MPMs from inflammation induced by stearic acid accumulation. MPMs were isolated from WT, TLR4-KO, and TLR2-KO mice and co-treated with stearic acid (18:0, 90 μM) and TC (2.5 μM) for 16 h in DMEM containing 5% FBS. A-D) Analysis of inflammatory markers in WT and TLR4-KO MPMs: A) Western blot of phospho-JNK 1/2, B-D) Real-time RT-PCR analysis of: B) *Il6*, C) *Il1b*, D) *Ccl2*. E-F) Analysis of inflammatory markers in WT and TLR2-KO MPMs: E) Western blot of phospho-JNK 1/2, F-H) Real-time RT-PCR analysis of: F) *Il6*, G) *Il1b*, H) *Ccl2*. Data are presented as mean ± SEM. * Treatment effect, $p < 0.05$; ** Treatment effect, $p < 0.01$; *** Treatment effect, $p < 0.001$; # Genotype effect, $p < 0.05$.

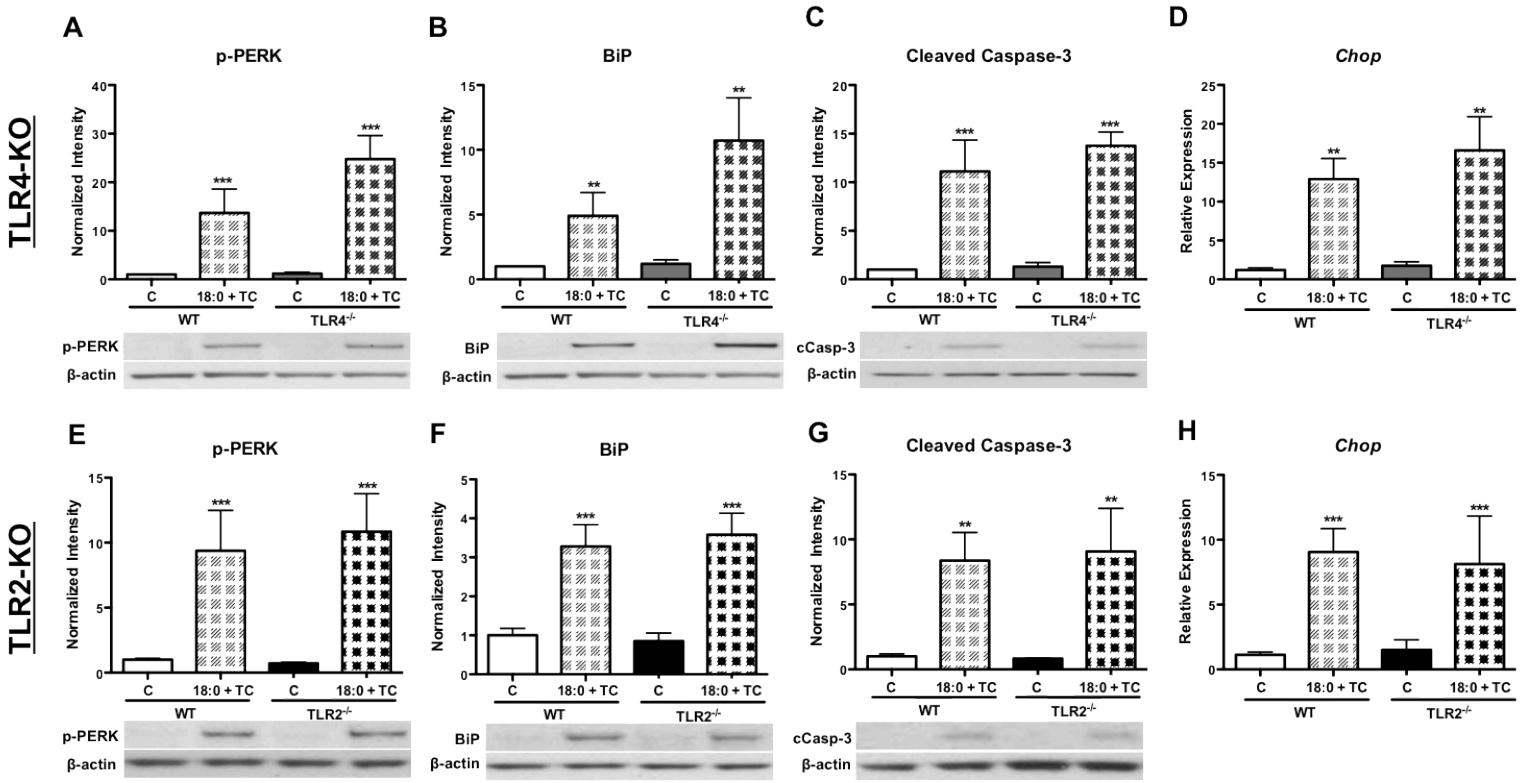
TLR4-KO
TLR2-KO
A
p-PERK
B
BiP
C
Cleaved Caspase-3
D
Chop
E
p-PERK
F
BiP
G
Cleaved Caspase-3
H
Chop
Normalized Intensity
Relative Expression
C
18:0 + TC
WT
TLR4-/-
TLR2-/-
p-PERK
BiP
cCasp-3
β-actin

Figure 3.8: Absence of TLR4 or TLR2 does not protect MPMs from ER stress or apoptosis induced by stearic acid accumulation. MPMs were isolated from WT, TLR4-KO, and TLR2-KO mice and co-treated with stearic acid (18:0, 90 μM) and TC (2.5 μM) for 16 h in DMEM containing 5% FBS. A-D) Analysis of ER stress and apoptotic markers in WT and TLR4-KO MPMs: A-C) Western blot analysis of: A) phospho-PERK, B) BiP, C) Cleaved caspase-3. D) Real-time RT-PCR analysis of *Chop* gene expression. E-F) Analysis of ER stress and apoptotic markers in WT and TLR2-KO MPMs: E-G) Western blot analysis of: E) phospho-PERK, F) BiP, G) Cleaved caspase-3. H) Real-time RT-PCR analysis of *Chop* gene expression. Data are presented as mean ± SEM. ** Treatment effect, $p<0.01$; *** Treatment effect, $p<0.001$.

Polarization of MPMs to an M1 phenotype increases susceptibility to inflammation and ER stress, but not apoptosis, in response to intracellular stearic acid accumulation

To determine if macrophage polarization state modulates the susceptibility of these cells to stearic acid-induced inflammation, ER-stress, and apoptosis, MPMs were polarized for 24 h with vehicle (Mθ, un-polarized macrophages), LPS (M1 macrophages), or IL-13 (M2 macrophages). Polarization was confirmed by real-time RT-PCR analysis of M1 and M2 gene expression (Figure 3.9). After polarization, each group was co-treated with stearic acid (90 μM) and TC (2.5 μM) in the presence of either vehicle (Mθ), LPS (M1), or IL-13 (M2) for an additional 16 h (40 h total treatment). To control for the effects of LPS and IL-13, a subset of macrophages was incubated with the respective polarizing agent in the absence of stearic acid and TC for the duration of the experiment. These control cells exhibited low JNK1/2 phosphorylation that was not modulated by macrophage phenotype (Figure 3.10A). Polarization in the absence of stearic acid and TC did not modulate the expression of ER stress or apoptotic markers (data not shown). However, when polarized macrophages were exposed to stearic acid and TC, M1 macrophages exhibited increased JNK 1/2 phosphorylation when compared to either Mθ or M2 macrophages (Figure 3.10A, $p<0.001$), suggesting that M1 polarized macrophages are more susceptible to stearic acid-induced inflammation.

Intracellular accumulation of stearic acid in M1 macrophages resulted in a 3-fold increase in PERK phosphorylation and a 45% increase in BiP protein levels when compared to M2 macrophages ($p<0.05$, Figure 3.10B-C). Protein

levels of IRE-1α remained similar among all groups (data not shown). There was a non-significant trend towards an increase in *Chop* gene expression in M1 macrophages (Figure 3.10D); however, there was no difference in TUNEL staining (Figure 3.10E) or caspase-3 cleavage (Figure 3.10F) between groups. Collectively, these results suggest that polarization of macrophages to an M1 phenotype increases susceptibility to stearic acid-induced inflammation and ER stress, but not apoptosis.

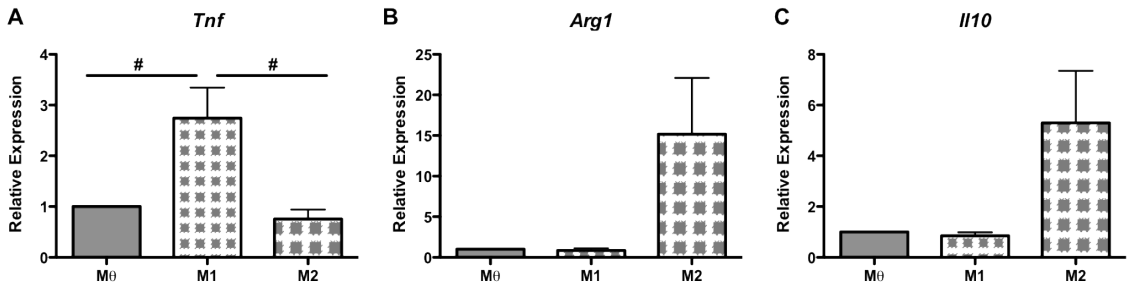

Figure 3.9: Confirmation of MPM Polarization State. MPMs were treated with vehicle, LPS (10 ng/mL), or IL-13 (4 ng/mL) for 24 h to induce a Mθ, M1, or M2 polarization state, respectively. A-C) RNA was collected and real-time RT-PCR was performed in order to confirm macrophage polarization: A) *Tnf*, B) *Arg1*, and C) *Il10*. Gene expression of *Nos2* (iNOS) was not detected in Mθ or M2 macrophages, but was seen in M1 macrophages. Data are presented as mean ± SEM, n = 3/group. # $p<0.05$ compared to M1.

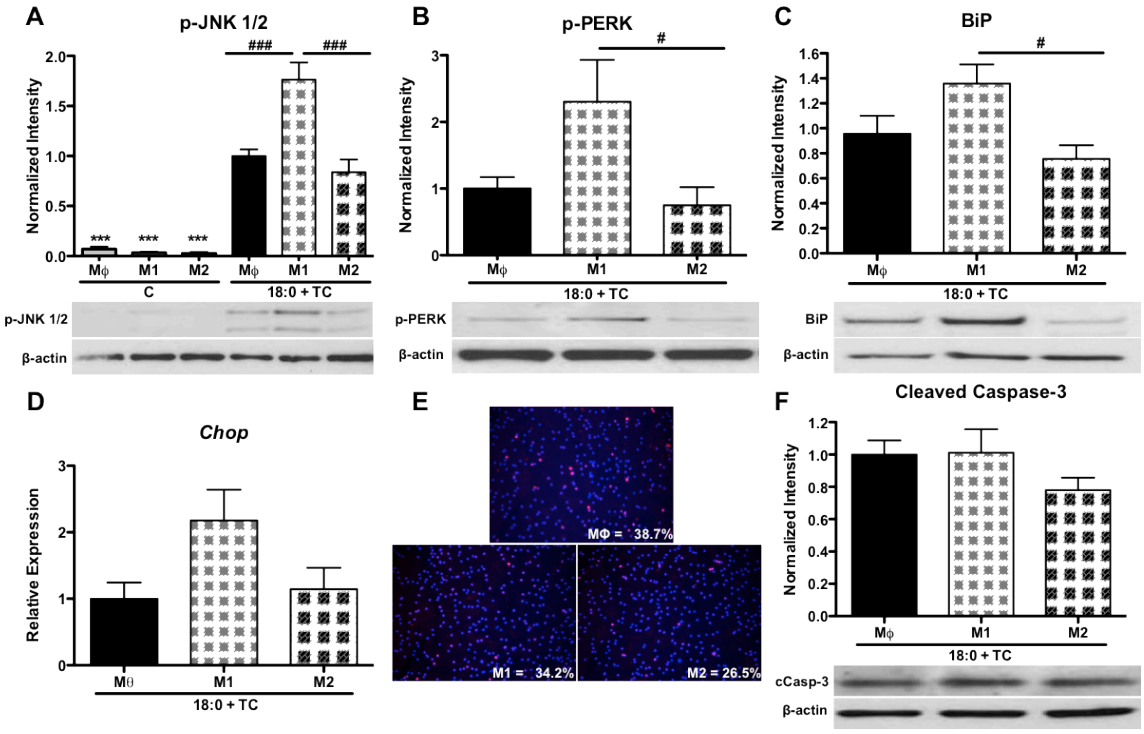

Figure 3.10: Polarization of MPMs to an M1 phenotype increases susceptibility to inflammation and ER stress in response to intracellular stearic acid accumulation. MPMs were polarized for 24 h with vehicle, LPS (10 ng/ml), or IL-13 (4 ng/ml) to induce a Mθ, M1, or M2 phenotype, respectively. Cells were then co-treated with stearic acid (18:0, 90 μM) and TC (2.5 μM) for 16 h in the presence of polarization agents. Controls were treated for 40 h with polarizing agents in the absence of stearic acid and TC. A-C) Western blot analysis for: A) phospho-JNK 1/2, B) phospho-PERK, C) BiP. D) Gene expression analysis of *Chop* mRNA by real-time RT-PCR. E) Detection of apoptotic cells by TUNEL (red) and DAPI (blue) staining. Magnification: 20X. F) Western blot analysis of cleaved caspase-3. Data are presented as mean ± SEM. n = 5-9/group. *** p<0.001 compared to Mθ of 18:0 + TC group, # p<0.05, ### p<0.001 compared to M1 of 18:0 + TC group.

Activation of lipolysis in the AT of obese mice does not modulate ER stress, inflammation, or apoptosis in the macrophage-enriched stromal vascular fraction

If macrophages residing in metabolic tissues, such as AT, undergo FFA-induced ER stress and apoptosis, it would be expected that activation of AT lipolysis would increase the exposure of macrophages to FFAs and, thus, activate these signaling pathways. To test this hypothesis, mice were fed a HF diet for 9 weeks and subsequently injected with CL316243, a β-3 adrenergic receptor agonist known to stimulate AT lipolysis (See Figure 3.11A for Study Design). Exposure to CL316243 resulted in a sustained ~4-fold increase in serum FFA levels throughout the time-course of the study ($p<0.001$ compared to saline-treated, Figure 3.11B), indicating that AT lipolysis was activated. Of note, this treatment did not modulate body weight (Figure 3.11C). To determine if increased AT lipolysis modulated ER stress and apoptotic signaling in resident macrophages, the macrophage-enriched SVF of the AT was isolated. Western blot analysis demonstrates that CL316243 treatment does not increase markers of ER stress (Figure 3.12A-C) or apoptosis (Figure 3.12D-F) in the SVF. Additionally, phosphorylation of JNK 1/2, a pro-inflammatory kinase, was not modulated (Figure 3.12C). These data indicate that activation of AT lipolysis does not induce ER stress, inflammation, or apoptosis in macrophages residing in AT.

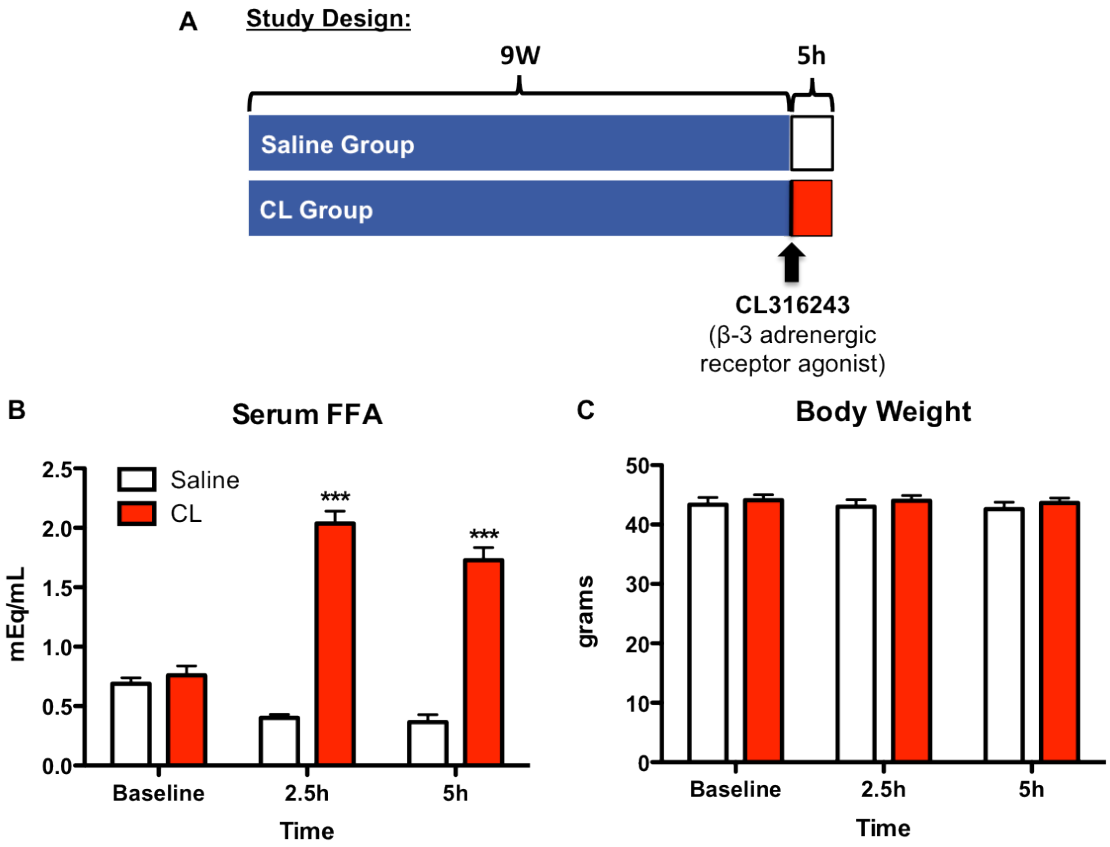

Figure 3.11. Administration of the β-3 adrenergic receptor agonist, CL316243, increases serum FFA concentrations in obese mice. A) Study design: mice were placed on a 60% high fat diet for 9 weeks and intraperitoneally injected with CL316243 (0.4 mg/kg) 5 h before sacrifice. B) Serum FFA concentrations at baseline, 2.5 h, and 5 h after injection. C) Body weight. Data are presented as mean ± SEM. n = 10/ group. *** treatment effect, $p<0.001$.

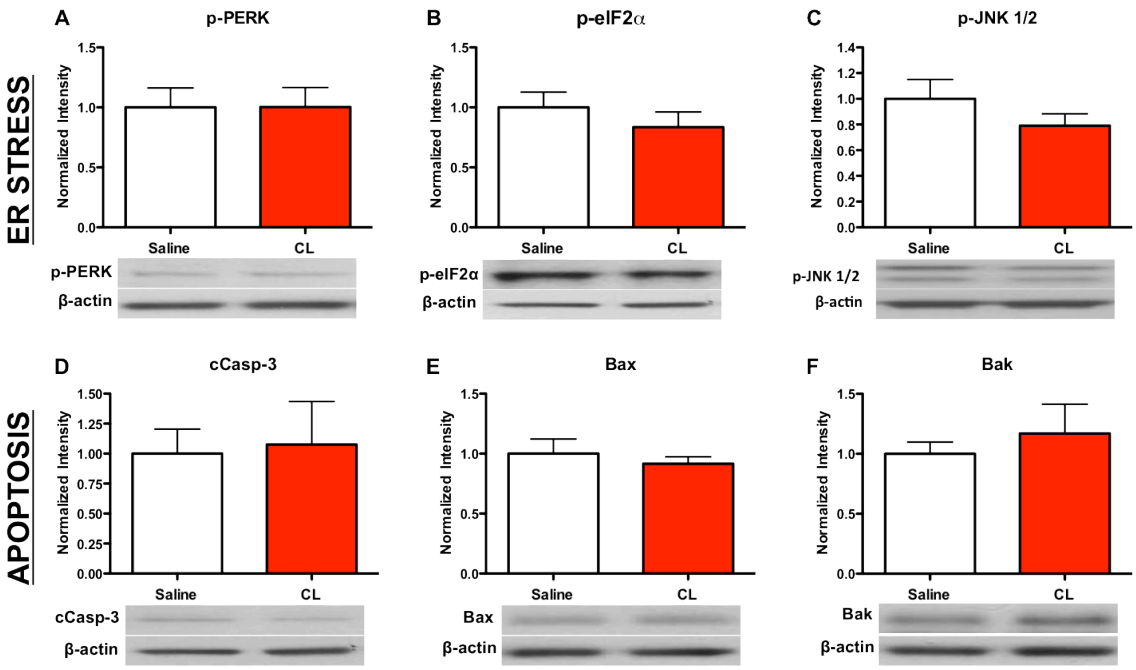

Figure 3.12. Activation of AT lipolysis in obese mice does not modulate SVF ER stress or apoptosis. Obese mice were injected with CL316243, as described in Figure 3.11. A-C) Western blot analysis for ER stress markers in the SVF: A) phospho-PERK, B) phospho-eIF2α, C) phospho-JNK 1/2. D-F) Western blot analysis of apoptotic markers in the SVF: D) cleaved caspase-3, E) Bax, and F) Bak. Data are presented as mean ± SEM. n = 10/ group.

DISCUSSION

Our previous studies have demonstrated that co-treatment of MPMs with low-level stearic acid and TC blocks ACSL activity, thus inducing intracellular FFA accumulation and lipotoxicity (169). Using this model, we now show that stearic acid accumulation in macrophages activates ER stress, inflammation, and apoptosis independent of TLR4/2 signaling. While exposure of macrophages to higher concentrations of stearic acid induced ER stress, inflammation, and apoptosis (Figure 3.3), exposure to low-level stearic acid in the absence of TC had no effect on these parameters (Figure 3.1), suggesting that intracellular accumulation of stearic acid accelerates lipotoxicity. It is possible that the ability of a macrophage to metabolize or store stearic acid is overwhelmed by higher concentrations of stearic acid, thus leading to intracellular FFA accumulation and lipotoxicity. Together, the PBA and SS studies demonstrate that stearic acid accumulation in MPMs initiates inflammatory signaling that culminates in the activation of ER stress-mediated apoptosis. Additionally, polarization of macrophages to a pro-inflammatory M1 phenotype increased stearic acid-induced inflammation and ER stress, but not apoptosis (See Figure 3.13 for Model).

These findings imply that macrophages residing in metabolic tissues such as AT, may be susceptible to FFA-induced inflammation, ER stress, and apoptosis. However, activation of AT lipolysis did not modulate these signaling pathways in the macrophage-enriched SVF of the AT, suggesting that these pathways may not be activated in ATMs during obesity. Instead, it is possible that

these *in vitro* findings may be more relevant to CVD and the development of atherosclerosis. Indeed, intracellular FFA accumulation (156) and ER stress-mediated apoptosis are observed in macrophages of atherosclerotic lesions (157; 166).

Research conducted in the past several decades has established a role for saturated FFAs in the development of CVD (72; 73). Additionally, recent studies indicate that macrophages of atherosclerotic plaques accumulate FFAs (154-156); however, the molecular consequences of intracellular FFAs remain relatively unknown. Increased partitioning of FFA to TG (via DGAT-1 overexpression) protects macrophages from FFA-induced inflammation (172), suggesting that accumulation of FFAs, rather than TG, in these immune cells may be responsible for inflammatory signaling. Our results support these findings and indicate that intracellular FFAs may be especially pathogenic, as blocking the incorporation of stearic acid into TG (through inhibition of ACSL activity) greatly increases the intracellular accumulation and lipotoxic potential of this FFA. Interestingly, studies have shown that polymorphisms in ACS genes, including ACSL-1 and medium-chain acyl-CoA synthetase 2, confer an increased risk for metabolic syndrome in human subjects (173; 174). Although the direct functional consequences of polymorphisms in these ACS genes are not known, it is believed that disruption of ACS activity is responsible for the increased risk for metabolic syndrome. Several studies have shown that insulin sensitizing thiazolidinediones (TZD) increase the transcription of ACSL-1 (the primary ACS isoform in macrophages) in the AT and liver (175; 176). Together with our current

data, these studies demonstrate that FFA accumulation occurs in plaque macrophages and may exacerbate inflammation during obesity/hyperlipidemia.

Previous studies have shown that over-activation of ER stress signaling can culminate in apoptotic cell death (163). Our results demonstrate that reducing ER stress signaling (via PBA) also abrogates apoptosis, indicating that stearic acid accumulation in MPMs induces ER stress-mediated apoptosis. Surprisingly, treatment with 6 mM PBA during stearic acid accumulation only decreased ER stress activation by 50%. This finding is in contrast to previously published studies showing that 3 mM PBA is sufficient to eliminate ER stress caused by extracellular exposure to high levels of palmitic acid (168). These results imply that intracellular and extracellular saturated FFAs may activate ER stress pathways by different mechanisms. Because correction of the protein folding defect only partially reduces the activation of UPR proteins, it is interesting to speculate that intracellular stearic acid accumulation may alter the composition of the ER membrane to activate ER stress signaling independently of an increase in unfolded proteins. In support of this hypothesis, a recent paper has shown that alterations in the lipid composition of the ER membrane during obesity results in inhibition of sarco/endoplasmic reticulum calcium ATPase activity, thus initiating ER stress signaling (177).

Activation of ER stress pathways has been shown to initiate inflammation through JNK and NF-κB (161; 162). However, in the current study, reducing ER stress during FFA accumulation in macrophages had no effect on inflammatory cytokine expression (Figure 3.4). Interestingly, PBA co-treatment was sufficient

to decrease the expression of the chemokine, *Ccl2*. These findings indicate that intracellular stearic acid activates inflammatory signaling independent of the ER stress response, whereas *Ccl2* expression is dependent upon ER stress signaling. Inhibition of inflammation by co-treatment with SS demonstrated that the inflammation generated by stearic acid accumulation initiates ER stress-mediated apoptosis, suggesting that inflammation is the main driving force for the lipotoxic effects of intracellular FFA accumulation.

Our data point to the importance of FFA-induced inflammation in activating macrophage ER stress and apoptosis. Some have suggested that saturated FFAs directly activate TLR4 or TLR2 (152; 153). However, our data support recent reports indicating that FFAs may not act through these pattern recognition receptors (48). We have shown that intracellular stearic acid accumulation potently activates inflammation, ER stress, and apoptosis in WT, TLR4-KO, and TLR2-KO macrophages. Additionally, low-level stearic acid in the absence of TC does not result in either FFA accumulation or inflammation. If cell surface TLR signaling were involved, extracellular exposure to stearic acid (as opposed to intracellular accumulation) should be a more potent activator of inflammation.

Interestingly, a recent study reported that saturated FFAs initiate inflammation by modifying the composition of the cell membrane rather than acting through extracellular receptors (178). Holzer and colleagues show that saturated FFAs alter the localization and activity of c-Src, a membrane-anchored tyrosine kinase involved in the activation of inflammation (178). Exposure of fibroblasts to palmitic or stearic acid partitions c-Src into intracellular lipid rafts

where the active kinase phosphorylates JNK, leading to inflammation (178). It is possible that c-Src also plays a role in saturated FFA-mediated inflammation in macrophages. In fact, c-Src is activated in macrophages of human atherosclerotic lesions and may contribute to plaque inflammation and instability (179).

Although the exact molecular mechanisms by which FFA accumulation leads to macrophage inflammation are not entirely understood, it is well accepted that pro-inflammatory M1 macrophages aberrantly accumulate in atherosclerotic lesions (150; 151), AT (180; 181), and liver (149), and during obesity. We have shown that polarization to an M1 phenotype increases the susceptibility of macrophages to stearic acid-induced inflammation and ER stress when compared to anti-inflammatory M2 macrophages. Our data demonstrate that FFA-induced inflammation is responsible for the initiation of macrophage ER stress (Figure 3.6). Therefore, the increased susceptibility of M1 macrophages to stearic acid-induced ER stress is likely due to increased inflammatory signaling in the presence of LPS. Although M1 polarization augmented inflammation and ER stress activation during stearic acid accumulation, there was no significant difference in the expression of apoptotic markers between M1 and M2 macrophages. Recent studies have demonstrated that engagement of TLRs reduces apoptotic cell death in response to ER stress by promoting the up-regulation of the guanine nucleotide exchange factor, eIF2B (182; 183). It is possible that this process also occurs when macrophages are polarized to an M1 phenotype. Thus, M1 macrophages would be protected from accelerated

apoptosis even in the presence of elevated ER stress signaling during FFA accumulation. These findings could suggest that M1 macrophages are particularly pathogenic because they resist apoptotic cell death and continue to secrete inflammatory cytokines into their local environment. This hypothesis will be explored in the next chapter.

ER stress activation and inflammation is observed in atherosclerotic lesions of obese/hyperlipidemic mice and humans (157; 166). Inflammatory M1 macrophages are recruited to these lesions during obesity and contribute to the development of CVD (150; 151). Our data suggest that FFA accumulation in macrophages residing in atherosclerotic plaques may play an essential role in the pathogenesis of obesity-related disorders. However, control of these signaling pathways appear to be different in macrophages residing in the AT, as activation of lipolysis does not modulate SVF ER stress or apoptosis. In support of this idea, recent studies have shown that AT foam cells (BODIPY-positive macrophages) are not significantly more inflammatory that non-lipid loaded ATMs (Shoelson and Glass, unpublished data). The above data indicate that activation of lipolysis does not increase ATM ER stress or apoptosis; however, in Chapters IV and V of this dissertation, will determine if obesity or weight loss modulates ER stress and apoptotic signaling in ATMs.

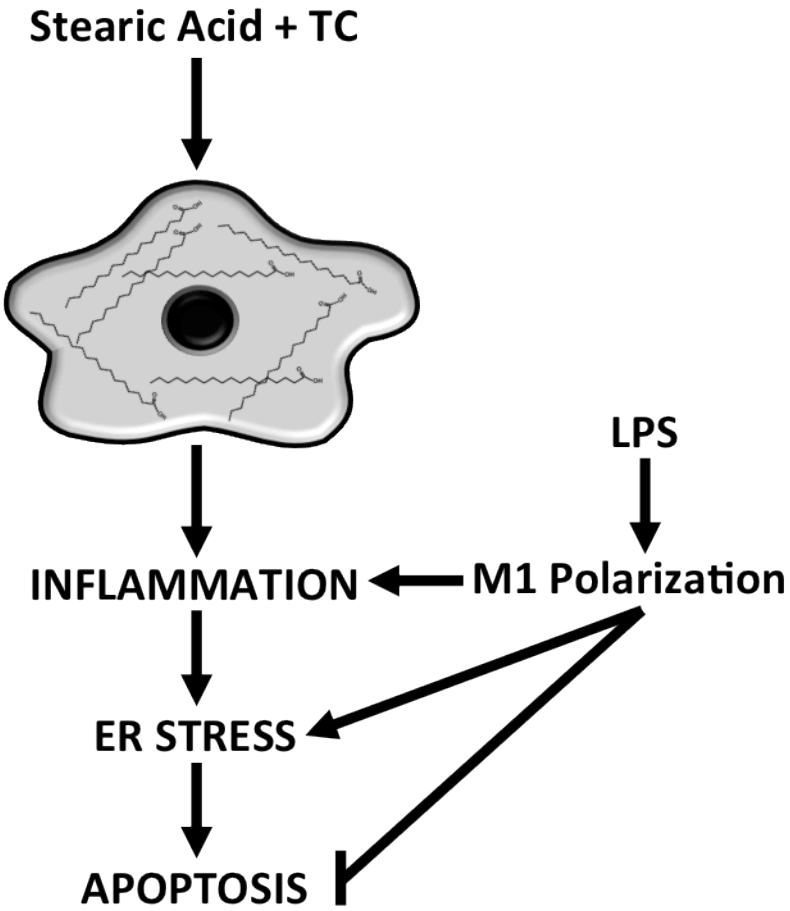

Figure 3.13: Consequences of Stearic Acid Accumulation in MPMs. Co-treatment of MPMs with stearic acid and TC increases intracellular stearic acid content, leading to TLR4/2-indepenedent inflammatory signaling. This inflammation results in ER stress-mediated apoptosis of macrophages. Polarization of MPMs to a pro-inflammatory M1 phenotype increases the susceptibility of the macrophages to inflammation and ER stress, but not apoptosis, during stearic acid accumulation.

CHAPTER IV

ATM apoptosis as a potential recruitment-independent mechanism regulating AT homeostasis

INTRODUCTION

In 2003, two seminal papers demonstrated that macrophages accumulate in AT during obesity (34; 35). ATM number is positively correlated with increasing adiposity, systemic inflammation, and IR, suggesting that these immune cells play an essential role in the pathogenesis of obesity (184). Recent findings demonstrate a role for additional immune cell subsets, including T cells (110; 113; 116; 118; 130; 185), B cells (117; 131), mast cells (104; 105), eosinophils (103), and neutrophils (107; 108) in the control of AT inflammation. However, macrophages are the most prevalent immune cell type in the AT and are a major source of inflammatory cytokines and chemokines secreted from the AT during obesity (1; 34; 35; 82). As a result of these discoveries, the immune system has come to the forefront of obesity research and much effort has been focused on determining mechanisms by which macrophages accumulate in obese AT.

Expression of many chemokines and chemokine receptors is increased in the AT of obese mice (35; 78-81). Additionally, labeling studies have shown that obesity results in recruitment of monocytes from the bone marrow to the AT (40). Therefore, the majority of published studies have sought to determine whether reducing the chemoattractant potential of AT can inhibit ATM accumulation

during obesity. However, in several instances, obese mice genetically lacking certain chemokines or chemokine receptors exhibit no metabolic abnormalities or change in ATM number (84; 95; 186). Additionally, even in studies showing that deficiency or antagonism of chemokines decreases ATM number during obesity, macrophage accumulation during HF diet feeding is never completely abolished (40; 187-191). These findings suggest that recruitment-independent mechanisms may also contribute to the accumulation of pro-inflammatory macrophages in the AT during obesity.

Since the original description of programmed cell death (143), it has become increasingly clear that proper control of apoptosis is essential for the homeostatic maintenance of cell number in many tissues (144). For example, accelerated apoptosis is observed in neurodegenerative disorders, while impaired apoptosis can contribute to tumorigenesis, autoimmunity, and inflammatory disorders (192). Interestingly, several recent studies have suggested that apoptosis of ATMs may decrease obesity-associated IR. Treatment with pioglitazone, a PPAR-γ agonist known to promote insulin sensitivity, increases apoptosis in human ATMs and decreases ATM content (193; 194). Additionally, clodronate-induced apoptosis of ATMs increases insulin sensitivity in obese mice (195). These findings demonstrate that pharmacological activation of ATM apoptosis decreases IR during obesity; however, it is not known whether macrophage apoptosis is modulated in AT during obesity.

In this study, we show that macrophage apoptosis occurs in AT of lean tissue, suggesting that this process could regulate ATM number. In support of

this hypothesis, ATM apoptosis is drastically decreased by diet-induced or genetic obesity and is “re-activated” during weight loss. The negative correlation between ATM apoptosis and macrophage number in AT suggests that ATM apoptosis is a metabolically regulated process that contributes to the recruitment-independent accumulation of macrophages locally in the AT.

RESULTS

Metabolic phenotype of diet-induced obese mice

To determine the impact of obesity on ATM apoptosis, mice were fed a 10% LF or a 60% HF diet for 9 weeks (Figure 4.1A). As expected, mice receiving the HF diet became obese (Figure 4.1B), gained lean (Figure 4.1C) and fat mass (Figure 4.1D), and were slightly hyperglycemic (Figure 4.1E) compared to lean controls. Additionally, *Emr1* (F4/80) gene expression in the SVF of AT was significantly increased by obesity (~25-fold increase, $p<0.001$, Figure 4.1F), confirming that 9 weeks of HF diet feeding is sufficient to promote the accumulation of macrophages in AT (113).

Diet-induced obesity may increase whole AT apoptosis

Recent studies suggest that obesity increases apoptosis in whole AT (196), likely due to adipocyte cell death as a result of local hypoxia or decreased vasculature (66-68). Consistent with these findings, HF diet feeding increased the expression the pro-apoptotic proteins, Bak ($p<0.01$, Figure 4.2B) and Bax

($p<0.001$, Figure 4.2C) in the AT, but did not affect caspase-3 cleavage (Figure 4.2C). These data suggest that obesity may increase apoptosis in the whole AT; however, the metabolic regulation of apoptosis in AT-resident macrophages has not been explored.

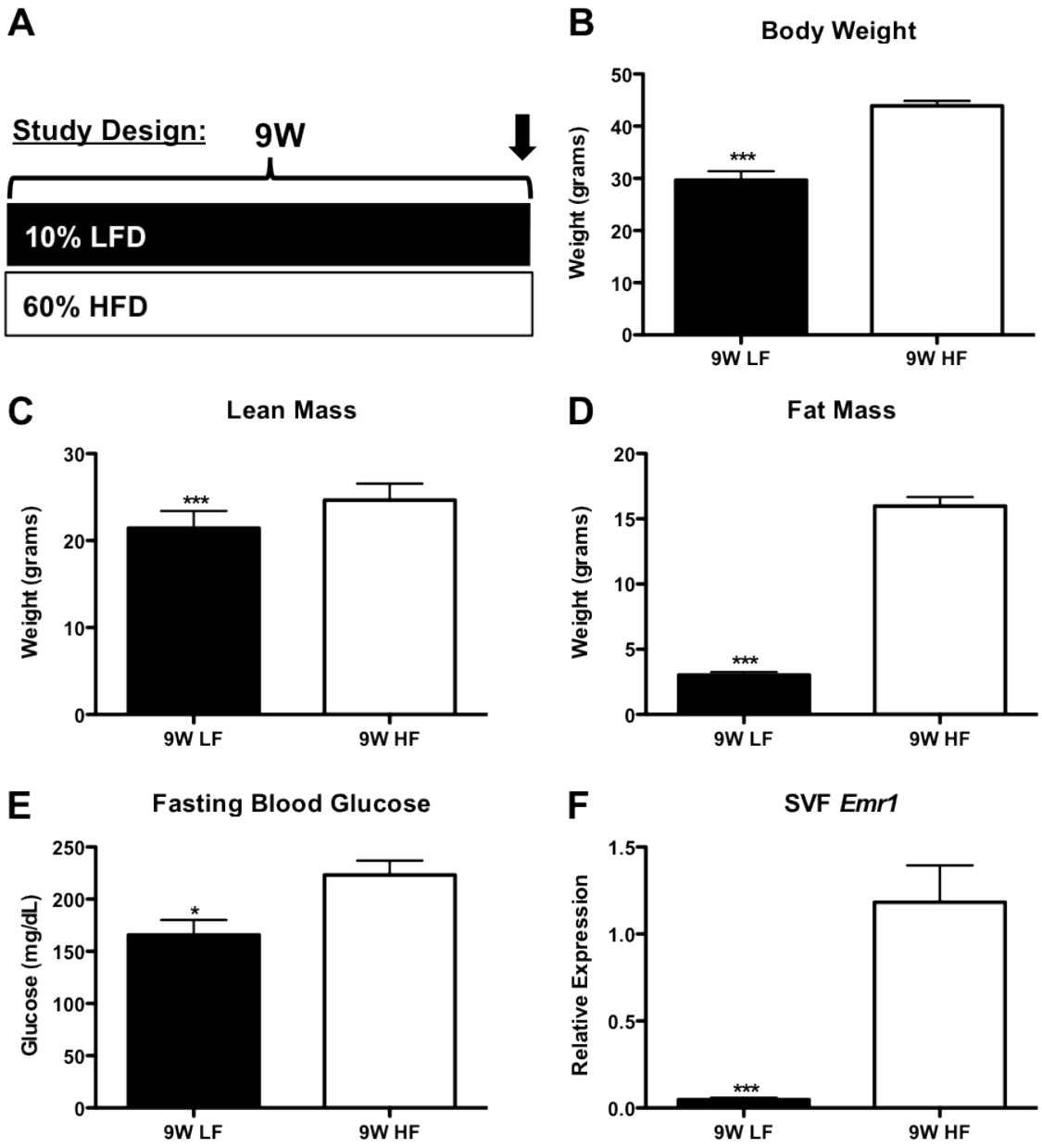

Figure 4.1: Metabolic phenotype of lean and obese mice. A) Study design: male C57Bl/6 mice were placed on a 10% LF diet or 60% HF diet for 9 weeks. B-E) Metabolic parameters were assessed at sacrifice: B) body weight, C) lean mass, D) fat mass, and E) fasting blood glucose concentrations. F) Real-time RT-PCR quantification of *Emr1* (F4/80) gene expression in the SVF of the AT. Data are presented as mean ± SEM, n = 11-12/group. * $p<0.05$, ** $p<0.01$, *** $p<0.001$ compared to 9W HF.

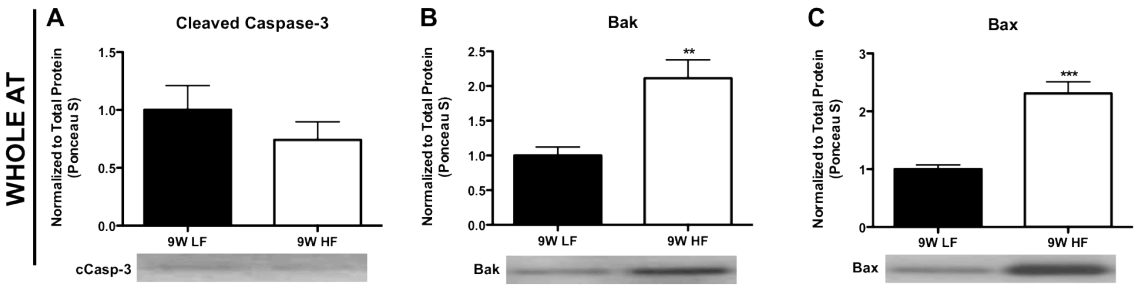

Figure 4.2: Obesity may increase apoptosis in whole AT. Male C57Bl/6 mice were placed on a 10% LF diet or a 60% HF diet for 9 weeks, as shown in Figure 4.1A. A-C: Whole AT was sonicated in 2% SDS and apoptotic markers were analyzed using Western blot: A) cleaved caspase-3, B) Bak, and C) Bax. Levels of specific proteins were normalized to total protein level, as measured by Ponceau S staining. Data are presented as mean ± SEM, n = 5/group. ** $p < 0.01$, *** $p < 0.001$ compared to 9W LF.

Diet-induced obesity decreases ATM apoptosis

To determine if obesity alters apoptotic signaling in ATMs, protein was isolated from the macrophage-enriched SVF of AT and assessed for apoptotic markers by Western blot analysis. Interestingly, obese mice demonstrated a 16-fold decrease in cleaved caspase-3 protein levels in the SVF ($p<0.001$ compared to 9W LF, Figure 4.3A), indicating that HF diet feeding drastically impairs AT immune cell apoptosis. Additionally, obesity decreased Bak protein levels in the SVF ($p<0.01$, Figure 4.3B), but did not modulate Bax expression (Figure 4.3C).

Although the SVF is a macrophage-enriched cell preparation, other leukocytes and pre-adipocytes are also contained within this fraction (34; 35; 197). To determine if obesity decreases apoptosis specifically in macrophages, AT was stained for F4/80, DAPI, and TUNEL. Interestingly, lean AT displayed high numbers of $F4/80^+$ $TUNEL^+$ apoptotic macrophages, while apoptotic macrophages were rarely observed in the AT of obese mice (Figure 4.3D). Quantification of confocal images demonstrated that nearly 25% of the macrophages in lean AT are apoptotic, while only 2.5% of macrophages in obese AT are $TUNEL^+$ ($p<0.001$, Figure 4.3E). Because obesity results in a striking increase in ATM content, it is possible that the same absolute numbers of macrophages undergo apoptosis in lean and obese AT. However, obesity also decreased the number of $F4/80^+$ $TUNEL^+$ apoptotic macrophages per high power field (Figure 4.3F). Additionally, the majority of apoptotic cells in the AT were $F4/80^+$ macrophages ($p<0.001$ compared to apoptotic $F4/80^-$ non-macrophage cells, Figure 4.3G), demonstrating that apoptosis occurs primarily in ATMs.

Nearly all of the apoptotic macrophages in lean AT were interstitially spaced, indicating that these cells are likely of an anti-inflammatory “M2” phenotype (Figure 4.3H). Interestingly, even in obese AT, the majority of apoptotic macrophages (~65%) were interstitially spaced, whereas only ~35% of apoptotic cells were localized to crown-like structures (Figure 4.3H). Taken together, these data indicate that apoptosis normally occurs in M2 macrophages in lean AT; however, this process is impaired as the AT becomes dysfunctional during obesity.

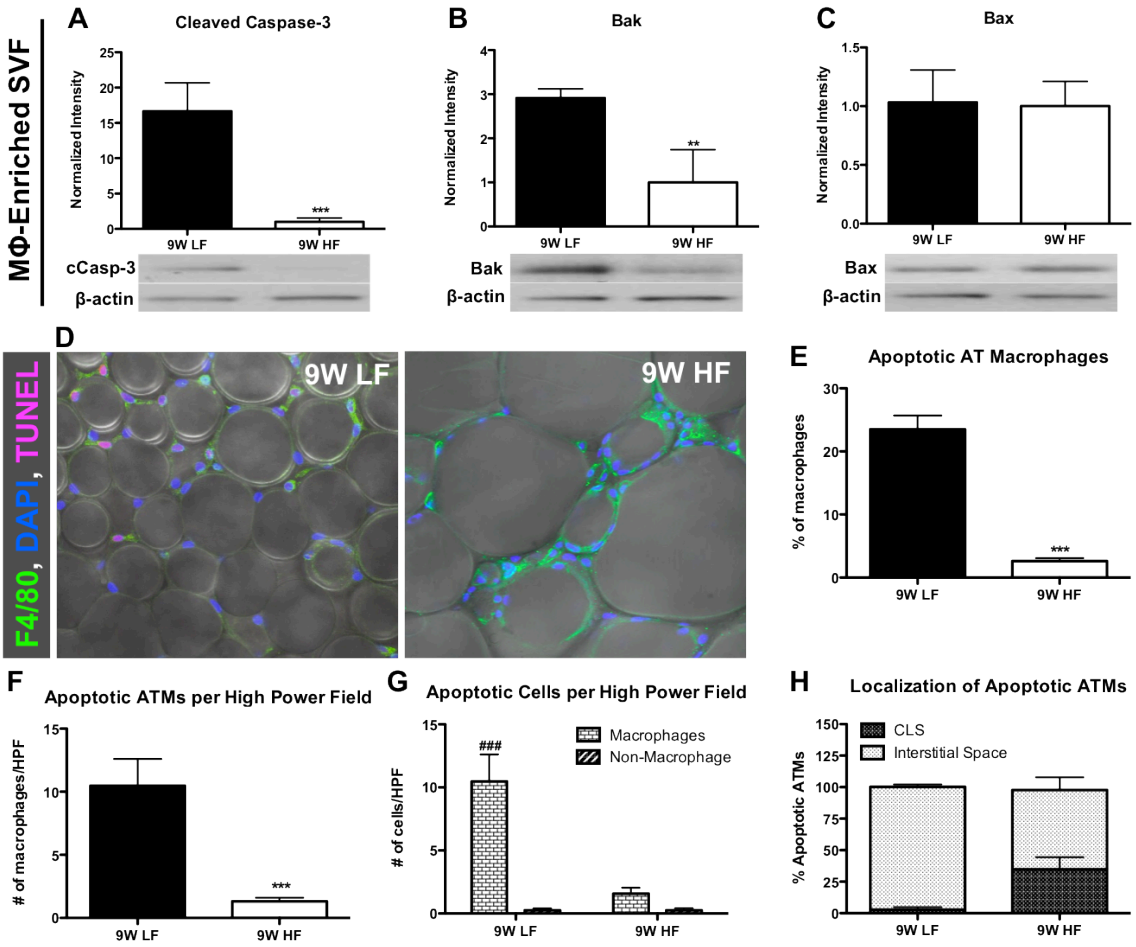

Figure 4.3: Diet-induced obesity decreases ATM apoptosis. Mice were placed on a 10% LF diet or 60% HF diet for 9 weeks, as described in Figure 4.1A. A-C) Western blot analysis of the macrophage-enriched SVF of the AT: A) cleaved caspase-3, B) bak, and C) bax. D-H) Confocal microscopy analysis to detect apoptotic macrophages using F4/80 (green), TUNEL (pink), and DAPI (blue) staining: D) Representative image from 9W LF and 9W HF groups. Magnification: 40X. Quantification of: E) the percent of macrophages that are apoptotic ($F4/80^+$, $TUNEL^+$), F) the number of apoptotic ATMs per high power field, G) the number of apoptotic macrophages ($F4/80^+$, $TUNEL^+$) versus non-macrophages ($F4/80^-$, $TUNEL^+$) per high power field, and H) localization of apoptotic ATMs in crown-like structures versus interstitial spaces. Data are presented as mean ± SEM, n = 6-8/group. ** p<0.01, *** p<0.001 compared to 9W HF; ### p<0.001 compared to non-macrophage.

Metabolic phenotype of genetically obese mice

Above, we demonstrated that diet-induced obesity decreased ATM apoptosis (Figure 4.3). To determine if this phenotype was the result of dietary composition or was due to overt obesity, we analyzed a mouse model of genetic obesity. Leptin-deficient ob/ob mice become obese on a standard chow diet, allowing for the analysis of the effects of obesity in the absence of a high fat, high calorie diet. Male ob/ob mice and lean littermate controls were maintained on a chow diet until 9-10 weeks of age (Figure 4.4A), at which point they were weight-matched with the HF diet-fed mice used previously (Figure 4.1B). As expected, ob/ob mice were obese compared to lean littermate control mice (Figure 4.4B), and the increase in body weight in the ob/ob mice was due to elevated fat mass, rather than lean mass (Figure 4.4C-D).

Genetic obesity decreases ATM apoptosis

To determine if genetic obesity decreases ATM apoptosis, the SVF of the AT was evaluated for apoptotic markers. Caspase-3 cleavage was significantly decreased in the SVF of ob/ob mice compared to lean controls (50% decrease, $p<0.01$, Figure 4.5A); however, Bak and Bax protein levels were not affected by genetic obesity (Figure 4.5B-C). AT was evaluated by confocal microscopy (as described above) to determine if genetic obesity decreased apoptosis specifically in macrophages. AT isolated from lean control mice displayed multiple $TUNEL^+$ apoptotic macrophages, while very few apoptotic cells were found in the AT of ob/ob mice (Figure 4.5D). Quantification of confocal images demonstrated that

macrophage apoptosis is significantly decreased in the AT of ob/ob mice compared to lean controls ($p<0.001$, Figure 4.5E-F). Additionally, almost all of the cells undergoing apoptosis in the AT of lean, chow-fed mice were F4/80$^+$ macrophages, rather than non-macrophage immune cells ($p<0.001$ compared to non-macrophages, Figure 4.5G). The majority of apoptotic macrophages were localized to interstitial spaces, rather than crown-like structures (Figure 4.5H), indicating that these cells are likely of an M2 phenotype. Thus, both diet-induced and genetic obesity result in decreased ATM apoptosis.

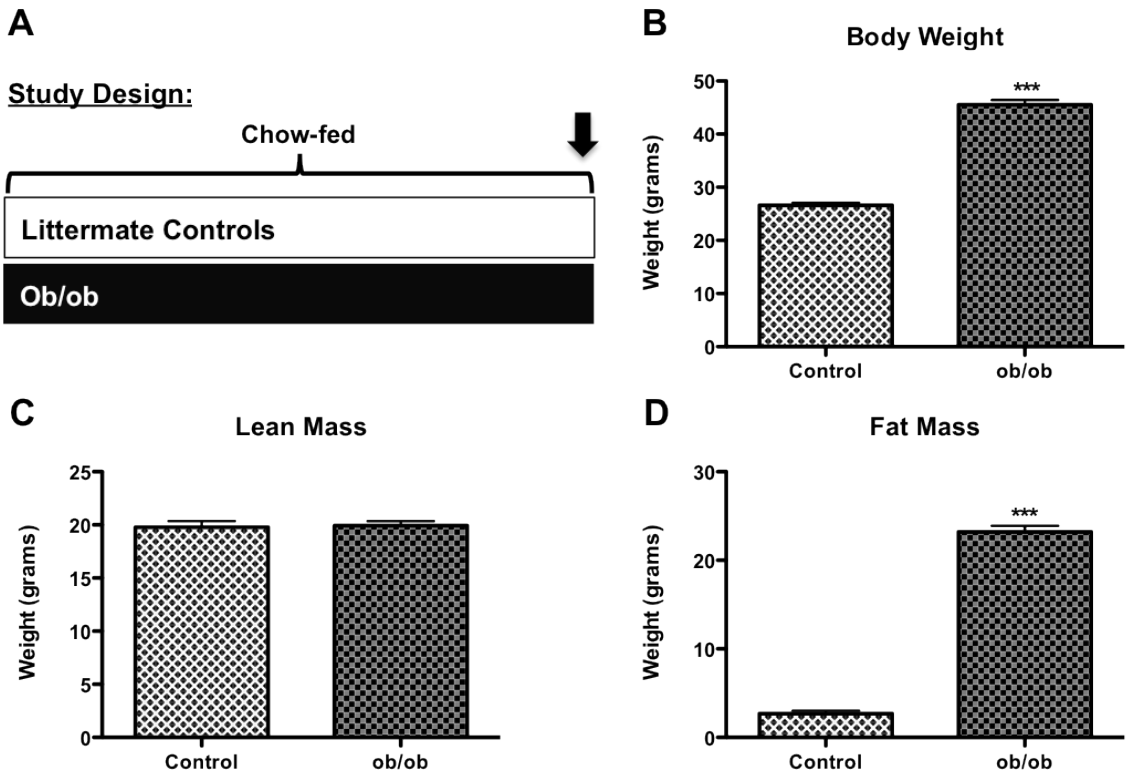

Figure 4.4: Metabolic phenotype of control and ob/ob mice. A) Study design: male ob/ob and littermate control mice were maintained on a standard rodent chow diet until 9-10 weeks of age. B-D) Metabolic parameters were assessed at sacrifice: B) body weight, C) lean mass, and D) fat mass. Data are presented as mean ± SEM, n = 8/group. *** $p<0.001$ compared to control.

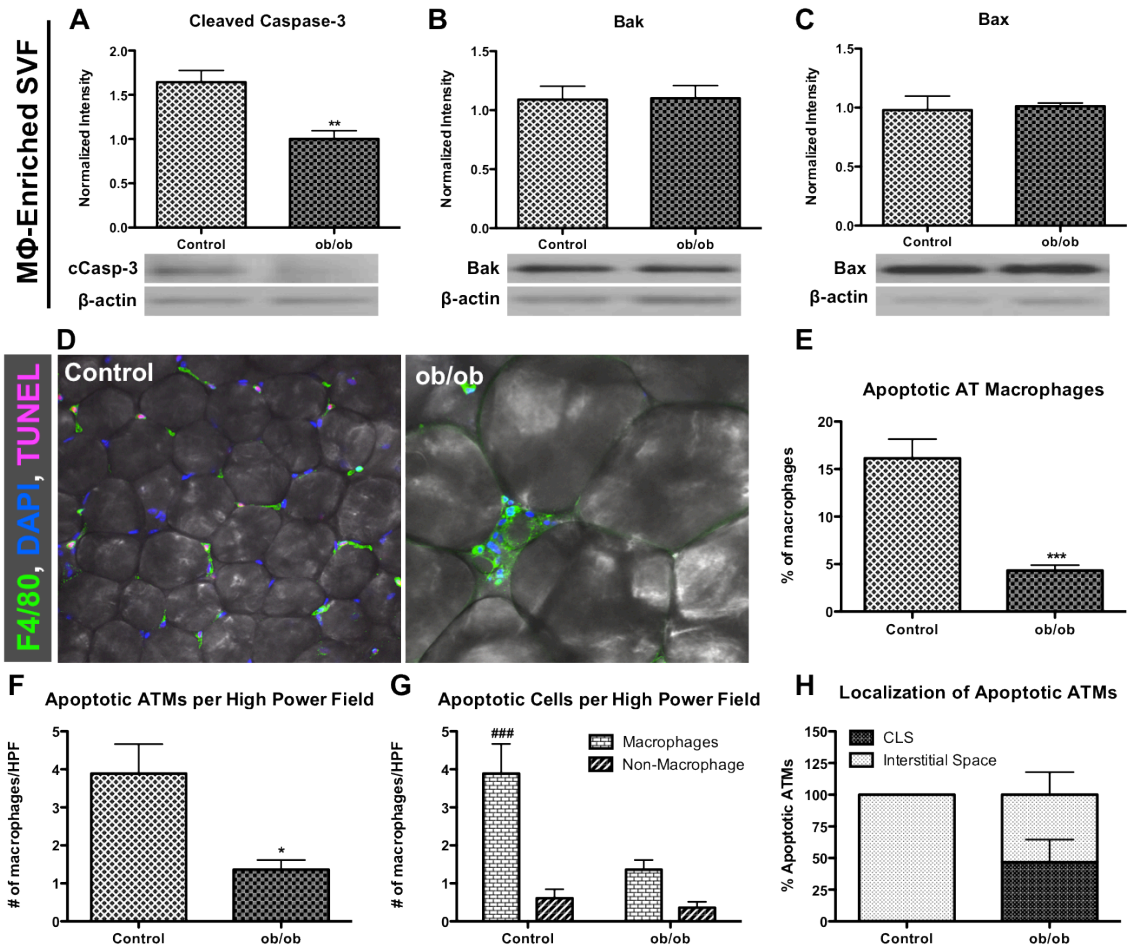

Figure 4.5: Genetic obesity decreases ATM apoptosis. Ob/ob and littermate control mice were maintained on a chow diet until 9-10 weeks of age, as described in Figure 4.6A. A-C) Western blot analysis of the macrophage-enriched SVF of the AT: A) cleaved caspase-3, B) bak, and C) bax. D-H) Confocal microscopy analysis to detect apoptotic macrophages using F4/80 (green), TUNEL (pink), and DAPI (blue) staining: D) Representative image from control and ob/ob groups. Magnification: 40X. Quantification of: E) the percent of macrophages that are apoptotic ($F4/80^+$, $TUNEL^+$), F) the number of apoptotic ATMs per high power field, G) the number of apoptotic macrophages ($F4/80^+$, $TUNEL^+$) versus non-macrophages ($F4/80^-$, $TUNEL^+$) per high power field, and H) localization of apoptotic ATMs in crown-like structures versus interstitial spaces. Data are presented as mean ± SEM, n = 5-6/group. * $p<0.05$, ** $p<0.01$, *** $p<0.001$ compared to control; ### $p<0.001$ compared to non-macrophage.

Metabolic phenotype of weight loss mice

The above findings indicate that ATM apoptosis is a metabolically regulated process. Therefore, weight loss would be expected to "re-activate" apoptotic signaling within ATMs. To test this hypothesis, mice were placed on a HF diet for 9 weeks, and then switched to a LF diet for 1 week to promote weight loss (Figure 4.7A). These "weight loss" mice, referred to as 1W S in the figures, were compared to the mice that had been maintained on a HF diet for 9 weeks. The diet-switch model of weight loss decreased body weight ($p<0.01$, Figure 4.6B), fat mass ($p<0.001$, Figure 4.6 D), and fasting blood glucose concentrations ($p<0.001$, Figure 4.6E), but did not significantly impact lean body mass (Figure 4.6C). Additionally, there was a trend towards a decrease in SVF F4/80 gene expression after 1 week of weight loss (Figure 4.6F).

Weight loss increases ATM apoptosis

AT was isolated from obese and weight loss mice and analyzed for apoptotic macrophages by confocal microscopy. As previously shown (Figure 4.3D), very few $TUNEL^+$ macrophages were found in the AT of obese mice (Figure 4.3D and Figure 4.7A). However, weight loss increased the number of $F4/80^+$ $TUNEL^+$ apoptotic ATMs ($p<0.001$, Figure 4.7A-D). Again, the majority of apoptotic macrophages were interstitially spaced (Figure 4.7E). In addition, protein levels of Bax ($p<0.05$, Figure 4.7F) and Bak ($p = 0.065$, Figure 4.7G) were increased in the SVF during weight loss. These findings indicate that weight loss increases ATM apoptosis to levels similar to what is seen in lean AT.

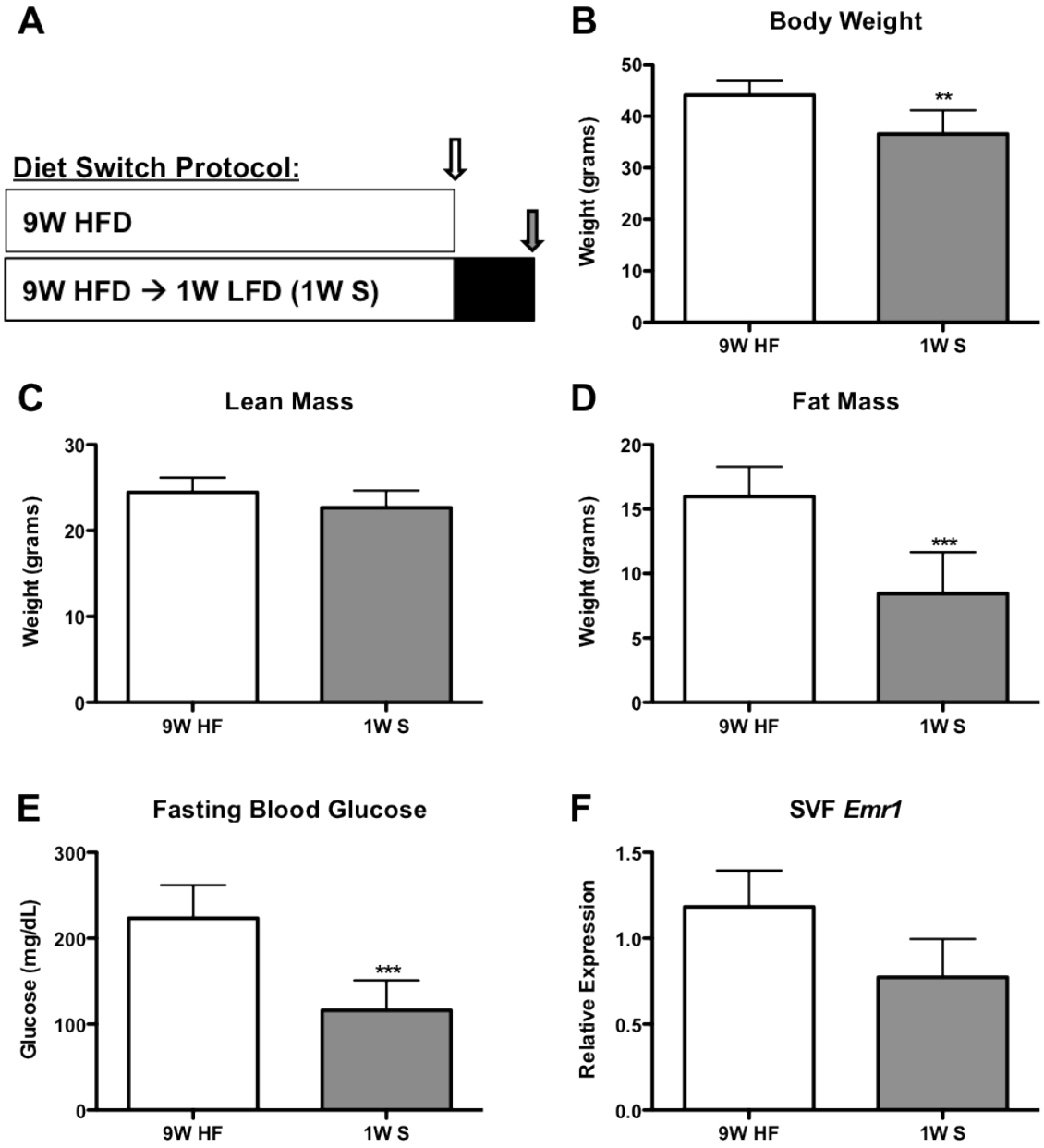

Figure 4.6: Metabolic phenotype of weight loss mice. A) Study design: male C57Bl/6 mice were placed on a 60% HF diet for 9 weeks. One group was sacrificed at this time-point, while the remaining mice were switched to a 10% LF diet for 1 week to promote weight loss. B-E) Metabolic parameters were assessed at sacrifice: B) body weight, C) lean mass, D) fat mass, and E) fasting blood glucose concentrations. F) Real-time RT-PCR quantification of *Emr1* gene expression in the SVF of the AT. Data are presented as mean ± SEM, n = 9-10/group. ** $p<0.01$, *** $p<0.001$ compared to 9W HF.

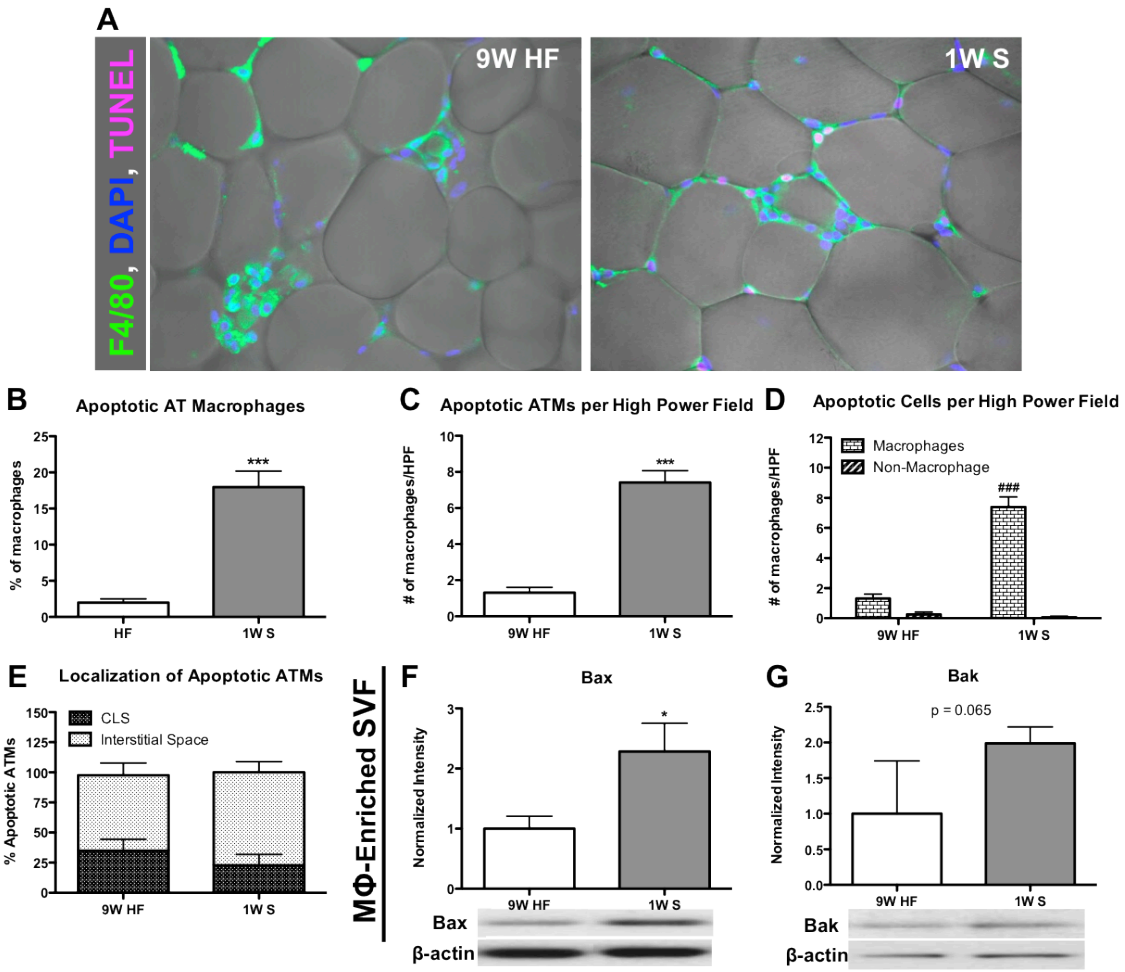

Figure 4.7: Weight loss increases ATM apoptosis. Mice were placed on the diet-switch protocol, as described in Figure 4.8A. A-E) Confocal microscopy analysis to detect apoptotic macrophages using F4/80 (green), TUNEL (pink), and DAPI (blue) staining: A) Representative image from 9W HF and 1W S groups. Magnification: 40X. Quantification of: B) the percent of macrophages that are apoptotic ($F4/80^+$, $TUNEL^+$), C) the number of apoptotic ATMs per high power field, D) the number of apoptotic macrophages ($F4/80^+$, $TUNEL^+$) versus non-macrophages ($F4/80^-$, $TUNEL^+$) per high power field, and E) localization of apoptotic ATMs in crown-like structures versus interstitial spaces. F-G) Western blot analysis of the macrophage-enriched SVF of the AT: F) bak and G) bax. Data are presented as mean ± SEM, n = 5-8/group. * $p<0.05$, *** $p<0.001$ compared to 9W HF; ### $p<0.001$ compared to non-macrophage.

Diet-induced obesity does not modulate apoptotic signaling in hepatocytes, liver-resident macrophages, or in the spleen

Above, we have shown that obesity increases whole AT apoptosis (Figure 4.2); however, ATM apoptosis is decreased during obesity (Figure 4.3). To determine if obesity modulates apoptosis in a similar manner in another metabolically relevant tissue, protein was isolated from liver hepatocytes and an F4/80-enriched non-parencymal fraction of lean and obese mice. Interestingly, markers of apoptosis, including protein levels of cleaved caspase-3, Bak, and Bak, were not modified by HF diet feeding in either the hepatocyte fraction (Figure 4.8) or the F4/80-enriched non-parenchymal fraction of the liver (Figure 4.9A-C). Additionally, obesity did not modulate apoptosis in the spleen, an immune cell-enriched organ (Figure 4.9D-F). Therefore, while obesity decreased apoptosis in AT-resident macrophages, this signaling pathway was not modulated in macrophages of the liver or in the spleen, indicating that this regulation is specific to the AT.

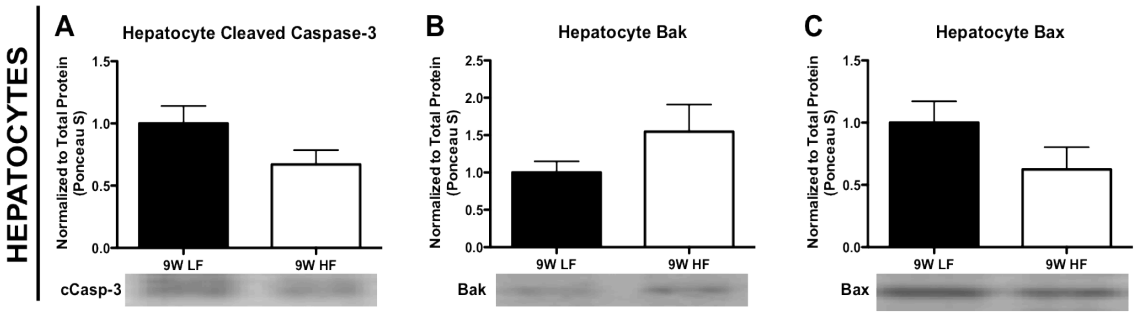

Figure 4.8: Obesity does not modulate apoptosis in the hepatocyte fraction of liver. Male C57Bl/6 mice were placed on a 10% LF diet or a 60% HF diet for 9 weeks, as shown in Figure 4.1A. A-C: The hepatocyte fraction of the liver was sonicated in 2% SDS apoptotic markers were analyzed using Western blot: A) cleaved caspase-3, B) bak, and C) bax. Levels of specific proteins were normalized to total protein level, as measured by Ponceau S staining. Data are presented as mean ± SEM, n = 6-9/group.

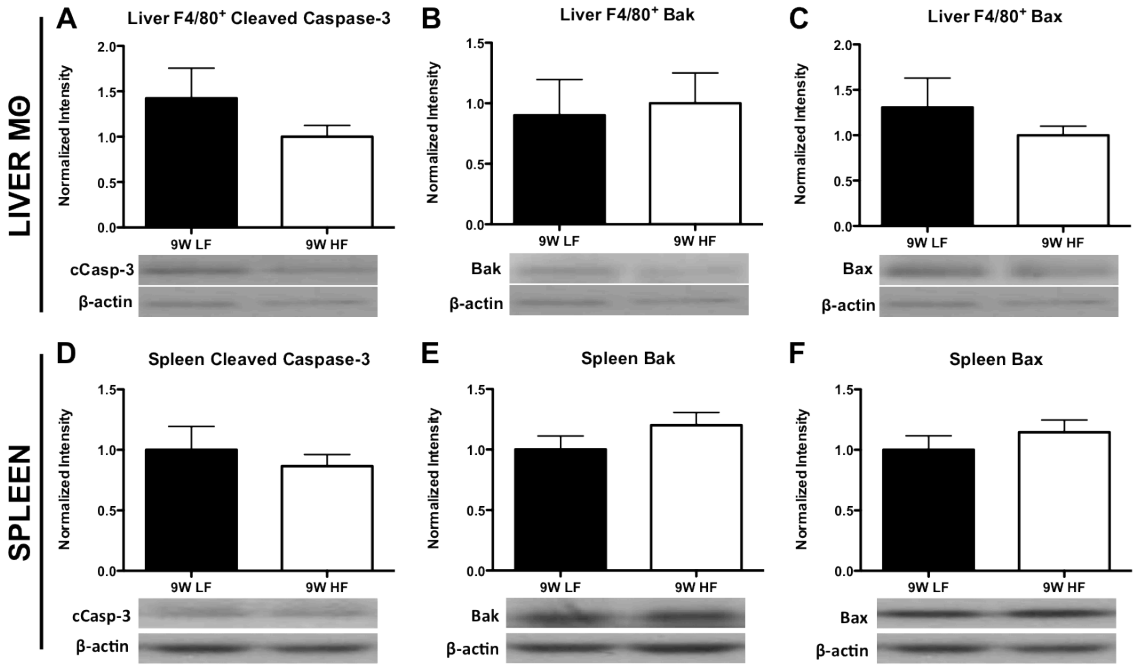

Figure 4.9: Obesity does not modulate apoptosis in an F4/80-enriched fraction of the liver or in the spleen. Male C57Bl/6 mice were placed on a 10% LF diet or a 60% HF diet for 9 weeks, as shown in Figure 4.1A. A-C: The non-parenchymal fraction of the liver was enriched for F4/80$^+$ macrophages using magnetic beads. Western blot analysis was performed for markers of apoptosis: A) cleaved caspase-3, B) bak, and C) bax. D-F: Whole spleen was sonicated in 2% SDS and Western blot analysis was performed: D) cleaved caspase-3, E) bak, and F) bax. Data are presented as mean ± SEM, n = 6-7/group.

Correlation between body weight, apoptotic ATMs, and ATM content

When combining the data from the lean, obese, and weight loss mice, it is apparent that the percentage of apoptotic macrophages in AT, but not liver, is inversely related to body weight (r^2 = 0.6477, $p<0.0001$) and positvely correlated with ATM content, as measured by SVF F4/80 gene expression (Figure 4.10, r^2 = 0.6585, $p<0.001$). Lean mice exhibit relatively high numbers of apoptotic ATMs and low F4/80 gene expression, while obese mice have very few apoptotic macrophages and high AT F4/80 gene expression (Figure 4.10). These findings suggest that macrophage apoptosis may be a recruitment-independent mechanism that contributes to the regulation of ATM number. Therefore, impaired macrophage apoptosis during obesity would increase the accumulation of these pro-inflammatory immune cells in the AT.

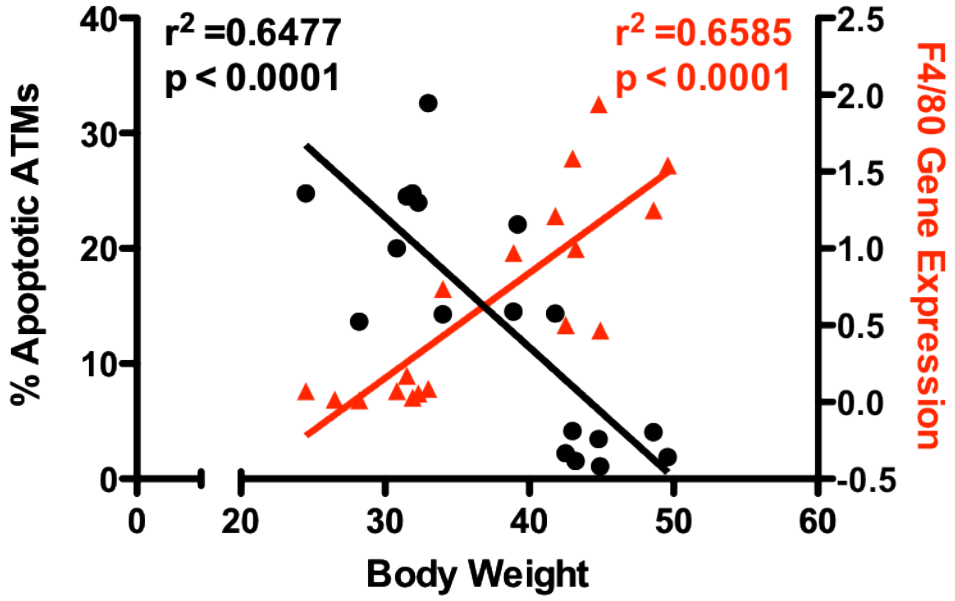

Figure 4.10: Correlation between body weight, apoptotic ATMs, and SVF F4/80 gene expression. Data from 9W LF, 9W HF, and 1W S mice. Negative correlation between body weight and ATM apoptosis (black). Positive correlation between body weight and SVF F4/80 gene expression (red).

DISCUSSION

During obesity, pro-inflammatory macrophages accumulate in metabolic tissues, including AT (34; 35), and contribute to obesity-associated IR both locally and systemically (36). Since this novel discovery, much effort has been focused on determining mechanisms by which macrophages accumulate in obese AT. The overwhelming majority of these studies have sought to establish whether recruitment of monocytes to the AT is responsible for the increase in ATM number during obesity. However, decreasing the chemoattractant potential of AT never completely abolishes macrophage accumulation in obese AT, suggesting that recruitment-independent mechanisms may also regulate ATM number. Here, we have shown that ATM apoptosis occurs in lean AT, is decreased during obesity, and is "re-activated" during weight loss. The negative correlation between macrophage apoptosis and ATM number suggests that macrophage apoptosis is a metabolically regulated process that contributes to the maintenance of AT homeostasis (Figure 4.11).

Compared to lean tissue, obese AT secretes high levels of various potent chemokines, including MCP-1 (78-81). Additionally, labeling studies have demonstrated that bone marrow-derived monocytes are recruited to the AT during obesity (40). Together, these studies have led to the hypothesis that increased recruitment of macrophage precursors to the AT is the sole mechanism leading to increased ATM number during obesity. However, many recent findings have called this concept into question. First, single gene deletion of multiple chemokines or chemokine receptors such as MIP-1α (95) and CXCR1

(94) does not modulate ATM number during HF diet feeding. Second, even in studies demonstrating that a chemokine or chemokine receptor plays a role in promoting macrophage accumulation in obese AT, ATM number is never normalized to levels observed in lean AT (81; 86-88). For example, deletion of CCR2, a key receptor for multiple chemokines, decreased macrophage number in obese AT by ~20-30%. However, CCR2 deficient mice still had approximately twice as many macrophages in their AT when compared to lean WT mice (81). Remarkably, this subtle decrease in ATM number due to CCR2 deficiency occurred despite a near absence of pro-inflammatory macrophage precursors in the blood of these mice (88; 99). Additionally, while increased macrophage number can be observed as early as 2 weeks after the initiation of HF diet feeding (131), studies in our laboratory (88) have shown that CCR2 deficiency does not decrease ATM content when compared to WT controls until much later (>20 weeks HF diet).

The disconnect between circulating blood monocyte number, chemokine/chemokine receptor deficiency, and ATM content suggests that recruitment-independent processes may also exist to regulate macrophage number. Potential mechanisms include increased proliferation of macrophages within the AT, decreased egress of macrophages from the AT to draining lymph nodes, or impaired ATM apoptosis during HF diet feeding (see Figure 1.3 in the Introduction section).

Interestingly, recent studies suggest that increasing macrophage apoptosis in the AT of obese mice and humans decreases the metabolic abnormalities associated with obesity. Feng, *et al*. have shown that activation of ATM apoptosis via treatment with liposomal clodronate decreased AT inflammation and improved systemic glucose tolerance and insulin sensitivity in a mouse model of obesity (195). Additionally, another study has reported that pioglitazone, an insulin sensitizing TZD, increased macrophage apoptosis in human AT, likely contributing to the reduced ATM number observed after treatment (193; 194). These findings demonstrate that activation of macrophage apoptosis in obese AT results in a physiologically relevant reduction in ATM content and decreased metabolic dysfunction. Therefore, the significant reduction in apoptosis observed in ATMs of obese mice likely leads to increased macrophage number in AT.

Additionally, our data contributes to this literature by demonstrating that ATM apoptosis is a metabolically regulated, recruitment-independent process that may modulate ATM number. In lean AT, macrophage apoptosis may allow for the normal turnover and removal of ATMs, thus maintaining tissue homeostasis. However, during obesity decreased ATM apoptosis, along with increased monocyte recruitment, could increase the accumulation of pro-inflammatory macrophages in AT, resulting in reduced insulin sensitivity. Additionally, weight loss increases ATM apoptosis, suggesting that macrophage

cell death may also be a mechanism to restore AT homeostasis during weight loss (Figure 4.11).

Currently, the processes regulating macrophage apoptosis in lean AT are not known. In Chapter V, we will determine whether ER stress signaling is upstream of ATM apoptosis in lean tissue. In addition, the mechanisms impairing ATM apoptosis during obesity have not been defined. Future studies not included in this dissertation will determine whether NF-κB activation in M1 polarized ATMs during obesity (198) is responsible for decreased macrophage apoptosis. NF-κB is well known for its pro-inflammatory properties (199); however, NF-κB is also a potent anti-apoptotic transcription factor (197). In addition, a recent study has shown that TLR4 engagement, and thus NF-κB activation, protects macrophages from ER stress-induced apoptosis (182; 183). Of note, the majority of apoptotic ATMs observed in our study were interstitially localized, indicating that they are likely M2, rather than M1, macrophages. These findings support the hypothesis that activation of NF-κB in M1 ATMs during obesity promotes the survival of these pro-inflammatory immune cells, thus increasing macrophage accumulation and IR in AT. Importantly, clinical trials to decrease NF-κB activation during obesity are currently underway (200). Preliminary results indicate that salicylate treatment reduces systemic inflammation and decreases fasting blood glucose concentrations (200), indicating improved metabolic control. It would be interesting to determine if, in addition to decreasing inflammation, salicylate treatment also promotes ATM apoptosis.

Taken together, the studies in this chapter demonstrate that ATM apoptosis is a metabolically regulated process that may contribute to the maintenance of AT homeostasis. Additionally, these findings indicate that recruitment-independent mechanisms also modulate ATM number during obesity. A further understanding of the relative contributions of monocyte recruitment, ATM proliferation, macrophage egress, and ATM apoptosis to the control of ATM number and inflammatory status could pave the way for the development of novel therapeutics targeting macrophages in obese AT.

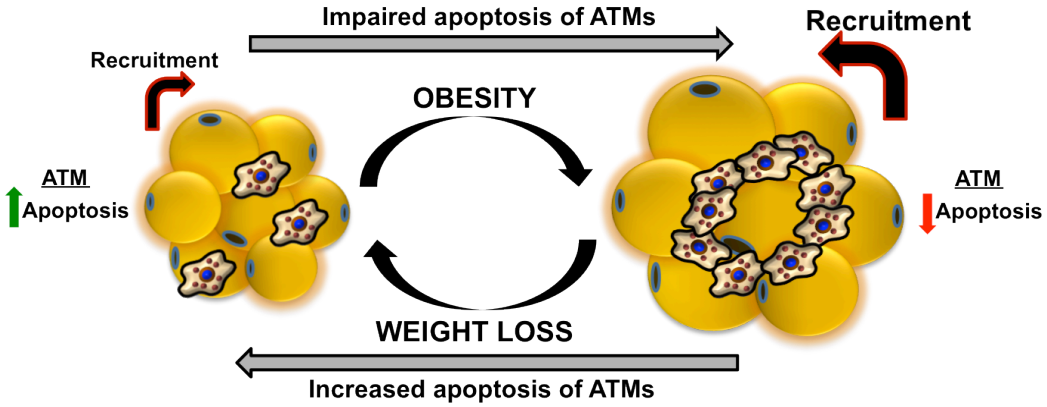

Figure 4.11: Apoptosis as a metabolically regulated mechanism to maintain and restore ATM homeostasis. Apoptosis may contribute to the normal regulation of macrophage number in lean AT. During obesity, ATM apoptosis is impaired, suggesting that macrophages are retained in the AT. This retention may contribute to macrophage accumulation in obese AT. Interestingly, ATM apoptosis is restored during weight loss. These findings suggest that macrophage apoptosis is a metabolically regulated process that contributes to the maintenance and restoration AT homeostasis. Impaired ATM apoptosis may lead to macrophage accumulation in obese AT.

CHAPTER V

Obesity decreases, while weight loss increases, stromal vascular fraction ER stress

INTRODUCTION

The first reports linking obesity and ER stress demonstrated that increased ER stress signaling in whole AT and liver contributes to the chronic low-grade inflammation associated with obesity (164; 167; 201; 202). In addition, blocking systemic ER stress activation using the chemical chaperone, PBA, improved tissue-specific and whole body insulin sensitivity (167). As a result of these novel findings, the concept that ER stress signaling in metabolic tissues is always detrimental has prevailed.

The above studies did not differentiate between ER stress activation in parenchymal cells (adipocytes and hepatocytes) and immune cells residing in these metabolic tissues. However, a recent study has attributed the increase in whole AT ER stress to the activation of this pathway in adipocytes, rather than macrophages (165). These data suggest that ER stress signaling may be differentially regulated in parenchymal cells versus non-parenchymal immune cells during obesity. Yet, the metabolic regulation and physiological role of AT immune cell ER stress has not been investigated.

Here, we show that, in contrast to whole AT, ER stress signaling is *decreased* in the macrophage-enriched SVF of AT during obesity. In addition,

weight loss re-activates SVF ER stress to levels near what is seen in lean mice. Although obesity increased ER stress activation in hepatocytes, HF diet feeding did not modulate markers of ER stress in an immune cell-enriched fraction of the liver. Interestingly, the pattern of ER stress activation in the SVF of the AT closely resembled the regulation of ATM apoptosis reported in the previous chapter (Chapter IV). The correlation between SVF ER stress activation and macrophage apoptosis, as well as the fact that ER stress signaling can culminate in apoptotic cell death, led to the hypothesis that activation of ER stress pathways is required to promote ATM apoptosis. However, SVF apoptosis was not decreased in mice globally deficient for CHOP, the primary protein involved in the activation of apoptosis downstream of ER stress. These findings indicate that ATM apoptosis does not require ER stress signaling.

RESULTS

Obesity increases whole AT ER stress activation

As previously mentioned, the first description of ER stress activation in metabolic tissues demonstrated an increase in ER stress signaling in whole AT (i.e. adipocyte fraction and SVF) of obese mice (164). To confirm this observation, male C57Bl/6 mice were placed on a 10% LF or a 60% HF diet for 9 weeks, as shown in Figure 4.1A. AT from lean and obese mice was assessed for markers of ER stress activation by Western blot. In agreement with previous literature (164), there was a trend towards an increase in BiP protein levels in the AT of

obese mice ($p = 0.068$, Figure 5.1A). Additionally, obesity resulted in a significant increase in the phosphorylated forms of both eIF2α and JNK 1/2 ($p<0.05$, Figure 5.1B-C), confirming that obesity activates ER stress signaling in whole AT.

Obesity decreases ER stress activation in the SVF of the AT

A recent study has suggested that the activation of ER stress pathways in whole AT is a consequence of increased ER stress signaling in adipocytes, rather than ATMs (165). To determine the impact of obesity on ER stress signaling specifically in ATMs, the macrophage-enriched SVF of the AT was isolated and analyzed by Western blot. Interestingly, obesity *decreased* the protein expression of the ER-resident chaperone protein, BiP, in the SVF of the AT ($p<0.001$, Figure 5.2A). In addition, protein levels of the phosphorylated forms of PERK ($p<0.001$, Figure 5.2B), eIF2α ($p<0.05$, Figure 5.2C), and JNK 1/2 ($p<0.001$, Figure 5.2C) were also significantly decreased in the SVF of the AT of obese compared to lean mice. These data demonstrate that obesity reduces ER stress activation specifically in the macrophage-enriched SVF of the AT.

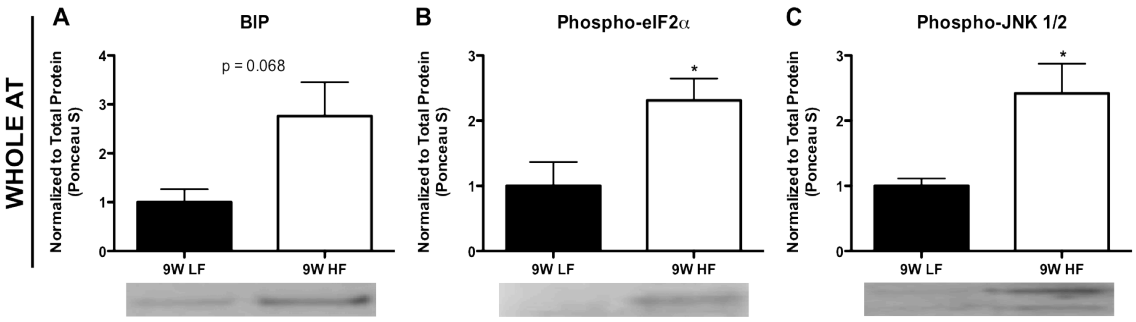

Figure 5.1: Obesity increases ER stress activation in whole AT. Male C57Bl/6 mice were placed on a 10% LF diet or a 60% HF diet for 9 weeks, as shown in Figure 4.1A. A-C: Whole AT was sonicated in 2% SDS and ER stress markers were analyzed using Western blot: A) BiP, B) phospho-eIF2α, C) phospho-JNK 1/2. Levels of specific proteins were normalized to total protein level, as measured by Ponceau S staining. Data are presented as mean ± SEM, n = 3-5/group. * p <0.05 compared to 9W LF.

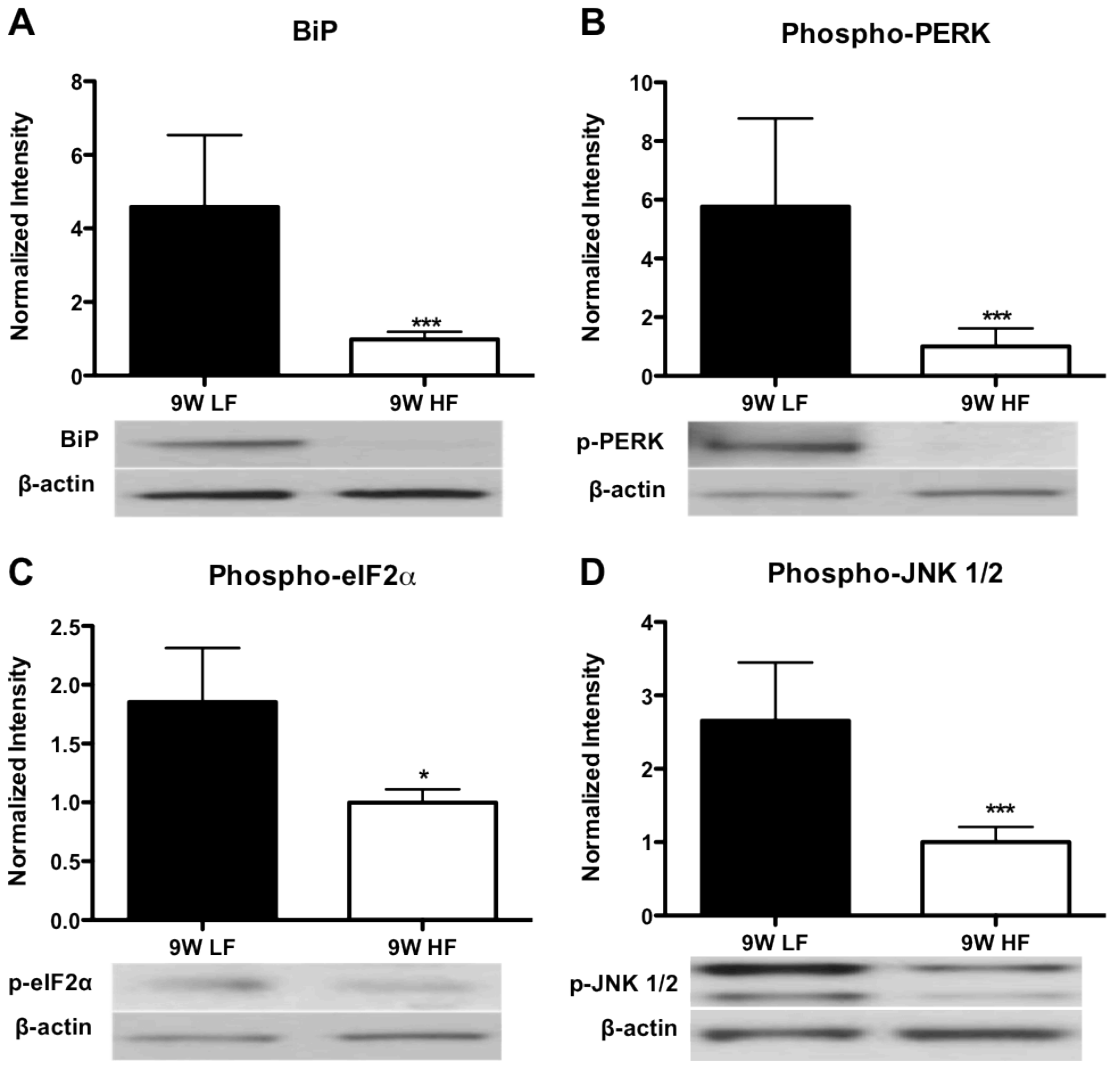

Figure 5.2: Obesity decreases ER stress activation in the SVF of AT. Male C57Bl/6 mice were placed on a 10% LF diet or a 60% HF diet for 9 weeks, as shown in Figure 4.1A. A-D: Protein was isolated from the SVF of the AT and ER stress markers were analyzed using Western blot: A) BiP, B) phospho-PERK, C) phospho-eIF2α, D) phospho-JNK 1/2. Data are presented as mean ± SEM, n = 7-12/group. * p <0.05, ***p<0.001 compared to 9W LF.

Weight loss increases ER stress activation in the SVF of the AT

To determine if weight loss modulates ER stress signaling in the SVF of AT, mice were placed on the diet-switch protocol shown in Figure 4.8A. Western blot analysis demonstrated that weight loss significantly increased the protein expression of BiP ($p<0.001$, Figure 5.3A) and phospho-PERK ($p<0.05$, Figure 5.3B) in the SVF. In addition, there was a trend towards an increase in the phosphorylated form of eIF2α ($p = 0.099$, Figure 5.3C) in the SVF during weight loss.

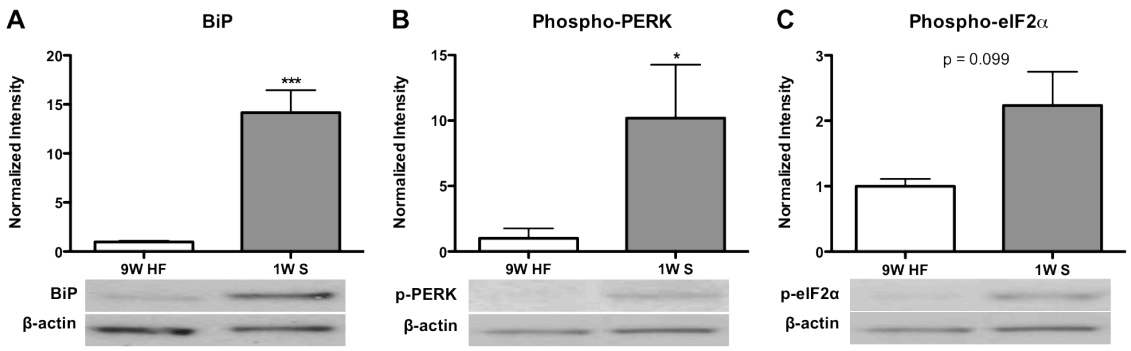

Figure 5.3: Weight loss increases ER stress activation in the SVF of the AT. Mice were placed on a 60% HF diet for 9 weeks. One group was sacrificed at this time-point, while the remaining mice were switched to a 10% LF diet for 1 week to promote weight loss. See Figure 4.5A for study design. A-C: Protein was isolated from the macrophage-enriched SVF of the AT and Western blot analysis was performed: A) BiP, B) phospho-PERK, and C) phospho-eIF2α. Data are presented as mean ± SEM, n = 4-8/group. * $p<0.05$, *** $p<0.001$ compared to 9W HF.

Obesity increases ER stress activation in the hepatocyte fraction of the liver

During obesity, ER stress activation is observed not only in whole AT, but also in other metabolically relevant tissues, including the liver (164). To determine if the increased ER stress in the liver is due to an up-regulation of these signaling pathways in the parenchymal fraction of the liver, hepatocytes were isolated from the livers of lean and obese mice. Western blot analysis demonstrated an increase in IRE-1α ($p<0.001$, Figure 5.4A) and BiP ($p<0.05$, Figure 5.4B) protein levels, but no change in eIF2α phosphorylation (Figure 5.4C) in the hepatocytes of obese mice, indicating that ER stress signaling is increased in the hepatocyte fraction of the liver during obesity.

Obesity does not alter ER stress activation in an F4/80-enriched non-parenchymal fraction of the liver or in the spleen

Above, we have demonstrated that obesity decreases ER stress activation in the macrophage-enriched SVF of the AT (Figure 5.2). To determine if obesity also reduces ER stress activation in macrophages in another metabolically relevant tissue, an F4/80-enriched non-parenchymal fraction was isolated from the liver. Obesity did not modulate the protein levels of IRE-1α, BiP, or phospho-eIF2α (Figure 5.5A-C). Additionally, obesity did not modulate ER stress markers in the spleen, an immune cell-enriched organ (Figure 5.5D-F). Therefore, while obesity decreased ER stress signaling in AT-resident macrophages, this signaling pathway was not modulated in macrophages of the liver or in the spleen, indicating that this phenomenon is specific to the AT.

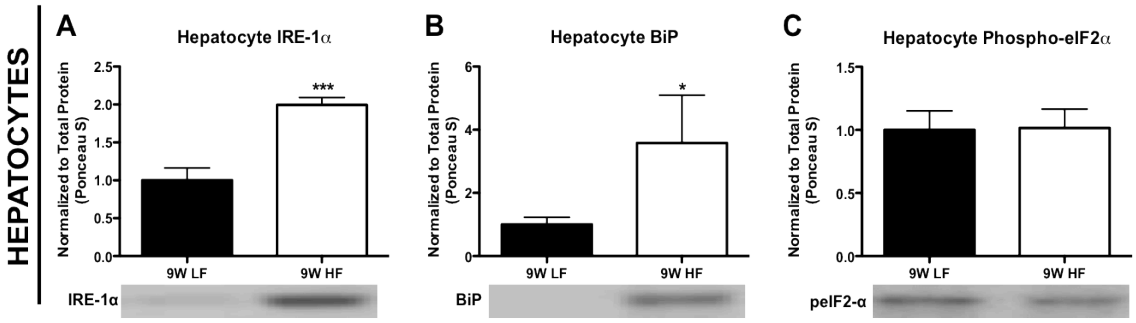

Figure 5.4: Obesity increases ER stress activation in the hepatocyte fraction of liver. Male C57Bl/6 mice were placed on a 10% LF diet or a 60% HF diet for 9 weeks, as shown in Figure 4.1A. A-C: The hepatocyte fraction of the liver was sonicated in 2% SDS and ER stress markers were analyzed using Western blot: A) IRE-1α, B) BiP, C) phospho-eIF2α. Levels of specific proteins were normalized to total protein level, as measured by Ponceau S staining. Data are presented as mean ± SEM, n = 6-9/group. * $p < 0.05$, *** $p < 0.001$ compared to 9W LF.

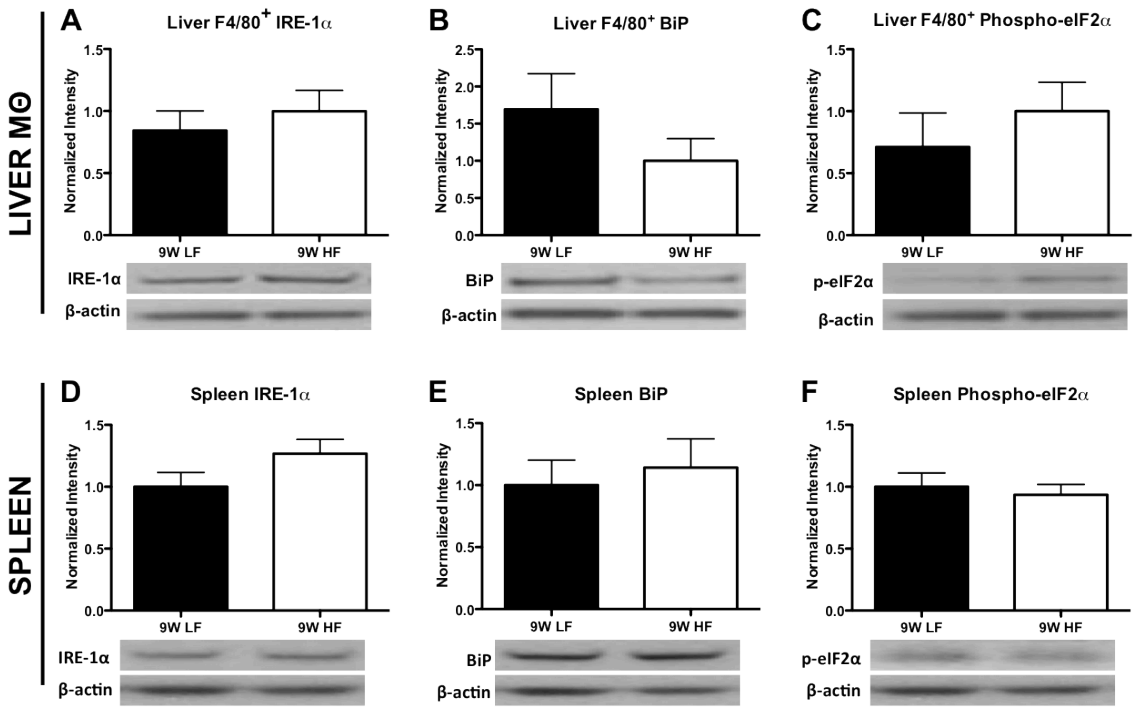

Figure 5.5: Obesity does not modulate ER stress signaling in an F4/80-enriched fraction of the liver or in the spleen. Male C57Bl/6 mice were placed on a 10% LF diet or a 60% HF diet for 9 weeks, as shown in Figure 4.1A. A-C: The non-parenchymal fraction of the liver was enriched for F4/80$^+$ macrophages using magnetic beads. Western blot analysis was performed for markers of ER stress: A) IRE-1α, B) BiP, and C) phospho-eIF2α. D-F: Whole spleen was sonicated in 2% SDS and Western blot analysis was performed: A) IRE-1α, B) BiP, and C) phospho-eIF2α. Data are presented as mean ± SEM, n = 6-7/group.

Correlation between ER stress activation and apoptosis in the SVF of AT during obesity and weight loss

Taken together, the above findings demonstrate that ER stress signaling is activated specifically in macrophages residing in lean AT, decreased during obesity, and re-activated by weight loss. In the previous chapter, we have demonstrated that ATM apoptosis follows a similar pattern of metabolic regulation (Figures 4.3 and 4.9). In fact, the protein levels of phosphorylated PERK in the SVF are significantly and positively correlated with the percent of apoptotic macrophages in the AT of lean, obese, and diet switch mice ($r^2 = 0.27$, $p<0.01$, data not shown). This positive correlation and the fact that macrophages are able to undergo ER stress-mediated apoptosis ((153; 157; 168) and Figure 3.4) led to the hypothesis that ER stress activation may culminate in apoptotic cell death in macrophages in lean AT.

CHOP deficiency does not decrease apoptosis in the SVF of AT

CHOP is a pro-apoptotic protein downstream of multiple signaling pathways activated during the ER stress response (203). Previous studies have shown that deletion of CHOP protects cells from ER stress-mediated apoptosis, while leaving other cell death pathways intact (163; 203). To determine if ER stress activation is the mechanism by which ATMs undergo apoptosis, WT and CHOP deficient mice were placed on a LF diet for 9 weeks (Figure 5.6A) and SVF apoptosis was analyzed. CHOP deficiency did not decrease cleaved caspase-3 levels in the SVF, indicating that ER stress-mediated apoptosis does not occur in AT-resident macrophages.

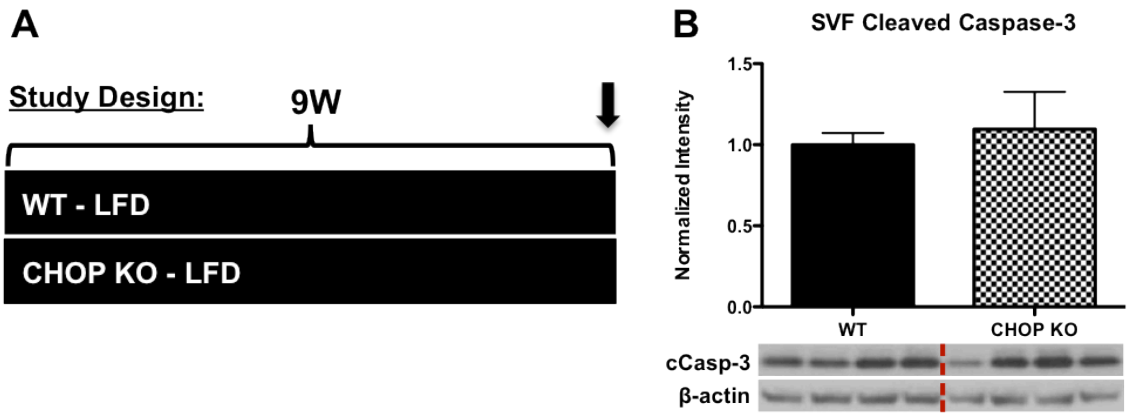

Figure 5.6: CHOP deficiency does not decrease SVF apoptosis. A) Study design: WT and CHOP deficient male C57Bl/6 mice were placed on a 10% LF diet for 9 weeks. B) Protein was isolated from the macrophage-enriched SVF of the AT and protein levels of cleaved caspase-3 were assessed using Western blot. Data are presented as mean ± SEM, n = 4-5/group.

DISCUSSION

Previous studies have shown that ER stress signaling in metabolic tissues, including whole AT and liver, contributes to the systemic inflammation and IR associated with obesity (164; 167). In agreement with this literature (164), we found that obesity *increased* ER stress signaling in whole AT and the hepatocyte fraction of the liver. In contrast, obesity *decreased* ER stress activation specifically in the macrophage-enriched SVF of the AT, but did not modulate ER stress levels in an immune cell fraction from the liver. These findings demonstrate that ER stress activation is differentially regulated in parenchymal versus non-parenchymal cells of the AT and liver during HF diet feeding. This novel concept brings up many questions regarding the physiological role of ER stress in AT immune cell populations.

Activation of ER stress pathways can ultimately result in apoptotic cell death (139). The data presented in the previous chapter (Chapter IV) suggest that macrophage apoptosis is a metabolically regulated process that contributes to the maintenance of AT homeostasis; however, the signaling pathways upstream of ATM apoptosis have not been identified. In this chapter, we demonstrate that, analogous to ATM apoptosis, ER stress signaling occurs in the immune cell fraction of lean AT, is decreased during obesity, and is restored after weight loss. The correlation between ER stress activation and ATM cell death suggests that ER stress-mediated apoptosis may occur in macrophages residing in lean AT. These findings would indicate that ER stress signaling plays a key role in regulating ATM number and, thus, AT insulin sensitivity. However, deletion

of CHOP, the primary protein involved in the activation of apoptosis downstream of ER stress, did not decrease ATM apoptosis.

The studies described above indicate that ER stress activation in macrophages residing in lean AT is not responsible for the initiation of apoptotic cell death. However, the functional role of ATM ER stress remains unknown. A recent *in vitro* study has indicated that ER stress activation may promote the polarization of macrophages to an M2 anti-inflammatory phenotype (204). Oh, *et al*. showed that polarization of primary human macrophages to an M2 phenotype (via treatment with IL-4) increased ER stress activation. Furthermore, co-treatment of macrophages with IL-4 and PBA decreased ER stress activation and blocked M2 polarization, demonstrating that ER stress signaling is necessary to promote an M2 macrophage phenotype (204).

These *in vitro* studies suggest that ER stress signaling in macrophages residing in lean AT may function not to activate ATM apoptosis, but instead to maintain M2 macrophage polarization. Decreased ATM ER stress signaling during obesity would be expected to promote a phenotypic switch from an M2 anti-inflammatory phenotype to an M1 pro-inflammatory phenotype. Therefore, it is possible that decreased ER stress activation in ATMs during obesity contributes to the increase in M1 macrophages and, thus, impaired AT insulin sensitivity. Future studies will determine whether blocking ER stress signaling in the ATMs of lean mice decreases the M2 polarization state of these cells.

Our data indicate that ER stress signaling is activated in lean ATMs and is decreased during obesity; however, the mechanism(s) by which macrophage ER

stress is regulated are not known. A recent study has demonstrated that eosinophils, granulocytic cells of the innate immune system, are the major IL-4 producing cell in the AT (103). As mentioned above, IL-4 promotes M2 macrophage polarization in an ER stress-dependent manner (204). Therefore, it is possible that eosinophils in lean AT secrete IL-4, which then activates ER stress signaling in ATMs to maintain an M2 polarized state. Of note, AT eosinophil number and IL-4 production are decreased during obesity (103). This reduction in eosinophil number may decrease ATM ER stress signaling, thus impairing M2 macrophage polarization during obesity.

Our data have shown that ER stress activation in metabolic tissues is differentially regulated in parenchymal cells versus non-parenchymal immune cells. While HF diet feeding increased ER stress signaling in whole AT and hepatocytes, obesity actually decreased the activation of this signaling pathway in AT-resident immune cells. Recent *in vitro* findings (204) suggest that this decreased ATM ER stress signaling during obesity may impair M2 macrophage polarization and contribute to the increase in pro-inflammatory M1 macrophages in the AT. Therefore, although pharmacological inhibition of ER stress would likely decrease adipocyte and hepatocyte inflammation and IR, these drugs could have off-target effects that promote an inflammatory immune cell phenotype.

CHAPTER VI

Weight Cycling Increases T Cell Accumulation in AT and Impairs Systemic Glucose Tolerance

(Adapted from Anderson, *et al*. In Revision at *Diabetes*, 2013)

INTRODUCTION

Obesity is associated with an increased risk for the development of numerous pathological conditions including IR, T2D, and CVD (36). Many of the metabolic consequences of obesity are the result of AT dysfunction. During obesity, AT releases FFAs and pro-inflammatory cytokines that interfere with insulin signaling, both locally and systemically (28; 36). Recent findings have implicated immune cell accumulation in AT as a key contributor to obesity-associated inflammation. It is well established that innate immune cells, including macrophages, accumulate in the AT during obesity and are the major source of AT-derived inflammatory cytokines/chemokines (34; 35; 148).

In addition to innate immune cells, recent evidence points to the involvement of the adaptive immune system in the initiation of AT inflammation during obesity. Upon HF diet feeding, the proportion of AT-resident anti-inflammatory lymphocytes, including $CD4^+$ T_{reg} cells (205) and T_H2 cells (206), is decreased. Furthermore, obesity promotes the influx of pro-inflammatory lymphocytes such as B-2 cells (131), NKT cells (126; 207), IFN-γ secreting $CD4^+$ T_H1 (110; 129; 130; 206), and $CD8^+$ cytotoxic T cells (113; 129; 130; 208) into AT.

The accumulation of T cells in AT appears to be antigen-driven (113; 206) and is also characterized by the formation of memory cells (129; 130). Interestingly, preventing the accumulation of pro-inflammatory T cell subsets in AT during obesity improves systemic glucose tolerance (113; 206), indicating that a shift towards a T_H1 immune response contributes to the development of AT inflammation and IR during obesity.

Weight loss is the ideal approach to counteract the negative consequences of obesity. Lifestyle or surgical interventions that promote weight loss result in decreased ATM number, reduced inflammation, and improved insulin sensitivity (41; 74; 132). However, even when weight loss is achieved, losses are rarely maintained. In fact, current estimates suggest that only 20% of individuals who lose greater than 10% of their body weight are able to maintain this loss (133). These bouts of weight regain lead to weight cycling. Although the literature regarding the impact of weight cycling on metabolic health remains controversial (209-212), multiple studies in humans indicate that weight cycling increases the risk of developing T2D and CVD (134-138). While the potentially deleterious effects of weight cycling are recognized, the mechanisms by which weight cycling increases metabolic dysfunction remain unknown. Additionally, it is not known whether weight cycling alters AT immune cell composition and/or inflammation.

In this study, mice were cycled between HF and LF diets to determine if weight cycling alters metabolic and immunological parameters when compared to mice that gain weight in the absence of cycling. We show that weight cycling

impairs systemic glucose tolerance and decreases AT insulin sensitivity. Weight cycling did not alter the HF diet-induced increase in ATM number or M1 polarization. However, both $CD4^+$ and $CD8^+$ T cell numbers were increased in the AT during weight cycling. In addition, $CD8^+$ effector memory T cell populations were increased during obesity and weight cycling. This intensified T cell-driven inflammatory response may contribute to the metabolic abnormalities associated with weight cycling.

RESULTS

Study design

To determine if weight cycling alters metabolic parameters or AT immune cell populations, male C57Bl/6 mice were fed diets to induce alternating obese and lean states. The study consisted of three 9-week diet periods in which mice had *ad libitum* access to either a 10% LF diet or a 60% HF diet. Three groups of mice were used (see study design, Figure 6.1A). The lean control group (designated as LF/LF/LF in Figures) was placed on the LF diet for the duration of the study (27 weeks). The weight gain group (designated as LF/HF/HF in Figures) was maintained on a LF diet for 9 weeks, then switched to the HF diet for the remaining 18 weeks of the study. The weight cycling group (designated as HF/LF/HF in Figures) was placed on a HF diet for 9 weeks to induce obesity and immune cell infiltration into AT; switched to a LF diet for 9 weeks to promote

weight loss; and placed on the HF diet during the last 9-week period to induce subsequent obesity.

Body weight and composition

When placed on a HF diet, mice gained weight as expected. After the mice in the weight cycling group were switched to a LF diet, their weight normalized (within 3-4 weeks) to the body weight of the lean control mice. Upon subsequent HF diet feeding, mice re-gained weight within 4 weeks and were weight-matched with the weight gain group for the final 5 weeks of the study (Figure 6.1B). At the end of the study, both groups that had received the HF diet for 18 weeks total (weight gain and weight cycling groups) had significantly increased body weight when compared to lean controls (Figure 1C, $p<0.05$). However, there was no difference in body weight between the weight gain group and the weight cycling group. Additionally, lean body mass (Figure 6.1D), fat mass (Figure 6.1E), and epididymal AT weight (Figure 6.1F) were increased by HF diet feeding ($p<0.05$), but were not modulated by weight cycling. Body weight and energy balance are key contributors to AT immune cell content and systemic glucose utilization (184; 213; 214). Because the weight gain and weight cycling mice were weight-matched and weight-stable for at least 4 weeks at the end of the study, the effects of weight cycling in the absence of altered body weight/composition could be analyzed.

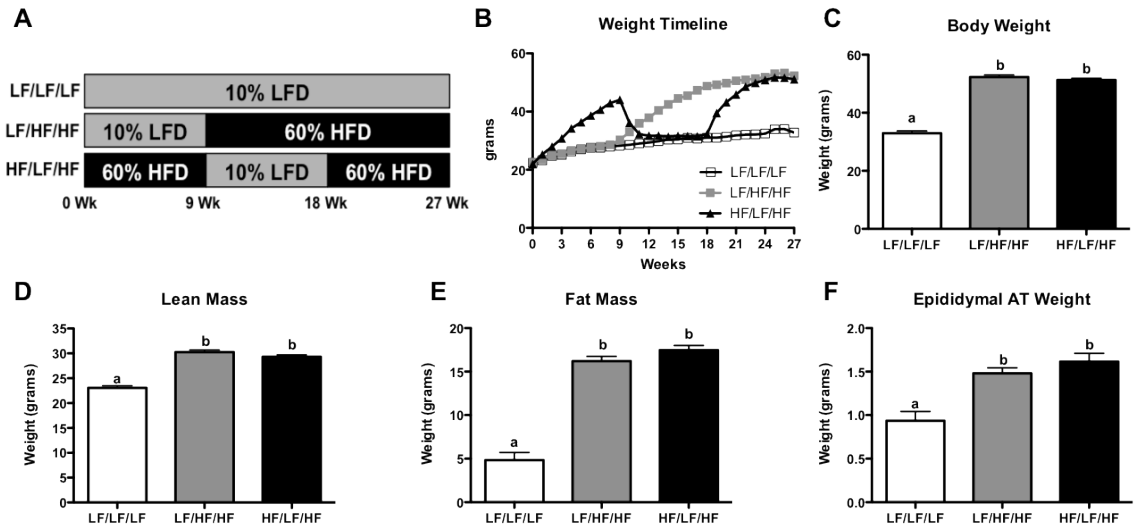

Figure 6.1. Metabolic characteristics of weight cycling mice. Male C57Bl/6 mice were placed on a 10% LF diet or a 60% HF diet for three 9-week intervals. A: Study design. B-F: Body weight and composition were determined. Body weight timeline for the duration of the study (B). Body weight after 27 weeks of diet (C). NMR was used to determine: Lean mass (D) and fat mass (E) after 27 weeks of diet. F: Epididymal AT weight after 27 weeks of diet. Data are presented as mean ± SEM, n = 15-17/group. Groups not connected by the same letter are significantly different, $p<0.05$.

Weight cycling impairs systemic glucose tolerance

To determine the systemic metabolic consequences of weight cycling, fasting plasma glucose and insulin levels were measured and an intraperitoneal GTT was performed. As expected, weight gain slightly increased blood glucose concentrations (Figure 6.2A, $p<0.05$ compared to LF/LF/LF). Interestingly, weight cycling resulted in an additional increase in fasting plasma glucose levels when compared to the weight gain group (Figure 6.2A, $p<0.05$). Fasting insulin concentrations were increased by HF diet feeding ($p<0.05$), but did not differ between the weight gain and weight cycling group (Figure 6.2B). In agreement with previous literature, glucose tolerance was decreased in the weight gain group when compared to lean controls (Figure 6.2C, $p<0.05$). Furthermore, weight cycling resulted in an additional impairment in glucose tolerance (Figure 2C, $p<0.05$ compared to LF/HF/HF).

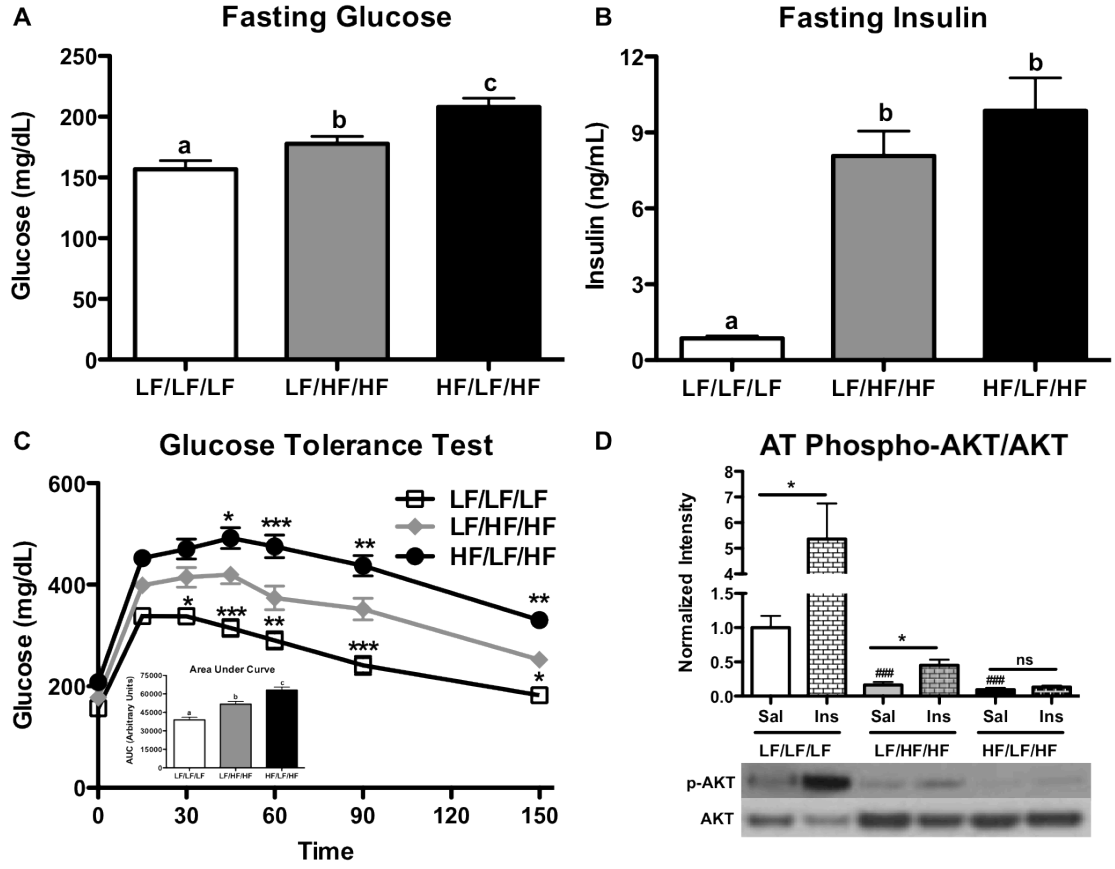

Figure 6.2. Weight cycling worsens systemic glucose tolerance and impairs AT insulin sensitivity. A-C: Metabolic parameters were evaluated in lean control, weight gain, and weight cycling mice after a 5 h fast. Fasting blood glucose (A) and plasma insulin (B) concentrations. Groups not connected by the same letter are significantly different, $p<0.05$. C: Glucose tolerance test (dose = 2 g/kg lean mass dextrose) and quantification of the area under the curve for the duration of the GTT (inset). * $p<0.05$, ** $p<0.01$, *** $p<0.001$ compared to the LF/HF/HF group. D: Mice were injected with saline or insulin (0.5 U/kg) 15 minutes before sacrifice. Protein was isolated from the epididymal AT. Western blot analysis of AT phospho-AKT (Ser 473) protein levels (relative to total AKT). * $p<0.05$ compared to saline-injected of same group. ### $p<0.001$ compared to LF/LF/LF saline-injected group. Data are presented as mean ± SEM, n =14-17 for glucose, insulin, and GTT; n = 4-6 for Westerns.

Weight loss reverses systemic metabolic dysfunction

It is possible that the impaired glucose tolerance observed in the weight cycling group at the end of the study (Figure 6.2) is the result of incomplete resolution of metabolic dysfunction during weight loss (weeks 9-18 of the study). To address this possibility, we completed metabolic analysis of mice at week 18 of the study (Figure 6.3). At this point, the weight cycling group had been on HF diet for 9 weeks, then switched to LF diet for 9 weeks to promote weight loss (Figure 6.3A). At this time point, the mice in the weight cycling group were weight-matched with the lean control group (Figure 6.3A-B). Similar results were seen with lean body mass and fat mass (Figure 6.3C-D). Fasting blood glucose and serum insulin concentrations were identical in the lean control mice and the weight cycling group at this time-point (Figure 6.3E-F). Additionally, a GTT revealed no difference in glucose tolerance between the two groups (Figure 6.3G-H). Therefore, incomplete resolution of metabolic defects during weight loss is not responsible for the worsened glucose tolerance observed at the end of the 27-week weight cycling study.

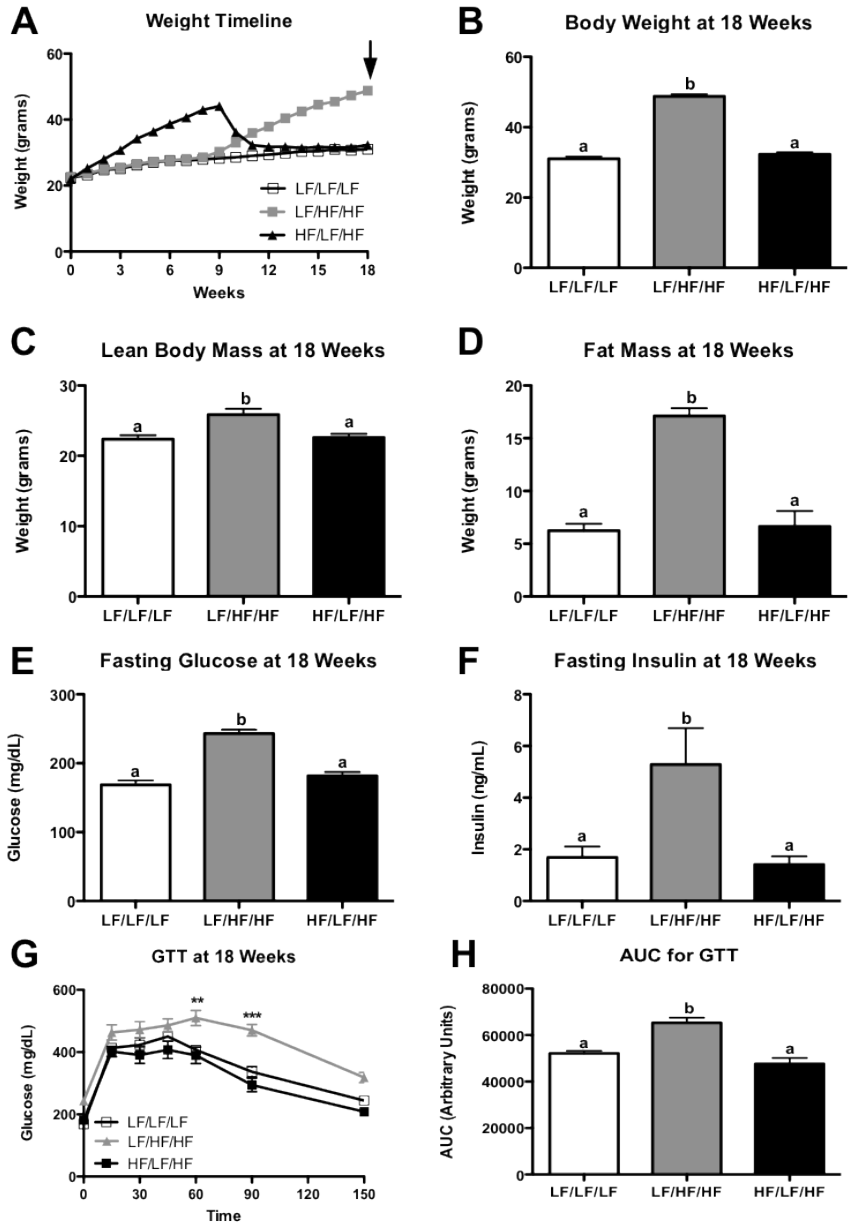

Figure 6.3: Weight loss reverses systemic metabolic dysfunction. A-D: Body mass and composition were measured at week 18 of the study. At this point, the weight cycling group had been on HF diet for 9 weeks, then switched to LF diet for an additional 9 weeks to promote weight loss. Body weight time-line (A), body weight (B), lean mass (C), and fat mass (D) at 18 weeks. E-H: Metabolic parameters were evaluated after a 5 h fast. Fasting blood glucose (D) and plasma insulin (E) concentrations at 18 weeks. Groups not connected by the same letter are significantly different, $p<0.05$. G-H: Glucose tolerance test (dose = 2 g/kg lean mass dextrose) (G). Quantification of the area under the curve of the GTT (H). ** $p<0.01$, *** $p<0.001$ compared to the LF/LF/LF group. Data are presented as mean ± SEM, n =7-11/group.

Weight cycling decreases AT insulin sensitivity

To determine if weight cycling modulates insulin signaling in the AT, mice were injected with saline or insulin (0.5 U/kg) 15 minutes prior to sacrifice. Insulin injection significantly increased the phosphorylation of AKT at ser473 in the AT of lean control mice ($p<0.05$ compared to LF/LF/LF saline, Figure 6.2D). As expected, HF diet feeding decreased insulin-stimulated AKT phosphorylation in the weight gain group; however, there remained a mild insulin response ($p<0.05$ compared to LF/HF/HF saline, Figure 6.2D). In contrast, weight cycling resulted in a complete loss of insulin-stimulated AKT phosphorylation in the AT, indicating that weight cycling further impaired AT insulin sensitivity (Figure 6.2D). Additionally, weight cycling impaired liver insulin signaling, but did not further decrease gastrocnemius muscle insulin signaling (Figure 6.4).

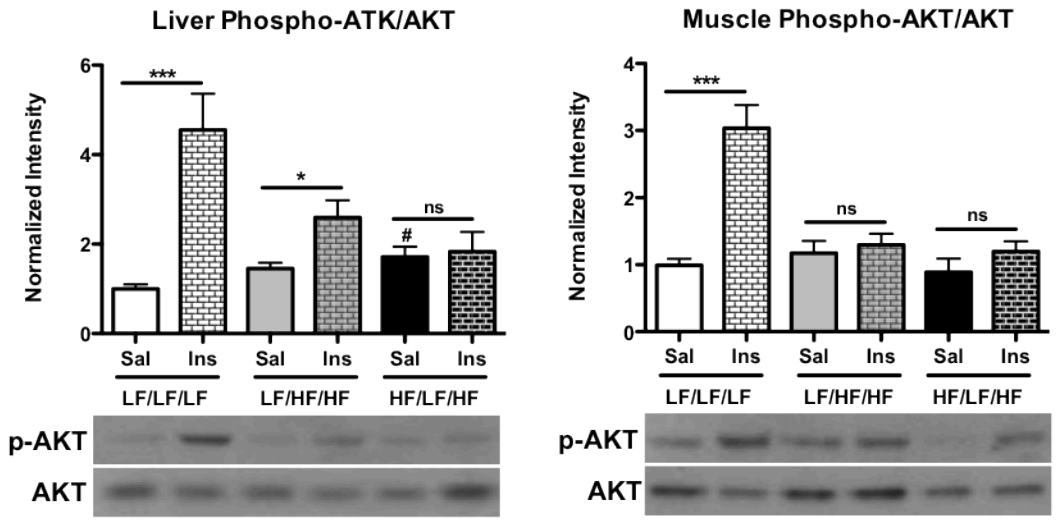

Figure 6.4: Weight cycling further impairs liver, but not muscle, insulin signaling. Mice were injected with saline or insulin (0.5 U/kg) 15 minutes before sacrifice. Protein was isolated from the liver or gastrocnemius muscle. A-B: Western blot analysis of phospho-AKT (Ser 473) protein levels (relative to total AKT) in liver (A) and muscle (B). * $p<0.05$ compared to saline-injected of same group. # $p<0.05$ compared to LF/LF/LF saline-injected group. Data are presented as mean ± SEM, n = 6-9/group.

Weight cycling does not alter ATM content

Because macrophage accumulation in obese AT contributes to the development of IR (36), we next performed flow cytometry on the SVF of the epididymal AT to determine if weight cycling impacts ATM content. For a detailed explanation of the gating strategy, see Figure 6.5. The percentage of $F4/80^+$ macrophages was increased by HF diet feeding ($p<0.05$ compared to LF/LF/LF), but did not differ between the weight gain and weight cycling groups (Figure 6.6G). HF diet significantly decreased the percentage of $F4/80^+CD11b^+CD11c^-$ macrophages in the AT ($p<0.05$ compared to LF/LF/LF), but there was no weight cycling effect (Figure 6.6G). Both $F4/80^+CD11b^-CD11c^+$ and $F4/80^+CD11b^+CD11c^+$ macrophages were increased in the AT during obesity ($p<0.05$ compared to LF/LF/LF, Figure 6.6G). Again, weight cycling did not modulate these immune cell populations. In addition to the flow cytometry data, real-time RT-PCR analysis demonstrates that weight cycling does not alter the HF diet-induced increase in AT expression of the macrophages markers, *Emr1*, *Cd68*, and *Itgam* (Figure 6.7A-C).

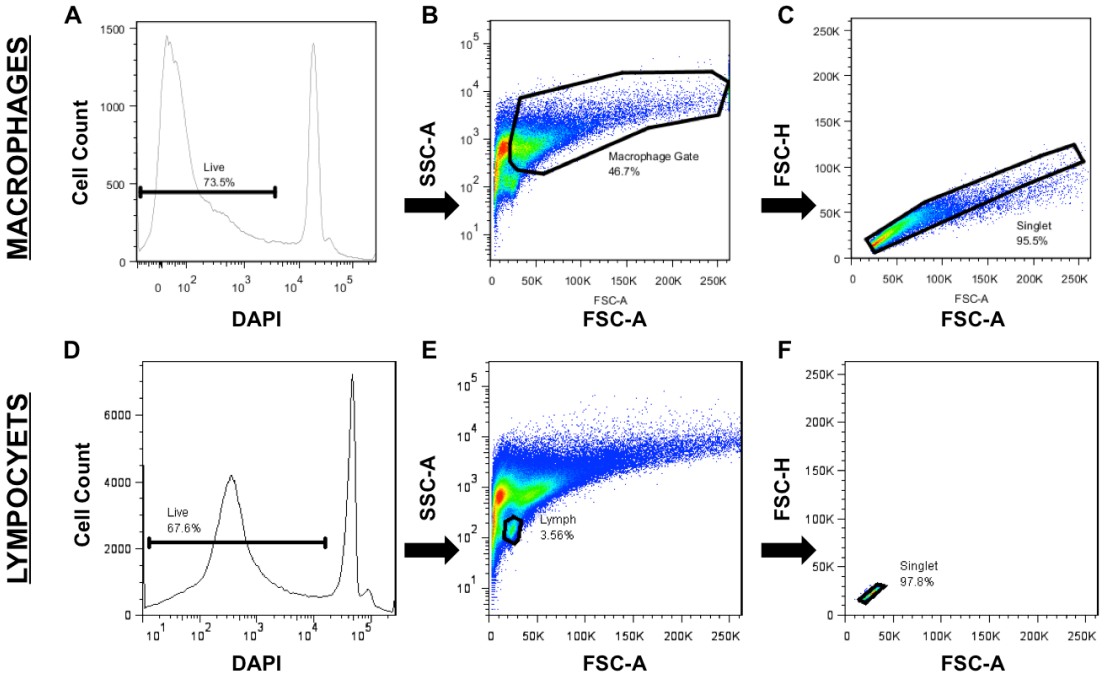

Figure 6.5: Gating strategy for flow cytometry analysis. SVF cells were isolated from the epididymal AT and analyzed by flow cytometry. A-C: Gating strategy for analysis of ATM populations: DAPI negative (live) cells were selected (A), then gated for the macrophage population based on forward and side scatter (B). Doublets were then excluded (C). D-F: Gating strategy for analysis of AT T cell populations: DAPI negative (live) cells were selected (A), then gated for the lymphocyte population based on forward and side scatter (B). Doublets were then excluded (C). This cell population was then used for further analysis with specific fluorophores. All flow cytometry data in the dissertation is presented as percent of DAPI negative (live) cells (A and D).

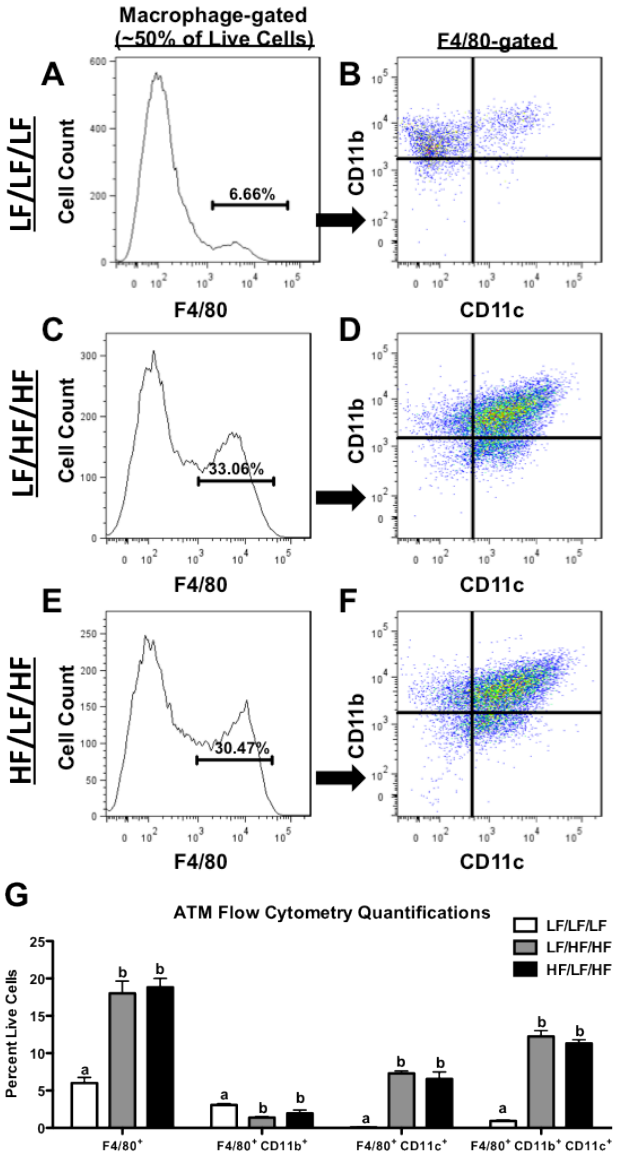

Figure 6.6: Weight cycling does not modulate ATM content. SVF cells were isolated from the epididymal AT and analyzed by flow cytometry. A-B: LF/LF/LF (lean control) group, C-D: LF/HF/HF (weight gain) group, E-F: HF/LF/HF (weight cycling) group. Representative flow cytometry histogram of F4/80 (A, C, E). Percentages on the histograms represent percent of previous gate (live, macrophage-gated, singlet cells). Flow cytometry dot plot of F4/80$^+$ cells analyzed for CD11b and CD11c (B, D, F). G: Quantification of ATM flow cytometry for all groups as percent of all live cells. Data are presented as mean ± SEM, n = 6-12/group. Groups not connected by the same letter within each cell population are significantly different, $p<0.05$.

Weight cycling does not alter ATM phenotype

To determine if weight cycling influences macrophage phenotype, gene expression of classical M1 and M2 macrophage markers was determined. AT expression of M1 (*Itgax*, *Tnf*, and *Ccr2*) and M2 (*Arg1* and *Clec10a*) macrophage markers was increased during obesity (215), but not altered by weight cycling (Figure 6.7D-H). Additionally, the M2 to M1 macrophage ratio (calculated by dividing the relative expression of either *Arg1* or *Clec10a* by the relative expression of *Itgax*) was decreased with HF diet feeding, but unchanged by weight cycling (Figure 6.7I).

Weight cycling increases T cell accumulation in AT

Recent evidence indicates that, in addition to macrophages, T cells also accumulate in AT during obesity and contribute to the development of IR (110; 111; 113; 206; 208). To determine if weight cycling modulates AT T cell subsets, live cells in the lymphocyte population of the SVF were analyzed for TCR-β (See Figure 6.5). The percentage of TCR-β^+ cells was increased in the AT of the weight cycling group (Figure 6.8G, $p<0.05$ compared to LF/LF/LF and LF/HF/HF). TCR-β^+ cells were subsequently analyzed for CD4 and CD8 (Figure 6.8B, D, and F). Weight cycling significantly increased the percentage of $CD4^+$ and $CD8^+$ T cells in the AT ($p<0.05$ compared to LF/LF/LF and LF/HF/HF, Figure 6.8G). In addition, real-time RT-PCR analysis demonstrated an increase in the expression of *Cd3, Cd4*, and *Cd8* in the AT of the weight-cycled mice (Figure 6.9A-C, $p<0.05$).

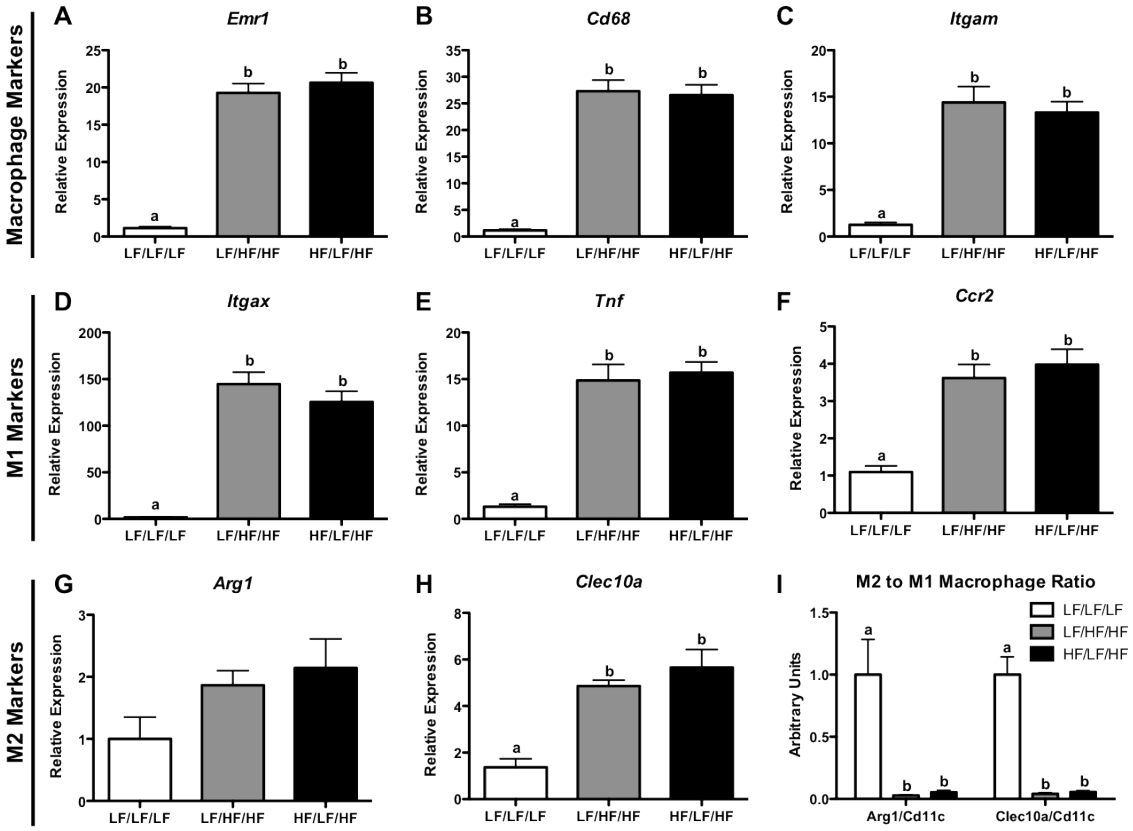

Figure 6.7: Weight cycling does not modulate ATM phentoype. RNA was isolated from the epididymal AT and gene expression was analyzed by real-time RT-PCR. A: *Emr1*, B: *Cd68*, C: *Itgam*, D: *Itgax*, E: *Tnf*, F: *Ccr2*, G: *Arg1*, H: *Clec10a*. I: M2 to M1 macrophage ratio calculated by dividing the relative expression of either *Arg1* or *Clec10a* (M2 markers) by the relative expression of *Itgax* (M1 marker). Data are presented as mean ± SEM, n = 8-14/group. Groups not connected by the same letter are significantly different, $p<0.05$.

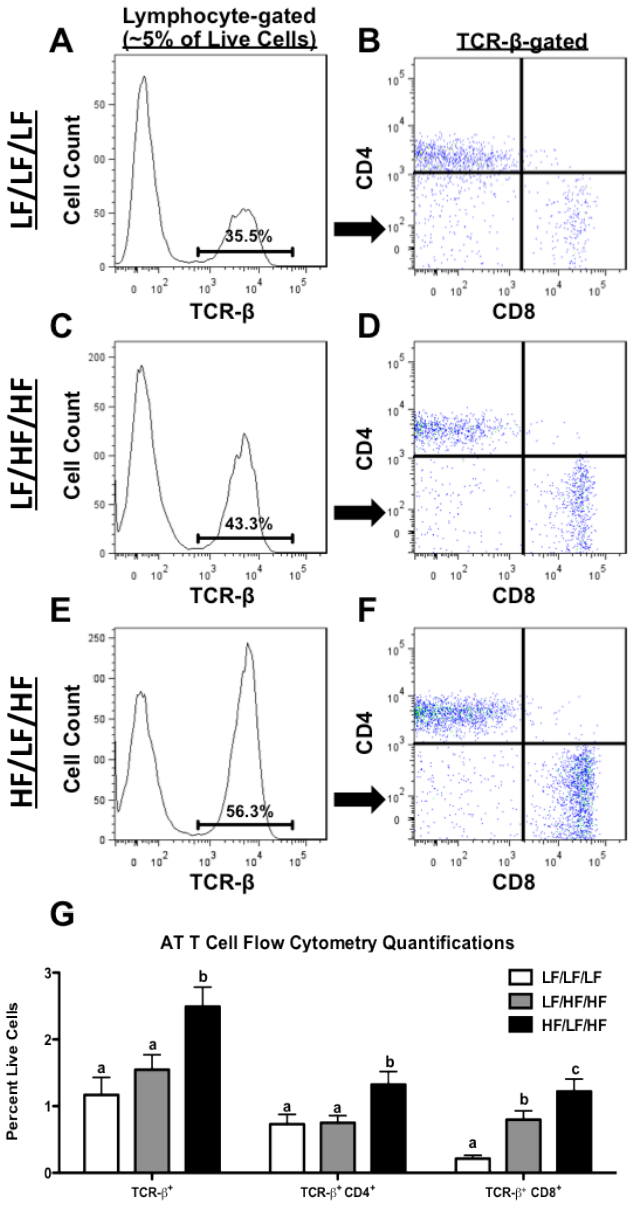

Figure 6.8: Weight cycling increases AT T cell populations. SVF cells were isolated from the epididymal AT and analyzed by flow cytometry. A-B: LF/LF/LF (lean control) group, C-D: LF/HF/HF (weight gain) group, E-F: HF/LF/HF (weight cycling) group. Representative flow cytometry histogram of TCR-β (A, C, E). Percentages on the histograms represent percent of previous gate (live, lymphocyte-gated, singlet cells). Flow cytometry dot plot of TCR-β^+ cells analyzed for CD4 and CD8 (B, D, F). G: Quantification of AT T cell flow cytometry from all groups as percent of all live cells. Data are presented as mean ± SEM, n = 10-12/group. Groups not connected by the same letter within each cell population are significantly different, $p<0.05$.

Weight cycling increases gene expression of CD4$^+$ T_H1- and CD8$^+$ T cell-derived cytokines in AT

Next, we determined the expression of genes relevant to T cell function and inflammatory status. T_H1 polarized CD4$^+$ T cells and cytotoxic CD8$^+$ T cells secrete high levels of the inflammatory cytokine, IFN-γ (216). Real-time RT-PCR analysis demonstrated that weight cycling further augments the HF diet-induced increase in *Ifng* gene expression (Figure 6.9D, $p<0.05$ compared to LF/HF/HF). IL-12 is a T_H1-stimulating cytokine involved in the production of IFN-γ (217). Weight cycling resulted in a striking 4.5-fold increase in AT *Il12* gene expression when compared to weight gain in the absence of cycling (Figure 6.9E, $p<0.05$). In addition, gene expression of *Il2*, a T_H1-derived cytokine required for the growth, differentiation, and survival of CD8$^+$ T cells (218), was increased 2-fold compared to the weight gain group (Figure 6.9F, $p<0.05$). Expression of the low-affinity IL-2 receptor, *Il2ra*, was not modulated by diet (Figure 6.9G). In contrast, the high-affinity IL-2 receptor, *Il2rb*, was increased during obesity and an additional 2-fold increase in gene expression was seen during weight cycling (Figure 6.9H, $p<0.05$ compared to LF/HF/HF). There was also a trend towards an increase in the gene expression of the T cell chemokine, *Ccl5*, in the AT of the weight cycling group (Figure 6.9I, $p=0.076$ compared to LF/HF/HF). Of note, weight cycling did not modulate the expression of the T_H2-derived cytokines: *Il4*, *Il10*, and *Il13* (Figure 6.10).

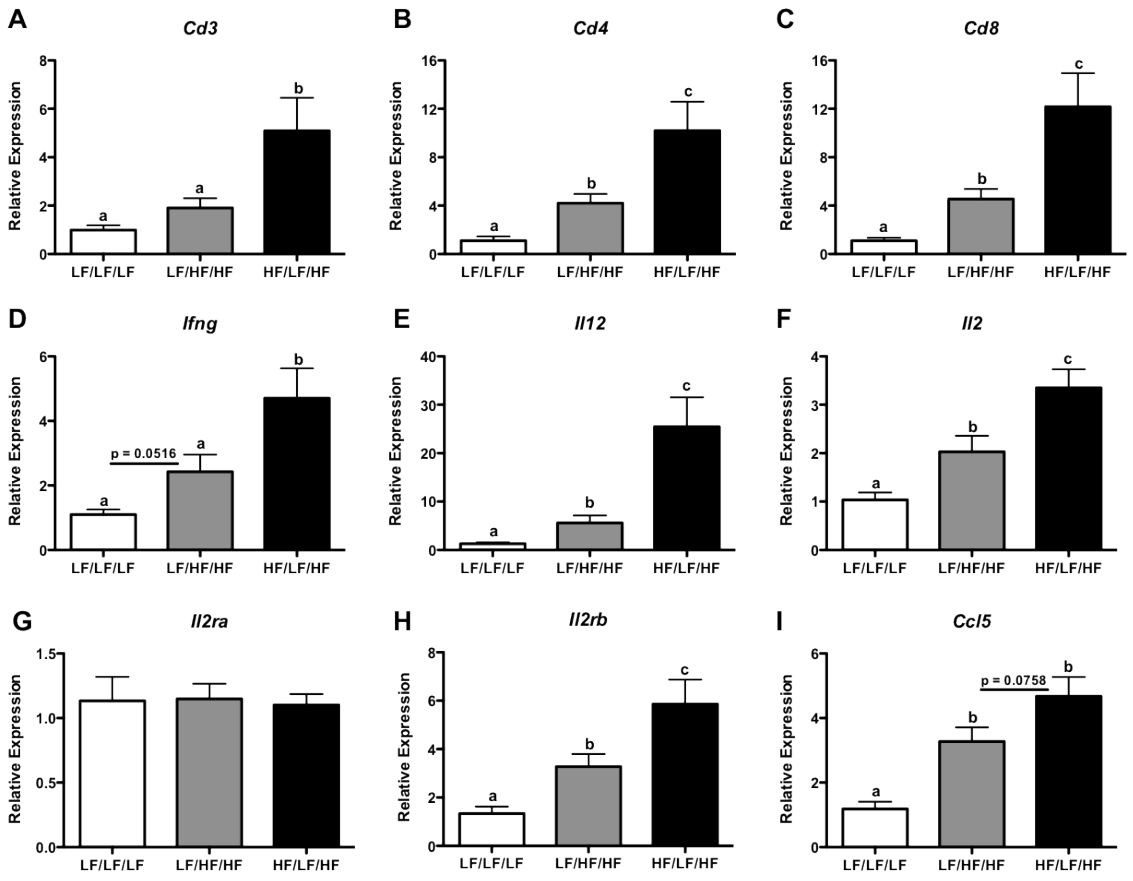

Figure 6.9: Weight cycling increases AT gene expression of T cell markers and CD4$^+$ T$_H$1- and CD8$^+$ T cell-derived cytokines. RNA was isolated from the epididymal AT and gene expression was analyzed by real-time RT-PCR. A: *Cd3*, B: *Cd4*, C: *Cd8,* D: *Ifng*, E: *Il12*, F: *Il2*, G: *Il2ra*, H: *Il2rb*, and I: *Ccl5*. Data are presented as mean ± SEM, n = 8-14/group. Groups not connected by the same letter are significantly different, $p<0.05$.

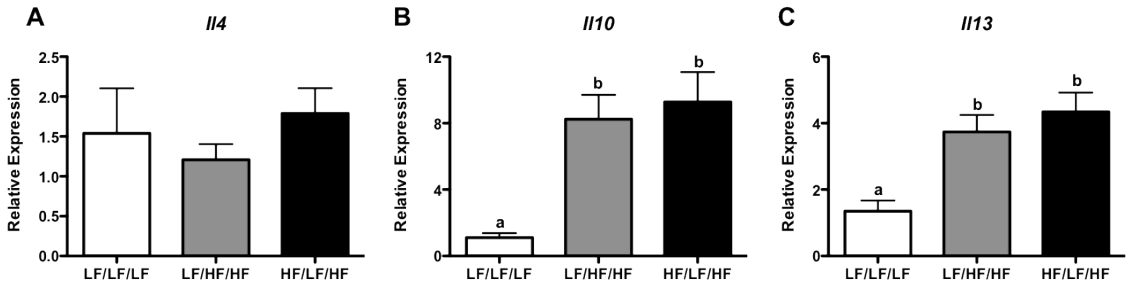

Figure 6.10: Weight cycling does not modulate T_H2-derived cytokine expression. RNA was isolated from the epididymal AT and gene expression of T_H2-derived cytokines was analyzed by real-time RT-PCR. A: *Il4*, B: *Il10*, C: *Il13*. Data are presented as mean ± SEM, n = 8-14/group. Groups not connected by the same letter are significantly different, $p<0.05$.

Obesity increases CD8$^+$ effector memory T cell accumulation in AT

One of the distinguishing features of an adaptive immune response is the development of cellular memory against specific antigens (219). To determine if weight cycling is associated with an increase in effector memory T cells, CD4$^+$ and CD8$^+$ T cells were analyzed for CD62L and CD44. CD4$^+$ effector memory T cells (CD62L^{lo} CD44^{hi}) were not modulated by either HF diet feeding or weight cycling (Figure 6.11A-D). However, in agreement with published literature (129; 130), we have found that obesity increases the number of CD8$^+$ effector memory T cells in the AT (Figure 6.11E-F, $p<0.05$ compared to LF/LF/LF). Additionally, there was a trend towards a further increase in CD8$^+$ effector memory T cell accumulation in the AT of weight-cycled mice (Figure 6.11F-G, $p = 0.075$ compared to LF/HF/HF). The above data indicate that an adaptive immune response, characterized by the accumulation of effector memory T cells, occurs in the AT during obesity and that weight cycling may further increase this memory response. (For quantification of all flow cytometry by number see Figure 6.12).

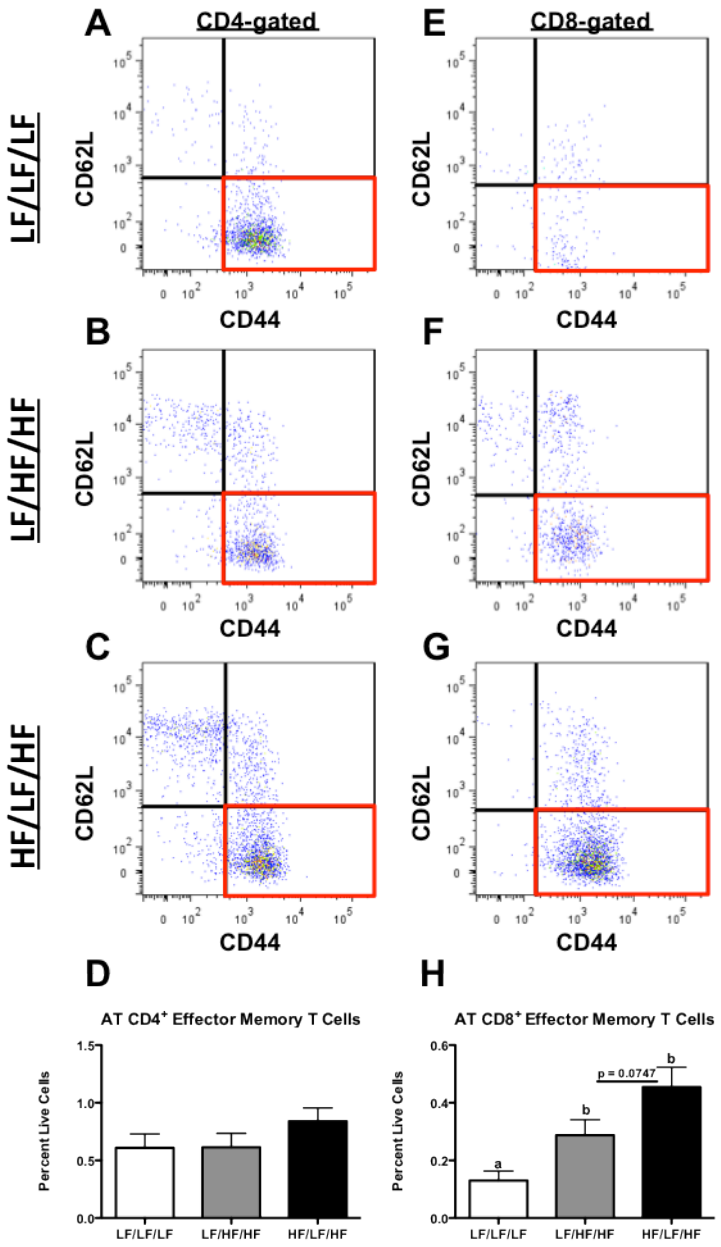

Figure 6.11: Increased CD8$^+$, but not CD4$^+$, effector memory T cell accumulation in AT during obesity. SVF cells were isolated from the epididymal AT and analyzed by flow cytometry. A, E: LF/LF/LF (lean control) group, B, F: LF/HF/HF (weight gain) group, C, G: HF/LF/HF (weight cycling) group. Representative flow cytometry dot plot of CD4$^+$ cells analyzed for CD62L and CD44 (A-C). D: Quantification of CD4$^+$ effector memory T cells (CD62L^{lo}CD44^{hi}) by flow cytometry. Representative flow cytometry dot plot of CD8$^+$ cells analyzed for CD62L and CD44 (E-G). H: Quantification of CD8$^+$ effector memory T cells (CD62L^{lo} CD44^{hi}) by flow cytometry. Data are presented as mean ± SEM, n = 6-12/group. Groups not connected by the same letter are significantly different, $p<0.05$.

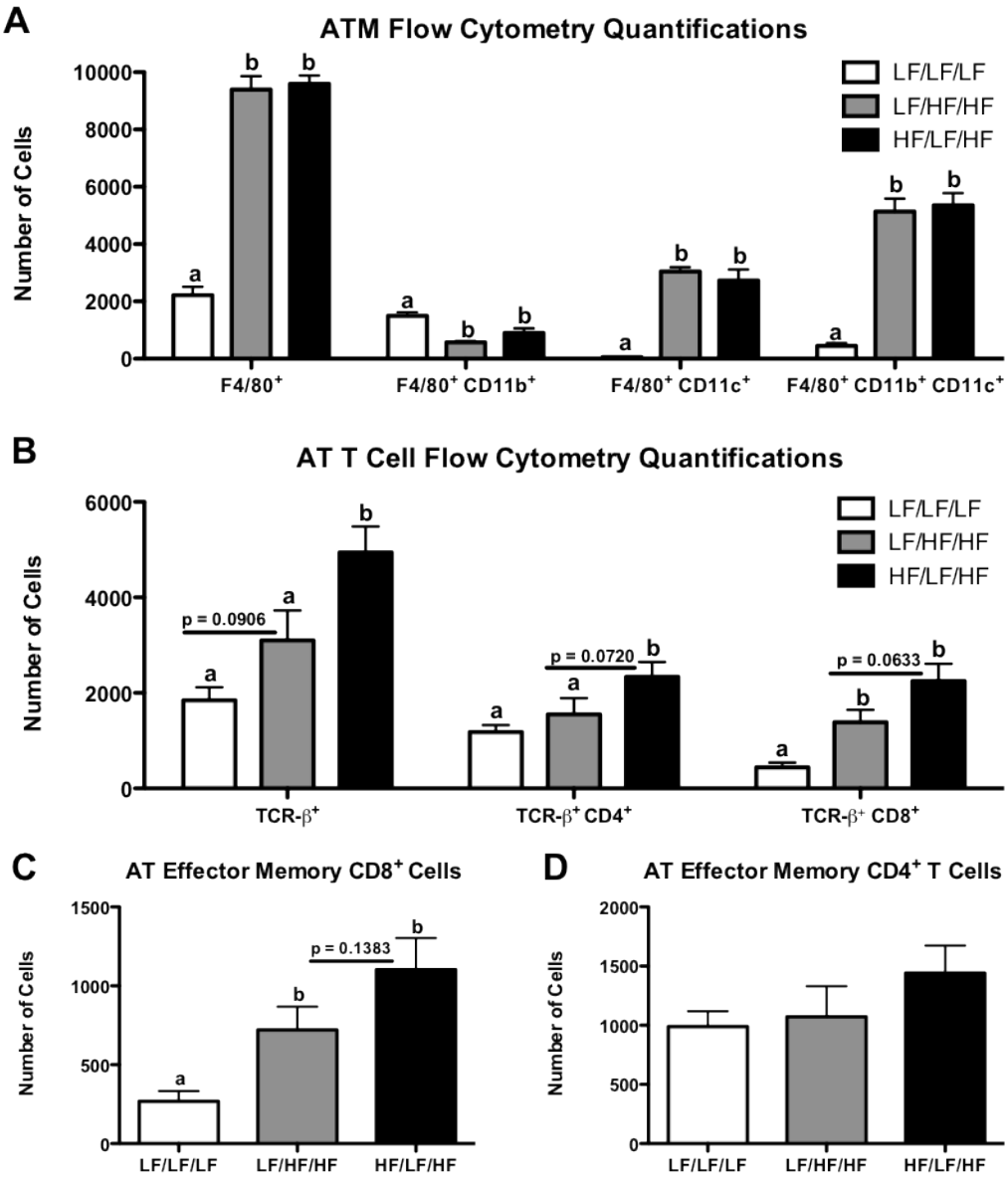

Figure 6.12: Analysis of flow cytometry data by number of cells. SVF cells were isolated from the epididymal AT and analyzed by flow cytometry. A: Quantification of ATM flow cytometry. B: Quantification of AT T cell flow cytometry. C-D: Quantification of AT effector memory $CD4^+$ (C) and $CD8^+$ (D) T cells. Data are presented as mean ± SEM, n = 6-12/group. Groups not connected by the same letter within each cell population are significantly different, $p<0.05$.

DISCUSSION

Multiple studies indicate that weight cycling is associated with worsened metabolic and cardiovascular outcomes (134-138). However, the mechanism(s) by which weight cycling promotes metabolic dysfunction are not known. Here, we show that weight cycling worsens obesity-associated systemic glucose intolerance and AT IR in mice. Accompanying these metabolic changes was an increase in $CD4^+$ T cells, $CD8^+$ T cells, and the expression of T_H1 cell-derived cytokines in the AT of weight-cycled mice. These novel findings suggest that an amplified T cell response occurs in the AT during weight cycling. (See Figure 6.13 for Model).

Previous reports have shown that weight cycling increases systemic IR in rats (220; 221). In addition, multiple human studies demonstrate that weight cycling increases the risk for development of CVD and T2D (134-138). One of the first studies addressing this issue reported a 10% increase in 25-year risk of coronary death in men who weight cycled when compared to those who gained weight but remained weight stable (135). Additionally, a recent study has shown that weight cycling is associated with an increased incidence of T2D in participants of the Framingham Heart Study (134).

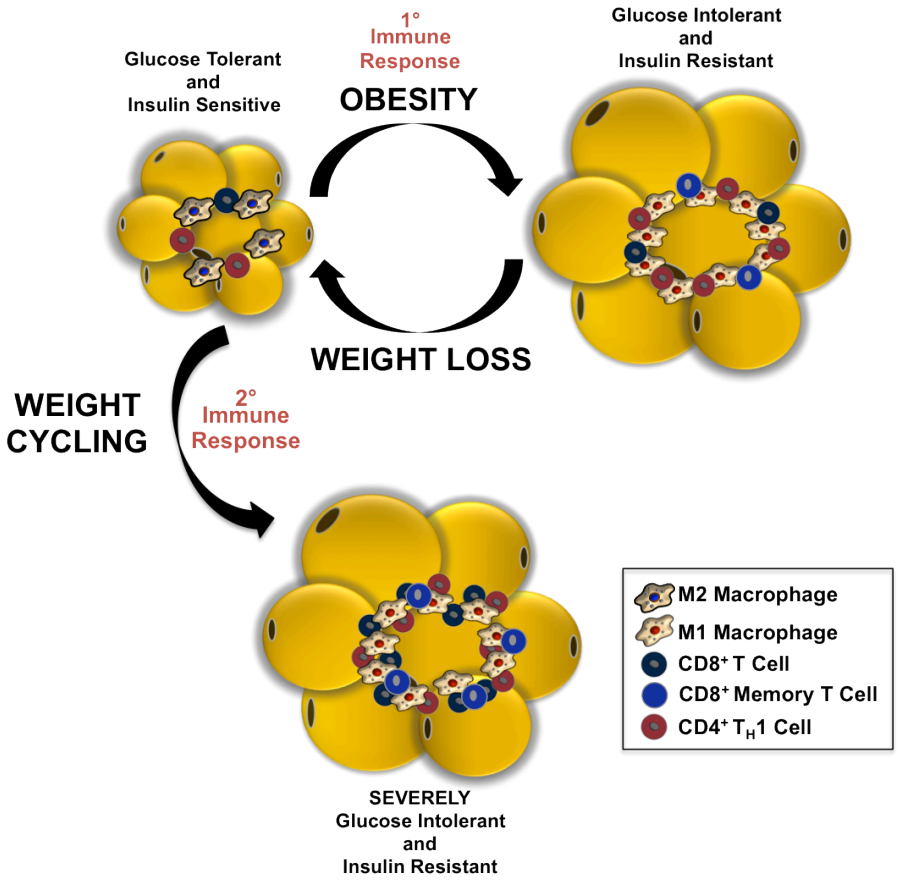

Figure 6.13: Metabolic and immunologic consequences of weight cycling. Weight cycling increases AT IR and systemic glucose tolerance, even when compared to weight-matched obese mice. This metabolic dysfunction is accompanied by an increase in pro-inflammatory AT T cell subsets, but no change in ATM number or phenotype. The presence of effector memory T cells in obese and weight-cycled AT suggests that weight cycling may initiate a more rapid and potent local secondary adaptive immune response, leading to increased AT T cell accumulation and tissue dysfunction.

In contrast to the above findings, other studies report no adverse effects of weight cycling (209-212). The controversy regarding the impact of weight cycling in humans may be due, in part, to variability of study design. Importantly, our data suggest that an exaggerated adaptive immune response in the AT may contribute to the negative effects of weight cycling. Indeed, $CD4^+$ T_H1 and T_H2, and $CD8^+$ T cells are known to play a role in the pathogenesis of human obesity (185). Therefore, if the extent of weight cycling or the time between cycles (as defined by the study design) was not sufficient to induce AT immune cell infiltration, the weight cycling effect on metabolism may not have been observed.

It was important to confirm that weight loss completely reversed obesity-associated metabolic dysfunction before subsequent weight gain. Metabolic phenotyping performed at week 18 of the study demonstrated that mice in the weight cycling group lose weight and become glucose tolerant when switched from a HF diet to a LF diet (Figure 6.3). In fact, at this time-point, the weight cycling mice have completely normalized to the body weight/composition and glucose tolerance of mice maintained on a LF diet for the duration of the study. These data indicate that glucose intolerance does not precede weight re-gain during this weight cycling protocol, and suggests that weight cycling, *per se*, is responsible for the metabolic dysfunction observed at the end of the study.

Our data demonstrate that weight cycling increases the accumulation of $CD4^+$ and $CD8^+$ T cells in the AT. Furthermore, gene expression of T_H1-derived cytokines and cytokine receptors, including *Ifng*, *Il12*, *Il2*, and *Il2rb*, was increased in the AT of weight-cycled mice when compared to mice maintained on

a HF diet (Figure 6.9). Recent studies have shown that mice lacking certain T cell-derived cytokines or pro-inflammatory T cell subsets are protected from many of the pathologies associated with obesity. For example, HF diet-induced glucose intolerance and AT inflammation is ameliorated in IFN-γ KO mice (222). Additionally, deletion of $CD8^+$ T cells improves systemic glucose tolerance and insulin sensitivity (113). These published studies suggest that increased T cell-mediated inflammation in the AT may contribute to the impaired AT insulin sensitivity and systemic glucose intolerance observed during weight cycling. In addition, we have performed regression analysis to determine if there is a correlation between AT T cell content and glucose tolerance in the mice in our study (Figure 6.14). These analyses demonstrate that impaired glucose tolerance (increased AUC of GTT) is significantly and positively correlated with the percent of $CD4^+$ and $CD8^+$ T cells in the AT, as well as the gene expression of the T_H1-derived cytokines, *Ifng* and *Il2* (Figure 6.14). Interestingly, when these correlations were corrected for changes in ATM number, the association remained significant. Therefore, these findings reinforce the conclusion that an increase in inflammatory T cell subsets, but not macrophages, in the AT during weight cycling contributes to impaired metabolic fitness.

Nishimura, *et al*. showed that $CD8^+$ T cell accumulation in AT preceded and was required for the infiltration of ATMs during obesity, suggesting that T cell-derived signals may direct the innate immune response in AT (113). However, subsequent findings have called this concept into question: two other studies have found that T cells actually accumulate in the AT well after ATM

infiltration is observed (114; 131). The reason for these differential findings is not clear, but this controversy does challenge the hypothesis that T cells "direct" macrophage infiltration into obese AT. Nevertheless, it has been shown that $CD8^+$ T cell depletion decreases AT inflammation and macrophage content (113); although the deletion of cytotoxic T cells does not completely normalize ATM content/inflammation to lean levels (113), suggesting that T cell-independent regulation of ATM accumulation does exist. Moreover, while T cell-derived cytokines have been shown to directly impact macrophages, these cytokines can also have an effect on other non-immune cells. For example, T cell-derived IFN-γ induces IR in adipocytes (223). Our data demonstrate that weight cycling increases AT IR and T cell content in the absence of a change in ATM number or phenotype. Therefore, these findings support the recently emerging concept that alterations in AT T cell populations may not always be accompanied by modulation of ATMs.

Adaptive immunity, in contrast to innate immunity, is characterized by an antigen-specific immune response that results in the formation and maintenance of memory cells. These long-lived memory cells are capable of mounting a more rapid and potent secondary immune response upon re-exposure to the same antigen (224). Interestingly, T cells in obese AT express a restricted T cell receptor repertoire, suggesting that these immune cells may recognize self-antigen in AT during obesity (113; 205; 206). Additionally, multiple studies, including our own (Figure 6.11), have shown that effector memory T cells accumulate in AT after HF diet feeding (129; 130). While the identity of the obese

AT antigens are not known, the concept of an antigen-specific T cell immune response during obesity has great implications for our current findings. Weight re-gain may “re-expose” T cells to obese AT antigens. Therefore, it is interesting to speculate that the increased accumulation of T cells observed in AT during weight cycling may be the result of a more potent and rapid memory cell-mediated secondary immune response. In fact, in our current study, the weight cycled mice trended towards a further increase in AT $CD8^+$ effector memory T cell number (Figure 6.11). Additional studies to establish whether effector memory T cells proliferate more rapidly during weight re-gain could confirm this hypothesis.

Our studies demonstrate that weight cycling increases systemic glucose intolerance and decreases AT insulin signaling. IR in the AT is a key contributor to systemic glucose intolerance during obesity; however, other metabolic tissues also play a significant role in maintaining glucose homeostasis. We have demonstrated that weight cycling impairs liver, but not muscle, insulin signaling. Thus, while our current report focuses on AT immune composition and IR, the impact of weight cycling on liver insulin sensitivity is an important area of future investigation.

Taken together, our studies show that weight cycling modulates AT T cell composition. These findings have important implications regarding the role of antigen-specific immune responses in the AT. The increase in pro-inflammatory T cell populations suggests that an exaggerated adaptive immune response in the AT contributes to the negative metabolic consequences of weight cycling.

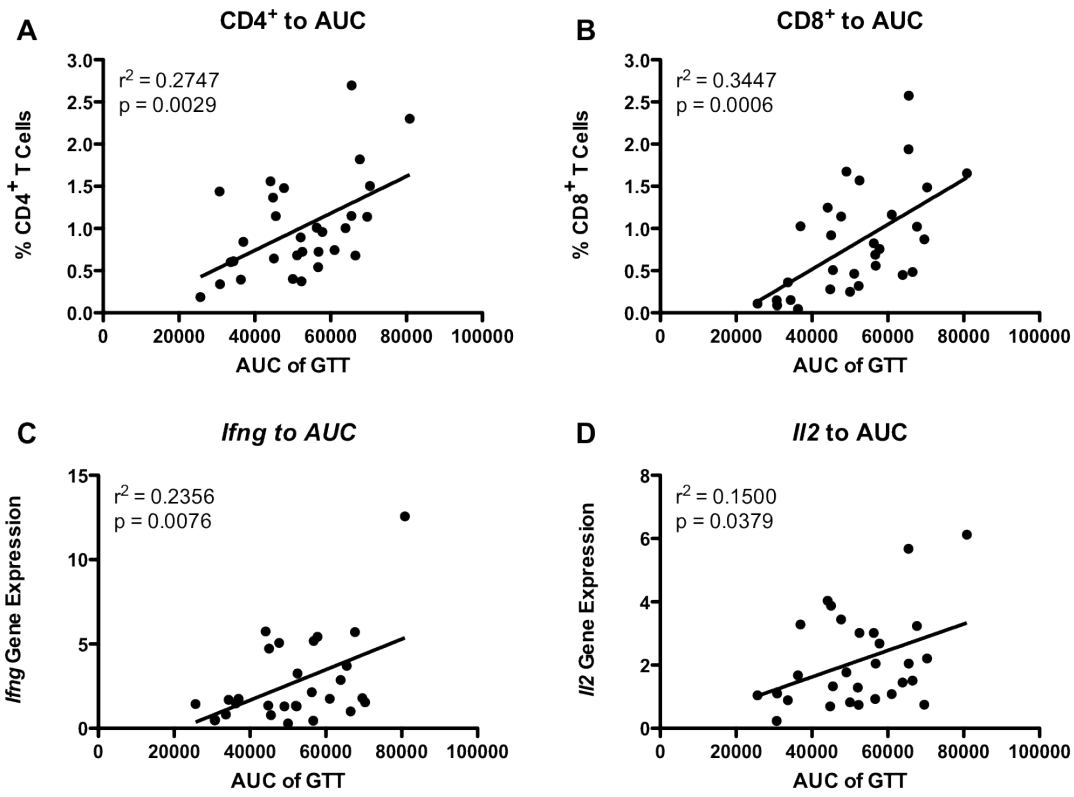

Figure 6.14: Correlation between immune cells/cytokine expression and glucose tolerance. Flow cytometry or real-time RT-PCR data from all groups was correlated with the area under the curve of the glucose tolerance test (Figure 2C, inset). A: Correlation between $CD4^+$ T cells and AUC of GTT. B: Correlation between $CD8^+$ T cells and AUC of GTT. C: Correlation between *Ifng* gene expression and AUC of GTT. D: Correlation between *Il2* gene expression and AUC of GTT.

CHAPTER VII

SUMMARY AND CONCLUSIONS

Obesity is a global epidemic effecting individuals of every age, sex, race, and socioeconomic status. Current estimates indicate that nearly two-thirds of American adults are either overweight or obese (2). The cost of treating diseases associated with obesity, including T2D and CVD, is a startling $147 billion per year (4; 6). Therefore, a better comprehension of the negative consequences of obesity is critical to the health and welfare of our society. A major breakthrough in the understanding of mechanisms by which obesity promotes metabolic dysfunction occurred one decade ago when it was discovered that pro-inflammatory immune cells, including macrophages, accumulate in obese AT and promote IR both locally and systemically (34; 35). Over the past 10 years, research in this newly emerging field of “immunometabolism” has begun to define the composition and activation status of AT-resident immune cells and has shed light upon the contribution of these cells to AT dysfunction during obesity.

Interestingly, many of the initial studies performed in the ATM field have been designed with the hypothesis that the biology of ATMs would be similar to the parameters already defined for macrophages of atherosclerotic lesions. This concept has led to many assumptions within the field; however, many of these expectations have not held up to rigorous experimentation. Below, I will discuss how the research performed during the completion of this dissertation has challenged and modified commonly held assumptions. Additionally, I will discuss

how these studies have begun to address multiple understudied areas in the newly emerging field of immunometabolism.

ATM lipotoxicity

Previous studies have established that accumulation of cholesterol in macrophages of atherosclerotic lesions increases inflammation and ER stress-mediated cell death, thus promoting atherogenesis (225). Therefore, it was assumed that increased FFA flux during obesity would promote lipid accumulation in ATMs, resulting in macrophage inflammation and lipotoxicity (76). In support of this hypothesis, obesity increases lipid storage in ATMs (75; 76). In addition, *in vitro* studies such as those presented in Chapter III of this dissertation have demonstrated that saturated FFAs activate inflammatory signaling in peritoneal macrophages, leading to ER stress-mediated apoptosis. However, our *in vivo* findings indicate that pharmacological activation of AT lipolysis does not promote inflammation, ER stress signaling, or apoptosis in ATMs (Chapter III). Additionally, we have found that obesity actually decreases ATM apoptosis (Chapter IV), suggesting that lipotoxicity does not occur in this cell population. In support of these findings, recent data presented at a Keystone Symposium indicate that lipid-laden AT foam cells are not significantly more inflammatory than non lipid-loaded macrophages (Shoelson and Glass, unpublished). Therefore, although *in vitro* exposure of macrophages to saturated FFAs increases inflammation and apoptosis, it does not appear as though ATM lipotoxicity occurs *in vivo* during obesity.

There are multiple possible explanations for why macrophage lipotoxicity does not occur in obese AT. First, the majority of FFAs lipolyzed from AT are either re-esterified into triglycerides or transported to peripheral tissues for oxidation (226). Therefore, AT FFA concentrations may not significantly increase during obesity. Second, our laboratory has shown that unsaturated FFAs prevent the lipotoxic effects of saturated FFAs on macrophages (75), suggesting that the mixture of FFAs found *in vivo* may not be sufficient to promote cell death. Interestingly, two recent studies have indicated that, instead of promoting lipotoxicity, increased AT lipolysis may induce chemotactic signals (74) and activate endothelial cells to promote monocyte extravasation into inflamed AT (74; 227).

Macrophage accumulation in AT

Studies in the cardiovascular field have shown that chemokine-mediated recruitment of monocytes to lesional areas plays a key role in the development of atherosclerosis and thrombosis (225). Obese AT secretes high levels of multiple chemokines (78-81), and labeling studies have shown that monocytes are recruited to AT during HF diet feeding (40). These findings have led to the assumption that, similar to what is observed during atherogenesis, monocyte recruitment to AT would be the sole mechanism explaining increased ATM number during obesity. However, recent studies by our laboratory and others have not supported this concept. Deletion of chemokines or chemokine receptors never completely ablates macrophage accumulation in obese AT (86-88; 90-95).

Additionally, mouse models of impaired monocyte mobilization from bone marrow do not demonstrate an equivalent reduction in ATM number during obesity (81; 96; 100).

Together, the above studies suggest that recruitment-independent mechanisms must also exist to regulate ATM number. It is possible that obesity increases ATM proliferation, decreases macrophage egress from AT, or reduces ATM apoptosis and turnover. In Chapter IV, we show that ATM apoptosis occurs in lean AT, is drastically decreased during obesity, and is re-activated during weight loss. Interestingly, the percent of apoptotic macrophages in the AT is negatively correlated with body weight and AT F4/80 gene expression. These findings indicate that macrophage apoptosis in lean AT may serve to promote turnover of ATMs, thus maintaining the proper number of immune cells within the AT. However, during obesity, ATM apoptosis is reduced, potentially leading to decreased cell turnover and increased retention of macrophages in AT. Decreased ATM apoptosis, in the presence of increased monocyte recruitment, could increase the number of pro-inflammatory macrophages in AT. In support of this hypothesis, two separate studies have demonstrated that increasing macrophage apoptosis during obesity decreases ATM number and systemic inflammation and IR (193; 195).

Our findings challenge the assumption that recruitment of macrophage precursors to inflamed tissue is the sole mechanism determining ATM number during obesity. We have shown that ATM apoptosis is a metabolically regulated process that could contribute to macrophage accumulation in obese AT.

Additional research will need to define the relative contributions of monocyte recruitment and macrophage proliferation, egress, and apoptosis to the maintenance of AT homeostasis. However, our exciting and novel findings indicate that drugs designed to induce ATM apoptosis during obesity may be have clinical efficacy.

ER stress in metabolic tissues

Obesity increases ER stress activation in multiple metabolic tissues, including whole AT and liver (164). Additionally, pharmacological reduction of ER stress signaling decreases systemic inflammation and IR (167). As a result of these studies, many in the field have assumed that ER stress activation in metabolic tissues is always detrimental. However, ER stress signaling often serves an adaptive role, either by allowing cells to secrete high levels of proteins (139) or by promoting cell turnover (228).

The previous studies demonstrating that ER stress contributes to metabolic dysfunction during obesity evaluated ER stress activation at the whole tissue level. However, our studies indicate that ER stress signaling is differentially regulated in parenchymal cells versus AT-resident immune cells (Chapter V). In contrast to what is observed in whole AT, we have found that obesity actually decreases ER stress signaling specifically in the macrophage-enriched SVF of AT. In addition, weight loss restores ATM ER stress activation to levels near what is observed in lean AT. The fact that macrophage ER stress activation is higher in healthy, non-inflamed AT suggests that this signaling

pathway may play a different role in immune cells than in adipocytes. Although our studies demonstrate that ER stress signaling does not promote ATM apoptosis and turnover *in vivo*, recent data indicate that this pathway may be essential for polarization of macrophages to an M2 phenotype (204). If this hypothesis is correct, decreasing ER stress in parenchymal cells may prevent inflammation, but reducing the activation of this signaling pathway in AT-resident macrophages could promote polarization to a pro-inflammatory M1 phenotype. Therefore, the beneficial systemic effects of ER stress inhibition (167) may be augmented if PBA treatment were targeted specifically to parenchymal cells and not immune cells.

Weight loss

In the 10 years since the discovery that pro-inflammatory macrophages promote AT IR, extensive research has focused on defining the time-course of immune cell accumulation and activation in AT during obesity (36). In contrast, very few studies have sought to understand the events occurring in AT during weight loss. Published findings (41; 74; 132) and our data presented in Chapters IV and VI demonstrate that weight loss reduces ATM number and decreases systemic inflammation and IR; however, mechanisms contributing to the improved AT phenotype during weight loss are not known. In Chapters IV and V of this dissertation, we demonstrate that ATM ER stress and apoptosis are increased during weight loss. It is possible that activation of these signaling pathways during weight loss promotes M2 polarization and enhances turnover of

ATMs, thus decreasing AT inflammation and macrophage content. An increased understanding of the mechanisms involved in the restoration of AT homeostasis during weight loss could lead to the development of novel therapeutics to target macrophages in obese AT.

Weight cycling

Weight loss is the ideal means to decrease the negative metabolic consequences associated with obesity. However, long-term maintenance of substantial weight loss is difficult to achieve, resulting in weight cycling. The majority of the literature on weight cycling was published several decades ago and sought to determine if fluctuations in body weight have a negative impact upon food efficiency or energy requirements (229-235). While this literature is controversial, additional studies have shown that weight cycling increases the risk of developing IR, T2D, and CVD (134-136; 220; 221). However, the mechanisms by which weight cycling promotes metabolic dysfunction are unknown. The data presented in Chapter VI demonstrate that in an extreme model of weight cycling, the number of pro-inflammatory T cells, but not macrophages, is increased in AT. This T cell-driven inflammation likely contributes to the increased AT IR and systemic glucose intolerance observed during weight cycling. These findings are the first to demonstrate a potential mechanism for increased metabolic dysfunction as a result of weight cycling.

Additionally, these studies give insight into the nutritional regulation of antigen-specific adaptive immune responses in AT. Previous studies have

suggested that T cells accumulate in obese AT in response to an unknown antigen (113; 116). Because weight cycling modulates adaptive, but not innate, immune cell populations, it is possible that a local secondary immune response occurs in AT. Initial weight gain may activate a primary immune response within AT, while weight cycling re-exposes the obese AT antigen(s) and induces a memory T cell-mediated secondary immune response. The above findings emphasize the importance of maintaining weight loss, as weight re-gain increases metabolic dysfunction and AT inflammation, potentially via an antigen-driven secondary immune response.

Relevance to human obesity

The ultimate goal of this dissertation work is to increase the understanding of human obesity and diabetes. As such, it is imperative to consider the benefits and limitations of the use of the mouse as a model system for human metabolic syndrome and inflammation. Similar to what is observed in the mouse, human obesity results in accumulation of pro-inflammatory macrophages (34) and T cells (110; 112; 113; 185) in subcutaneous and visceral AT. Our findings indicate that increasing ATM apoptosis during obesity may have beneficial clinical effects (Chapter IV). In support of this hypothesis, recent human data indicate that insulin-sensitizing TZDs decrease macrophage accumulation in the AT of obese individuals via an increase in the apoptosis of these immune cells (193; 194). In addition, our data show that a mouse model of weight cycling recapitulates the metabolic dysfunction observed in humans (Chapter VI), and suggest that

alterations in the immunometabolic function of AT may underlie these systemic abnormalities. Therefore, studies in humans support many of the findings presented in this dissertation, indicating that mice are an appropriate model system in which to study metabolic syndrome.

Although human obesity is associated with an accumulation of immune cells in the AT, recent evidence indicates that activation of systemic inflammatory pathways in response to acute stressors such as trauma, burn, and endotoxemia may vary widely between the mouse and the human (236). Therefore, it is possible that obesity could activate different inflammatory pathways in these two species. However, recent genome-wide association studies have shown significant overlap between genes associated with obesity and body mass index in mouse models and humans (237), indicating that mice may appropriately mimic human obesity. Despite these similarities, multiple anti-inflammatory therapies that have shown promising results in obese mouse models have been relatively ineffective in clinical trials (238). These findings emphasize the importance of verifying data obtain from model systems before continuing to clinical trials. However, the mouse model remains an important and valid system in which to discover novel processes and signaling pathways occurring during obesity and inflammation.

Conclusions

Overall, the studies in this dissertation have shown the dynamic regulation of AT immune cell populations during obesity, weight loss, and weight cycling.

These findings have modified commonly held assumptions in our field and have begun to address understudied aspects of immunometabolism. Although *in vitro* accumulation of saturated FFAs in macrophages results in ER stress-mediated apoptosis (Chapter III), we have shown that these pathways are not activated in ATMs during obesity (Chapters III and IV). In fact, ATM apoptosis is actually *decreased* during obesity. Additionally, weight loss increases macrophage apoptosis to levels near what is observed in lean AT. These findings suggest that ATM apoptosis is a metabolically regulated, recruitment-independent mechanism that contributes to the accumulation of pro-inflammatory macrophages in AT (Chapters IV and V). In addition, studies in this dissertation have provided insight into the changes occurring in the AT during weight cycling (Chapter VI). Our findings suggest that weight re-gain may activate a nutritionally regulated secondary immune response in the AT, leading to increase inflammation and IR. See Figure 7.1 for an overall model of the contributions that this dissertation research has made to the field of immunometabolism.

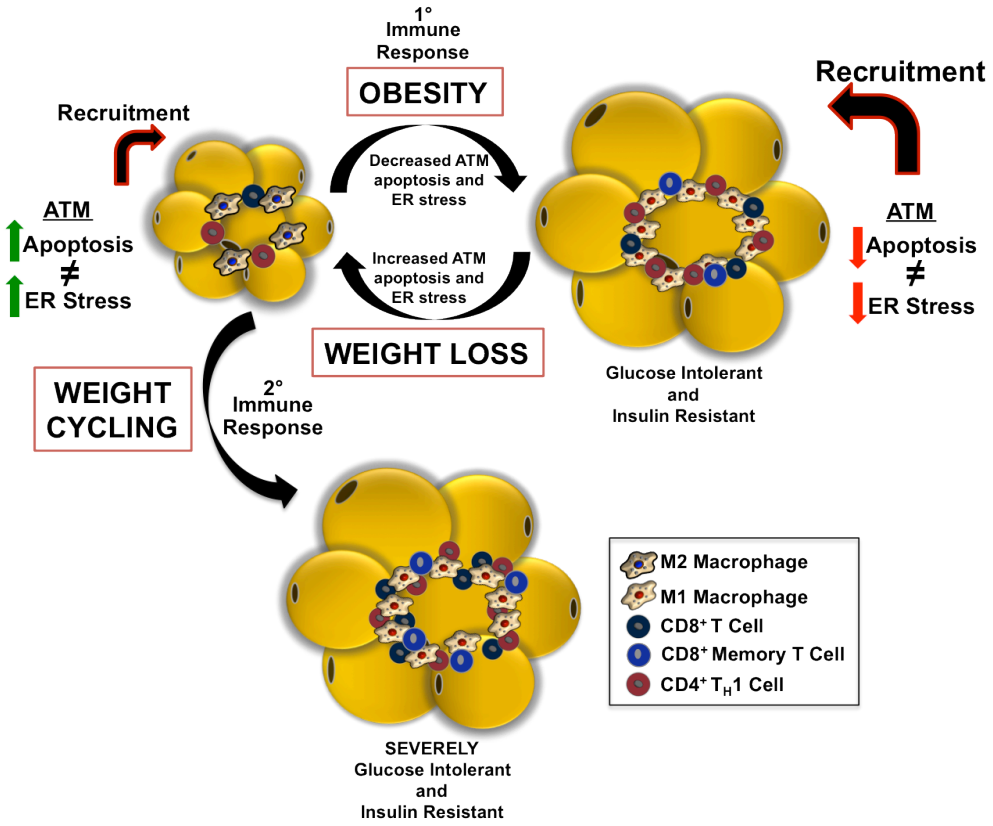

Figure 7.1: Overall contribution of dissertation research to the field of immunometabolism. The studies in this dissertation have further defined the changes occurring in AT immune cell populations during various nutritional conditions including obesity, weight loss, and weight cycling. Our findings indicate that macrophage apoptosis is a metabolically regulated process that contributes to the maintenance and restoration of AT homeostasis. Additionally, our studies demonstrate that weight cycling increases AT T cell numbers, suggesting that a secondary adaptive immune response may occur in the AT.

CHAPTER VIII

FUTURE DIRECTIONS

Chapter III: Intracellular accumulation of saturated FFAs in macrophages activates inflammatory signaling, leading to ER stress-mediated apoptosis. Interestingly, FFA-induced inflammation was not initiated through the extracellular receptors, TLR2 and 4. However, the mechanism(s) by which intracellular FFAs do activate inflammation is not known and future studies will address this important area. A recent study has suggested that saturated FFAs activate inflammatory signaling in fibroblasts not by interacting with extracellular receptors, but by modulating the lipid composition of the cell membrane. Specifically, palmitic acid was found to increase the partitioning of c-Src, an inflammatory tyrosine kinase, to lipid raft regions of the cell membrane, thus facilitating the signaling of this kinase (178). Upon FFA stimulation, raft-associated c-Src was able to activate JNK, leading to an inflammatory cascade (178). Future studies could determine if intracellular accumulation of stearic acid in macrophages initiates inflammatory signaling by increasing lipid raft stability and activating membrane-associated kinases, including c-Src.

Chapter IV: The findings presented in this chapter demonstrate that ATM apoptosis is decreased as a result of diet- or genetic-induced obesity. In addition, weight loss restores ATM apoptosis to levels close to those seen in lean AT.

These findings suggest that ATM apoptosis may be a recruitment-independent mechanism by which AT homeostasis is maintained and restored. Many exciting future directions are being pursued based upon these findings:

1) Generation of a mouse model of impaired ATM apoptosis: In response to death signals, the pro-apoptotic Bcl-2 family members, Bax and Bak, oligomerize in the mitochondrial outer membrane. Mitochondrial permeabilization results in the release of cytochrome c and subsequent activation of the caspase cascade. Cells lacking either *Bax* or *Bak* display normal apoptotic responses; however, deletion of both genes confers resistance to multiple apoptotic stimuli. To determine the consequences of impaired macrophage apoptosis, we will cross *Bak* KO, *Bax* fl/fl mice with mice expressing Cre recombinase under the macrophage-specific promoter, LysM. We hypothesis that inhibition of macrophage apoptosis in lean mice will increase ATM content, leading to local and systemic metabolic dysfunction.

2) To determine the signal(s) that regulate macrophage apoptosis in lean tissue: Our hypothesis is that ATM apoptosis in lean mice is a regulated process that contributes to the proper turnover of these cells. Therefore, cytokines or cells that are present at a higher level in lean compared to obese AT may initiate apoptotic signaling. Two possible candidates are the insulin sensitizing adipokine, adiponectin, and the innate immune cell, the eosinophil. Our preliminary data show that *in vitro* treatment of primary mouse macrophages with adiponectin increases apoptosis. Additionally, in a mouse model of AT eosinophilia (CCR2 KO mice, (88)), we have observed a significant increase in

ATM apoptosis. In fact, the increased ATM apoptosis was positively correlated with markers of eosinophils. Future studies will determine whether adiponectin or eosinophils are necessary to promote macrophage apoptosis and turnover in AT.

3) To determine the signal(s) that impair ATM apoptosis during obesity: Obesity is associated with chronic low-grade inflammation and activation of NF-κB in ATMs (36). NF-κB is classically known as a pro-inflammatory transcription factor (199); however, this protein also possesses potent anti-apoptotic properties (197). Therefore, it is possible that activation of NF-κB may prevent normal macrophage apoptosis in the AT of obese animals. Mouse models of macrophage-specific NF-κB activation and inhibition will be utilized to test this hypothesis.

4) To determine if obesity impairs ATM apoptosis in humans: We are currently working with the Naji Abumurad laboratory at Vanderbilt University to obtain human samples for confocal analysis of ATM apoptosis.

Chapter V: The results of the studies in this chapter indicate that ER stress pathways are increased in the SVF of lean AT, decreased during obesity, and re-activated during weight loss. In the previous chapter, we demonstrated that ATM apoptosis is regulated in a similar manner, leading to the hypothesis that ER stress-mediated apoptosis may occur in macrophages residing in lean AT. However, deletion of CHOP, the primary protein involved in ER stress-mediated apoptosis, did not modulate ATM apoptosis, suggesting that ER stress is not leading to apoptosis. Future studies will determine the non-apoptotic role of ER

stress signaling in lean ATMs. A recent study has shown that ER stress activation is critical for *in vitro* polarization of macrophages to an anti-inflammatory M2 phenotype (204). Therefore, it is possible that the increased ER stress observed in lean ATMs is indicative of increased M2 polarization. Decreasing ER stress signaling in lean ATMs via genetic or pharmacological means may decrease M2 macrophage polarization, leading to metabolic dysfunction.

Chapter VI: In this chapter, we demonstrate that a mouse model of weight cycling recapitulates the metabolic dysfunction reported in multiple human studies. Accompanying these metabolic defects was a decrease in AT insulin signaling and an increase in the number of $CD4^+$ T_H1 cells and $CD8^+$ cytotoxic T cells in the AT. Additionally, $CD8^+$ effector memory T cells were present in the AT of obese and weight-cycled mice. Future directions associated with these findings are listed below:

1) To determine if weight cycling induces a T cell-driven secondary immune response in AT: Our preliminary studies show an enhanced T cell response and the presence of $CD8^+$ effector memory T cells in the AT of weight-cycled mice. However, we have not determined whether this amplified response is indicative of a local secondary immune response in the AT. To test this hypothesis, we will perform two separate experiments.

i. Mice will be taken through the weight cycling protocol, while blocking the influx of T cells into the AT during the initial phase of weight gain using anti-CD8

or CD4 antibody. This experimental design will allow us to test the hypothesis that inhibition of T cell infiltration during the first phase of weight gain will ameliorate the secondary immune response during subsequent weight gain. If our hypothesis is correct, we would expect that blocking the initial influx of T cells into obese AT would eliminate the increased immunological and metabolic dysfunction observed during weight cycling. These studies will also allow us to determine whether a cause-effect relationship exists between T cell accumulation in AT and systemic glucose intolerance during weight cycling.

ii. Next, we want to determine whether subsequent exposure of AT T cells to obese AT antigens is sufficient to recapitulate the immunological and metabolic defects associated with weight cycling. “Antigen-experienced” T cells from the AT of obese mice or “antigen-naïve” cells from lean mice will be adoptively transferred to chow-fed mice that are then placed on a HF diet. Using this study design, the recipient mice will not be weight-cycled; however, the “antigen-experienced” T cells originally isolated from the AT of HF fed mice will have experienced two phases of weight gain. Our hypothesis is that “antigen-experienced” T cells isolated from the AT of HF fed mice will exhibit a secondary immune response during weight gain, while “antigen-naïve” T cells isolated from lean mice will display a less inflammatory primary immune response.

2) To determine if IFN-γ is necessary for the metabolic consequences of weight cycling: The experiments outlined above will determine whether a T cell-driven secondary immune response occurs during weight cycling. However,

the mechanism(s) by which T cells contribute to the metabolic defects associated with weight cycling remain unknown. As shown in Figure 6.9D, weight cycling increases AT expression of *Ifng,* an immunomodulatory cytokine secreted by $CD4^+$ T_H1 cells, $CD8^+$ T cells, and NK cells (216). Published data demonstrate that IFN-γ contributes to obesity-associated systemic glucose intolerance and AT inflammation (222). Therefore, we hypothesize that weight-cycled IFN-KO mice will not exhibit the increased metabolic dysfunction observed during weight cycling in WT mice.

In conclusion, the studies performed during the completion of this dissertation have provided insight into the dynamic regulation of AT immune cell composition during various metabolic conditions including obesity, weight loss, and weight cycling. These findings suggest that recruitment-independent processes exist to regulate ATM number, and that weight cycling initiates a local secondary adaptive immune response in AT. Thus, this body of work has increased the understanding of mechanisms and consequences of immune cell accumulation in AT.

REFERENCES

1. Anderson EK, Gutierrez DA, Hasty AH: Adipose tissue recruitment of leukocytes. Curr Opin Lipidol 21:172-177
2. Flegal KM, Carroll MD, Ogden CL, Curtin LR: Prevalence and trends in obesity among US adults, 1999-2008. JAMA 303:235-241
3. Ogden CL, Carroll MD, Kit BK, Flegal KM: Prevalence of obesity and trends in body mass index among US children and adolescents, 1999-2010. JAMA : the journal of the American Medical Association 2012;307:483-490
4. Jeffrey Levi LMS, Rebecca St. Laurent, Albert Land, Jack Rayburn: F as in Fat: How Obesity Threatens America's Future. 2012;
5. Whitlock G, Lewington S, Sherliker P, Clarke R, Emberson J, Halsey J, Qizilbash N, Collins R, Peto R: Body-mass index and cause-specific mortality in 900 000 adults: collaborative analyses of 57 prospective studies. Lancet 2009;373:1083-1096
6. Finkelstein EA, Trogdon JG, Cohen JW, Dietz W: Annual medical spending attributable to obesity: payer-and service-specific estimates. Health Aff (Millwood) 2009;28:w822-831
7. Guo SS, Chumlea WC: Tracking of body mass index in children in relation to overweight in adulthood. Am J Clin Nutr 1999;70:145S-148S
8. Narayan KM, Boyle JP, Thompson TJ, Sorensen SW, Williamson DF: Lifetime risk for diabetes mellitus in the United States. JAMA : the journal of the American Medical Association 2003;290:1884-1890
9. Johnson AR, Milner JJ, Makowski L: The inflammation highway: metabolism accelerates inflammatory traffic in obesity. Immunol Rev 2012;249:218-238
10. Hotamisligil GS, Budavari A, Murray D, Spiegelman BM: Reduced tyrosine kinase activity of the insulin receptor in obesity-diabetes. Central role of tumor necrosis factor-alpha. The Journal of clinical investigation 1994;94:1543-1549
11. Hotamisligil GS, Murray DL, Choy LN, Spiegelman BM: Tumor necrosis factor alpha inhibits signaling from the insulin receptor. Proc Natl Acad Sci U S A 1994;91:4854-4858
12. Bandyopadhyay GK, Yu JG, Ofrecio J, Olefsky JM: Increased p85/55/50 expression and decreased phosphotidylinositol 3-kinase activity in insulin-resistant human skeletal muscle. Diabetes 2005;54:2351-2359
13. Hirosumi J, Tuncman G, Chang L, Gorgun CZ, Uysal KT, Maeda K, Karin M, Hotamisligil GS: A central role for JNK in obesity and insulin resistance. Nature 2002;420:333-336
14. Itani SI, Ruderman NB, Schmieder F, Boden G: Lipid-induced insulin resistance in human muscle is associated with changes in diacylglycerol, protein kinase C, and IkappaB-alpha. Diabetes 2002;51:2005-2011
15. Chang-Chen KJ, Mullur R, Bernal-Mizrachi E: Beta-cell failure as a complication of diabetes. Rev Endocr Metab Disord 2008;9:329-343
16. Kennedy GC: The role of depot fat in the hypothalamic control of food intake in the rat. Proc R Soc Lond B Biol Sci 1953;140:578-596
17. Greenberg AS, Obin MS: Obesity and the role of adipose tissue in inflammation and metabolism. Am J Clin Nutr 2006;83:461S-465S

18. Coleman DL: Effects of parabiosis of obese with diabetes and normal mice. Diabetologia 1973;9:294-298
19. Zhang Y, Proenca R, Maffei M, Barone M, Leopold L, Friedman JM: Positional cloning of the mouse obese gene and its human homologue. Nature 1994;372:425-432
20. Campfield LA, Smith FJ, Guisez Y, Devos R, Burn P: Recombinant mouse OB protein: evidence for a peripheral signal linking adiposity and central neural networks. Science 1995;269:546-549
21. Halaas JL, Gajiwala KS, Maffei M, Cohen SL, Chait BT, Rabinowitz D, Lallone RL, Burley SK, Friedman JM: Weight-reducing effects of the plasma protein encoded by the obese gene. Science 1995;269:543-546
22. Pelleymounter MA, Cullen MJ, Baker MB, Hecht R, Winters D, Boone T, Collins F: Effects of the obese gene product on body weight regulation in ob/ob mice. Science 1995;269:540-543
23. Hu E, Liang P, Spiegelman BM: AdipoQ is a novel adipose-specific gene dysregulated in obesity. The Journal of biological chemistry 1996;271:10697-10703
24. Combs TP, Berg AH, Obici S, Scherer PE, Rossetti L: Endogenous glucose production is inhibited by the adipose-derived protein Acrp30. The Journal of clinical investigation 2001;108:1875-1881
25. Wu X, Motoshima H, Mahadev K, Stalker TJ, Scalia R, Goldstein BJ: Involvement of AMP-activated protein kinase in glucose uptake stimulated by the globular domain of adiponectin in primary rat adipocytes. Diabetes 2003;52:1355-1363
26. Yamauchi T, Kamon J, Minokoshi Y, Ito Y, Waki H, Uchida S, Yamashita S, Noda M, Kita S, Ueki K, Eto K, Akanuma Y, Froguel P, Foufelle F, Ferre P, Carling D, Kimura S, Nagai R, Kahn BB, Kadowaki T: Adiponectin stimulates glucose utilization and fatty-acid oxidation by activating AMP-activated protein kinase. Nature medicine 2002;8:1288-1295
27. Wang C, Mao X, Wang L, Liu M, Wetzel MD, Guan KL, Dong LQ, Liu F: Adiponectin sensitizes insulin signaling by reducing p70 S6 kinase-mediated serine phosphorylation of IRS-1. The Journal of biological chemistry 2007;282:7991-7996
28. Hotamisligil GS, Shargill NS, Spiegelman BM: Adipose expression of tumor necrosis factor-alpha: direct role in obesity-linked insulin resistance. Science 1993;259:87-91
29. Hotamisligil GS, Arner P, Caro JF, Atkinson RL, Spiegelman BM: Increased adipose tissue expression of tumor necrosis factor-alpha in human obesity and insulin resistance. The Journal of clinical investigation 1995;95:2409-2415
30. Hotamisligil GS, Spiegelman BM: Tumor necrosis factor alpha: a key component of the obesity-diabetes link. Diabetes 1994;43:1271-1278
31. Berg AH, Scherer PE: Adipose tissue, inflammation, and cardiovascular disease. Circ Res 2005;96:939-949
32. Hotamisligil GS: Inflammation and metabolic disorders. Nature 2006;444:860-867

33. Ravussin E: Adiponectin enhances insulin action by decreasing ectopic fat deposition. Pharmacogenomics J 2002;2:4-7
34. Weisberg SP, McCann D, Desai M, Rosenbaum M, Leibel RL, Ferrante AW, Jr.: Obesity is associated with macrophage accumulation in adipose tissue. J Clin Invest 2003;112:1796-1808
35. Xu H, Barnes GT, Yang Q, Tan G, Yang D, Chou CJ, Sole J, Nichols A, Ross JS, Tartaglia LA, Chen H: Chronic inflammation in fat plays a crucial role in the development of obesity-related insulin resistance. J Clin Invest 2003;112:1821-1830
36. Olefsky JM, Glass CK: Macrophages, inflammation, and insulin resistance. Annu Rev Physiol 2010;72:219-246
37. Mantovani A, Sica A, Sozzani S, Allavena P, Vecchi A, Locati M: The chemokine system in diverse forms of macrophage activation and polarization. Trends Immunol 2004;25:677-686
38. Lumeng CN, Bodzin JL, Saltiel AR: Obesity induces a phenotypic switch in adipose tissue macrophage polarization. J Clin Invest 2007;117:175-184
39. Nguyen MT, Favelyukis S, Nguyen AK, Reichart D, Scott PA, Jenn A, Liu-Bryan R, Glass CK, Neels JG, Olefsky JM: A subpopulation of macrophages infiltrates hypertrophic adipose tissue and is activated by free fatty acids via Toll-like receptors 2 and 4 and JNK-dependent pathways. The Journal of biological chemistry 2007;282:35279-35292
40. Lumeng CN, DelProposto JB, Westcott DJ, Saltiel AR: Phenotypic switching of adipose tissue macrophages with obesity is generated by spatiotemporal differences in macrophage subtypes. Diabetes 2008;57:3239-3246
41. Li P, Lu M, Nguyen MT, Bae EJ, Chapman J, Feng D, Hawkins M, Pessin JE, Sears DD, Nguyen AK, Amidi A, Watkins SM, Nguyen U, Olefsky JM: Functional heterogeneity of CD11c-positive adipose tissue macrophages in diet-induced obese mice. The Journal of biological chemistry 2010;285:15333-15345
42. Patsouris D, Li PP, Thapar D, Chapman J, Olefsky JM, Neels JG: Ablation of CD11c-positive cells normalizes insulin sensitivity in obese insulin resistant animals. Cell metabolism 2008;8:301-309
43. Takeda K, Akira S: Toll-like receptors in innate immunity. Int Immunol 2005;17:1-14
44. Guha M, Mackman N: LPS induction of gene expression in human monocytes. Cell Signal 2001;13:85-94
45. Caricilli AM, Nascimento PH, Pauli JR, Tsukumo DM, Velloso LA, Carvalheira JB, Saad MJ: Inhibition of toll-like receptor 2 expression improves insulin sensitivity and signaling in muscle and white adipose tissue of mice fed a high-fat diet. J Endocrinol 2008;199:399-406
46. Lee JY, Zhao L, Youn HS, Weatherill AR, Tapping R, Feng L, Lee WH, Fitzgerald KA, Hwang DH: Saturated fatty acid activates but polyunsaturated fatty acid inhibits Toll-like receptor 2 dimerized with Toll-like receptor 6 or 1. The Journal of biological chemistry 2004;279:16971-16979
47. Shi H, Kokoeva MV, Inouye K, Tzameli I, Yin H, Flier JS: TLR4 links innate immunity and fatty acid-induced insulin resistance. J Clin Invest 2006;116:3015-3025

48. Erridge C, Samani NJ: Saturated fatty acids do not directly stimulate Toll-like receptor signaling. Arteriosclerosis, thrombosis, and vascular biology 2009;29:1944-1949
49. Himes RW, Smith CW: Tlr2 is critical for diet-induced metabolic syndrome in a murine model. Faseb J 2010;24:731-739
50. Suganami T, Mieda T, Itoh M, Shimoda Y, Kamei Y, Ogawa Y: Attenuation of obesity-induced adipose tissue inflammation in C3H/HeJ mice carrying a Toll-like receptor 4 mutation. Biochem Biophys Res Commun 2007;354:45-49
51. Poggi M, Bastelica D, Gual P, Iglesias MA, Gremeaux T, Knauf C, Peiretti F, Verdier M, Juhan-Vague I, Tanti JF, Burcelin R, Alessi MC: C3H/HeJ mice carrying a toll-like receptor 4 mutation are protected against the development of insulin resistance in white adipose tissue in response to a high-fat diet. Diabetologia 2007;50:1267-1276
52. Davis JE, Gabler NK, Walker-Daniels J, Spurlock ME: Tlr-4 deficiency selectively protects against obesity induced by diets high in saturated fat. Obesity (Silver Spring) 2008;16:1248-1255
53. Saberi M, Woods NB, de Luca C, Schenk S, Lu JC, Bandyopadhyay G, Verma IM, Olefsky JM: Hematopoietic cell-specific deletion of toll-like receptor 4 ameliorates hepatic and adipose tissue insulin resistance in high-fat-fed mice. Cell Metab 2009;10:419-429
54. Orr JS, Puglisi MJ, Ellacott KL, Lumeng CN, Wasserman DH, Hasty AH: Toll-like receptor 4 deficiency promotes the alternative activation of adipose tissue macrophages. Diabetes 2012;61:2718-2727
55. Solinas G, Vilcu C, Neels JG, Bandyopadhyay GK, Luo JL, Naugler W, Grivennikov S, Wynshaw-Boris A, Scadeng M, Olefsky JM, Karin M: JNK1 in hematopoietically derived cells contributes to diet-induced inflammation and insulin resistance without affecting obesity. Cell metabolism 2007;6:386-397
56. Han MS, Jung DY, Morel C, Lakhani SA, Kim JK, Flavell RA, Davis RJ: JNK expression by macrophages promotes obesity-induced insulin resistance and inflammation. Science 2013;339:218-222
57. Arkan MC, Hevener AL, Greten FR, Maeda S, Li ZW, Long JM, Wynshaw-Boris A, Poli G, Olefsky J, Karin M: IKK-beta links inflammation to obesity-induced insulin resistance. Nature medicine 2005;11:191-198
58. Odegaard JI, Ricardo-Gonzalez RR, Goforth MH, Morel CR, Subramanian V, Mukundan L, Red Eagle A, Vats D, Brombacher F, Ferrante AW, Chawla A: Macrophage-specific PPARgamma controls alternative activation and improves insulin resistance. Nature 2007;447:1116-1120
59. Odegaard JI, Ricardo-Gonzalez RR, Red Eagle A, Vats D, Morel CR, Goforth MH, Subramanian V, Mukundan L, Ferrante AW, Chawla A: Alternative M2 activation of Kupffer cells by PPARdelta ameliorates obesity-induced insulin resistance. Cell Metab 2008;7:496-507
60. Ohashi K, Parker JL, Ouchi N, Higuchi A, Vita JA, Gokce N, Amstrup Pedersen A, Kalthoff C, Tullin S, Sams A, Summer R, Walsh K: Adiponectin promotes macrophage polarization towards an anti-inflammatory phenotype. J Biol Chem 2009;

61. Sato K, Imai Y, Higashi N, Kumamoto Y, Onami TM, Hedrick SM, Irimura T: Lack of antigen-specific tissue remodeling in mice deficient in the macrophage galactose-type calcium-type lectin 1/CD301a. Blood 2005;106:207-215
62. Han J, Lee JE, Jin J, Lim JS, Oh N, Kim K, Chang SI, Shibuya M, Kim H, Koh GY: The spatiotemporal development of adipose tissue. Development 2011;138:5027-5037
63. Sun K, Kusminski CM, Scherer PE: Adipose tissue remodeling and obesity. The Journal of clinical investigation 2011;121:2094-2101
64. Faust IM, Johnson PR, Stern JS, Hirsch J: Diet-induced adipocyte number increase in adult rats: a new model of obesity. Am J Physiol 1978;235:E279-286
65. Trayhurn P: Hypoxia and adipose tissue function and dysfunction in obesity. Physiol Rev 2013;93:1-21
66. Cinti S, Mitchell G, Barbatelli G, Murano I, Ceresi E, Faloia E, Wang S, Fortier M, Greenberg AS, Obin MS: Adipocyte death defines macrophage localization and function in adipose tissue of obese mice and humans. J Lipid Res 2005;46:2347-2355
67. Alkhouri N, Gornicka A, Berk MP, Thapaliya S, Dixon LJ, Kashyap S, Schauer PR, Feldstein AE: Adipocyte apoptosis, a link between obesity, insulin resistance, and hepatic steatosis. The Journal of biological chemistry 2010;285:3428-3438
68. Murano I, Barbatelli G, Parisani V, Latini C, Muzzonigro G, Castellucci M, Cinti S: Dead adipocytes, detected as crown-like structures, are prevalent in visceral fat depots of genetically obese mice. Journal of lipid research 2008;49:1562-1568
69. Pajvani UB, Trujillo ME, Combs TP, Iyengar P, Jelicks L, Roth KA, Kitsis RN, Scherer PE: Fat apoptosis through targeted activation of caspase 8: a new mouse model of inducible and reversible lipoatrophy. Nature medicine 2005;11:797-803
70. Feng D, Tang Y, Kwon H, Zong H, Hawkins M, Kitsis RN, Pessin JE: High-fat diet-induced adipocyte cell death occurs through a cyclophilin D intrinsic signaling pathway independent of adipose tissue inflammation. Diabetes 2011;60:2134-2143
71. Duncan RE, Ahmadian M, Jaworski K, Sarkadi-Nagy E, Sul HS: Regulation of lipolysis in adipocytes. Annu Rev Nutr 2007;27:79-101
72. Pankow JS, Duncan BB, Schmidt MI, Ballantyne CM, Couper DJ, Hoogeveen RC, Golden SH: Fasting plasma free fatty acids and risk of type 2 diabetes: the atherosclerosis risk in communities study. Diabetes Care 2004;27:77-82
73. Mathew M, Tay E, Cusi K: Elevated plasma free fatty acids increase cardiovascular risk by inducing plasma biomarkers of endothelial activation, myeloperoxidase and PAI-1 in healthy subjects. Cardiovasc Diabetol 2010;9:9
74. Kosteli A, Sugaru E, Haemmerle G, Martin JF, Lei J, Zechner R, Ferrante AW, Jr.: Weight loss and lipolysis promote a dynamic immune response in murine adipose tissue. The Journal of clinical investigation 2010;120:3466-3479
75. Saraswathi V, Hasty AH: Inhibition of long-chain acyl coenzyme A synthetases during fatty acid loading induces lipotoxicity in macrophages. Arterioscler Thromb Vasc Biol 2009;29:1937-1943

76. Prieur X, Mok CY, Velagapudi VR, Nunez V, Fuentes L, Montaner D, Ishikawa K, Camacho A, Barbarroja N, O'Rahilly S, Sethi JK, Dopazo J, Oresic M, Ricote M, Vidal-Puig A: Differential lipid partitioning between adipocytes and tissue macrophages modulates macrophage lipotoxicity and M2/M1 polarization in obese mice. Diabetes 2011;60:797-809
77. Comerford I, McColl SR: Mini-review series: focus on chemokines. Immunol Cell Biol 2011;89:183-184
78. Dahlman I, Kaaman M, Olsson T, Tan GD, Bickerton AS, Wahlen K, Andersson J, Nordstrom EA, Blomqvist L, Sjogren A, Forsgren M, Attersand A, Arner P: A unique role of monocyte chemoattractant protein 1 among chemokines in adipose tissue of obese subjects. J Clin Endocrinol Metab 2005;90:5834-5840
79. Huber J, Kiefer FW, Zeyda M, Ludvik B, Silberhumer GR, Prager G, Zlabinger GJ, Stulnig TM: CC chemokine and CC chemokine receptor profiles in visceral and subcutaneous adipose tissue are altered in human obesity. J Clin Endocrinol Metab 2008;93:3215-3221
80. Kanda H, Tateya S, Tamori Y, Kotani K, Hiasa K, Kitazawa R, Kitazawa S, Miyachi H, Maeda S, Egashira K, Kasuga M: MCP-1 contributes to macrophage infiltration into adipose tissue, insulin resistance, and hepatic steatosis in obesity. J Clin Invest 2006;116:1494-1505
81. Weisberg SP, Hunter D, Huber R, Lemieux J, Slaymaker S, Vaddi K, Charo I, Leibel RL, Ferrante AW, Jr.: CCR2 modulates inflammatory and metabolic effects of high-fat feeding. J Clin Invest 2006;116:115-124
82. Surmi BK, Hasty AH: Macrophage infiltration into adipose tissue: initiation, propagation and remodeling. Future Lipidol 2008;3:545-556
83. Kamei N, Tobe K, Suzuki R, Ohsugi M, Watanabe T, Kubota N, Ohtsuka-Kowatari N, Kumagai K, Sakamoto K, Kobayashi M, Yamauchi T, Ueki K, Oishi Y, Nishimura S, Manabe I, Hashimoto H, Ohnishi Y, Ogata H, Tokuyama K, Tsunoda M, Ide T, Murakami K, Nagai R, Kadowaki T: Overexpression of monocyte chemoattractant protein-1 in adipose tissues causes macrophage recruitment and insulin resistance. J Biol Chem 2006;281:26602-26614
84. Inouye KE, Shi H, Howard JK, Daly CH, Lord GM, Rollins BJ, Flier JS: Absence of CC chemokine ligand 2 does not limit obesity-associated infiltration of macrophages into adipose tissue. Diabetes 2007;56:2242-2250
85. Kirk EA, Sagawa ZK, McDonald TO, O'Brien KD, Heinecke JW: Macrophage chemoattractant protein-1 deficiency fails to restrain macrophage infiltration into adipose tissue. Diabetes 2008;57:1254-1261
86. Tamura Y, Sugimoto M, Murayama T, Ueda Y, Kanamori H, Ono K, Ariyasu H, Akamizu T, Kita T, Yokode M, Arai H: Inhibition of CCR2 ameliorates insulin resistance and hepatic steatosis in db/db mice. Arterioscler Thromb Vasc Biol 2008;28:2195-2201
87. Ito A, Suganami T, Yamauchi A, Degawa-Yamauchi M, Tanaka M, Kouyama R, Kobayashi Y, Nitta N, Yasuda K, Hirata Y, Kuziel WA, Takeya M, Kanegasaki S, Kamei Y, Ogawa Y: Role of CC chemokine receptor 2 in bone marrow cells in the recruitment of macrophages into obese adipose tissue. J Biol Chem 2008;283:35715-35723

88. Gutierrez DA, Kennedy A, Orr JS, Anderson EK, Webb CD, Gerrald WK, Hasty AH: Aberrant accumulation of undifferentiated myeloid cells in the adipose tissue of CCR2-deficient mice delays improvements in insulin sensitivity. Diabetes 2011;60:2820-2829
89. Galastri S, Zamara E, Milani S, Novo E, Provenzano A, Delogu W, Vizzutti F, Sutti S, Locatelli I, Navari N, Vivoli E, Caligiuri A, Pinzani M, Albano E, Parola M, Marra F: Lack of CC chemokine ligand 2 differentially affects inflammation and fibrosis according to the genetic background in a murine model of steatohepatitis. Clin Sci (Lond) 2012;123:459-471
90. Nara N, Nakayama Y, Okamoto S, Tamura H, Kiyono M, Muraoka M, Tanaka K, Taya C, Shitara H, Ishii R, Yonekawa H, Minokoshi Y, Hara T: Disruption of CXC motif chemokine ligand-14 in mice ameliorates obesity-induced insulin resistance. J Biol Chem 2007;282:30794-30803
91. Chavey C, Lazennec G, Lagarrigue S, Clape C, Iankova I, Teyssier J, Annicotte JS, Schmidt J, Mataki C, Yamamoto H, Sanches R, Guma A, Stich V, Vitkova M, Jardin-Watelet B, Renard E, Strieter R, Tuthill A, Hotamisligil GS, Vidal-Puig A, Zorzano A, Langin D, Fajas L: CXC ligand 5 is an adipose-tissue derived factor that links obesity to insulin resistance. Cell Metab 2009;9:339-349
92. Neels JG, Badeanlou L, Hester KD, Samad F: Keratinocyte-derived Chemokine in Obesity: Expression, Rregulation, And Role in Adipose Macrophage Infiltration and Glucose Homeostasis. J Biol Chem 2009;284:20692-20698
93. Kitade H, Sawamoto K, Nagashimada M, Inoue H, Yamamoto Y, Sai Y, Takamura T, Yamamoto H, Miyamoto K, Ginsberg HN, Mukaida N, Kaneko S, Ota T: CCR5 plays a critical role in obesity-induced adipose tissue inflammation and insulin resistance by regulating both macrophage recruitment and M1/M2 status. Diabetes 2012;61:1680-1690
94. Morris DL, Oatmen KE, Wang T, DelProposto JL, Lumeng CN: CX3CR1 deficiency does not influence trafficking of adipose tissue macrophages in mice with diet-induced obesity. Obesity 2012;20:1189-1199
95. Surmi BK, Webb CD, Ristau AC, Hasty AH: Absence of macrophage inflammatory protein-1{alpha} does not impact macrophage accumulation in adipose tissue of diet-induced obese mice. Am J Physiol Endocrinol Metab 2010;299:E437-445
96. Tsou CL, Peters W, Si Y, Slaymaker S, Aslanian AM, Weisberg SP, Mack M, Charo IF: Critical roles for CCR2 and MCP-3 in monocyte mobilization from bone marrow and recruitment to inflammatory sites. The Journal of clinical investigation 2007;117:902-909
97. Gordon S, Taylor PR: Monocyte and macrophage heterogeneity. Nat Rev Immunol 2005;5:953-964
98. Geissmann F, Jung S, Littman DR: Blood monocytes consist of two principal subsets with distinct migratory properties. Immunity 2003;19:71-82
99. Tsou CL, Peters W, Si Y, Slaymaker S, Aslanian AM, Weisberg SP, Mack M, Charo IF: Critical roles for CCR2 and MCP-3 in monocyte mobilization from bone marrow and recruitment to inflammatory sites. J Clin Invest 2007;117:902-909

100. Westcott DJ, Delproposto JB, Geletka LM, Wang T, Singer K, Saltiel AR, Lumeng CN: MGL1 promotes adipose tissue inflammation and insulin resistance by regulating 7/4hi monocytes in obesity. J Exp Med 2009;
101. Thomas J. Kindt RAG, and Barbara A. Osborne: Kuby Immunology. 2007;6
102. Rothenberg ME, Hogan SP: The eosinophil. Annu Rev Immunol 2006;24:147-174
103. Wu D, Molofsky AB, Liang HE, Ricardo-Gonzalez RR, Jouihan HA, Bando JK, Chawla A, Locksley RM: Eosinophils sustain adipose alternatively activated macrophages associated with glucose homeostasis. Science 2011;332:243-247
104. Liu J, Divoux A, Sun J, Zhang J, Clement K, Glickman JN, Sukhova GK, Wolters PJ, Du J, Gorgun CZ, Doria A, Libby P, Blumberg RS, Kahn BB, Hotamisligil GS, Shi GP: Genetic deficiency and pharmacological stabilization of mast cells reduce diet-induced obesity and diabetes in mice. Nat Med 2009;15:940-945
105. Divoux A, Moutel S, Poitou C, Lacasa D, Veyrie N, Aissat A, Arock M, Guerre-Millo M, Clement K: Mast cells in human adipose tissue: link with morbid obesity, inflammatory status, and diabetes. The Journal of clinical endocrinology and metabolism 2012;97:E1677-1685
106. Nathan C: Neutrophils and immunity: challenges and opportunities. Nat Rev Immunol 2006;6:173-182
107. Elgazar-Carmon V, Rudich A, Hadad N, Levy R: Neutrophils transiently infiltrate intra-abdominal fat early in the course of high-fat feeding. Journal of lipid research 2008;49:1894-1903
108. Talukdar S, Oh da Y, Bandyopadhyay G, Li D, Xu J, McNelis J, Lu M, Li P, Yan Q, Zhu Y, Ofrecio J, Lin M, Brenner MB, Olefsky JM: Neutrophils mediate insulin resistance in mice fed a high-fat diet through secreted elastase. Nature medicine 2012;18:1407-1412
109. Schipper HS, Prakken B, Kalkhoven E, Boes M: Adipose tissue-resident immune cells: key players in immunometabolism. Trends Endocrinol Metab 2012;23:407-415
110. Kintscher U, Hartge M, Hess K, Foryst-Ludwig A, Clemenz M, Wabitsch M, Fischer-Posovszky P, Barth TF, Dragun D, Skurk T, Hauner H, Bluher M, Unger T, Wolf AM, Knippschild U, Hombach V, Marx N: T-lymphocyte infiltration in visceral adipose tissue: a primary event in adipose tissue inflammation and the development of obesity-mediated insulin resistance. Arterioscler Thromb Vasc Biol 2008;28:1304-1310
111. Wu H, Ghosh S, Perrard XD, Feng L, Garcia GE, Perrard JL, Sweeney JF, Peterson LE, Chan L, Smith CW, Ballantyne CM: T-cell accumulation and regulated on activation, normal T cell expressed and secreted upregulation in adipose tissue in obesity. Circulation 2007;115:1029-1038
112. Rausch ME, Weisberg S, Vardhana P, Tortoriello DV: Obesity in C57BL/6J mice is characterized by adipose tissue hypoxia and cytotoxic T-cell infiltration. Int J Obes (Lond) 2008;32:451-463
113. Nishimura S, Manabe I, Nagasaki M, Eto K, Yamashita H, Ohsugi M, Otsu M, Hara K, Ueki K, Sugiura S, Yoshimura K, Kadowaki T, Nagai R: CD8+ effector

T cells contribute to macrophage recruitment and adipose tissue inflammation in obesity. Nat Med 2009;15:914-920
114. Strissel KJ, DeFuria J, Shaul ME, Bennett G, Greenberg AS, Obin MS: T-cell recruitment and Th1 polarization in adipose tissue during diet-induced obesity in C57BL/6 mice. Obesity 2010;18:1918-1925
115. Murphy KM, Reiner SL: The lineage decisions of helper T cells. Nat Rev Immunol 2002;2:933-944
116. Winer S, Chan Y, Paltser G, Truong D, Tsui H, Bahrami J, Dorfman R, Wang Y, Zielenski J, Mastronardi F, Maezawa Y, Drucker DJ, Engleman E, Winer D, Dosch HM: Normalization of obesity-associated insulin resistance through immunotherapy. Nat Med 2009;15:921-929
117. Duffaut C, Galitzky J, Lafontan M, Bouloumie A: Unexpected trafficking of immune cells within the adipose tissue during the onset of obesity. Biochem Biophys Res Commun 2009;384:482-485
118. Feuerer M, Herrero L, Cipolletta D, Naaz A, Wong J, Nayer A, Lee J, Goldfine AB, Benoist C, Shoelson S, Mathis D: Lean, but not obese, fat is enriched for a unique population of regulatory T cells that affect metabolic parameters. Nat Med 2009;15:930-939
119. Brigl M, Brenner MB: CD1: antigen presentation and T cell function. Annu Rev Immunol 2004;22:817-890
120. Lynch L, O'Shea D, Winter DC, Geoghegan J, Doherty DG, O'Farrelly C: Invariant NKT cells and CD1d(+) cells amass in human omentum and are depleted in patients with cancer and obesity. Eur J Immunol 2009;39:1893-1901
121. Wu L, Parekh VV, Gabriel CL, Bracy DP, Marks-Shulman PA, Tamboli RA, Kim S, Mendez-Fernandez YV, Besra GS, Lomenick JP, Williams B, Wasserman DH, Van Kaer L: Activation of invariant natural killer T cells by lipid excess promotes tissue inflammation, insulin resistance, and hepatic steatosis in obese mice. Proc Natl Acad Sci U S A 2012;109:E1143-1152
122. Ohmura K, Ishimori N, Ohmura Y, Tokuhara S, Nozawa A, Horii S, Andoh Y, Fujii S, Iwabuchi K, Onoe K, Tsutsui H: Natural Killer T Cells Are Involved in Adipose Tissues Inflammation and Glucose Intolerance in Diet-Induced Obese Mice. Arterioscler Thromb Vasc Biol 2009;
123. Ji Y, Sun S, Xu A, Bhargava P, Yang L, Lam KS, Gao B, Lee CH, Kersten S, Qi L: Activation of natural killer T cells promotes M2 Macrophage polarization in adipose tissue and improves systemic glucose tolerance via interleukin-4 (IL-4)/STAT6 protein signaling axis in obesity. The Journal of biological chemistry 2012;287:13561-13571
124. Lynch L, Nowak M, Varghese B, Clark J, Hogan AE, Toxavidis V, Balk SP, O'Shea D, O'Farrelly C, Exley MA: Adipose tissue invariant NKT cells protect against diet-induced obesity and metabolic disorder through regulatory cytokine production. Immunity 2012;37:574-587
125. Schipper HS, Rakhshandehroo M, van de Graaf SF, Venken K, Koppen A, Stienstra R, Prop S, Meerding J, Hamers N, Besra G, Boon L, Nieuwenhuis EE, Elewaut D, Prakken B, Kersten S, Boes M, Kalkhoven E: Natural killer T cells in adipose tissue prevent insulin resistance. The Journal of clinical investigation 2012;122:3343-3354

126. Mantell BS, Stefanovic-Racic M, Yang X, Dedousis N, Sipula IJ, O'Doherty RM: Mice lacking NKT cells but with a complete complement of CD8+ T-cells are not protected against the metabolic abnormalities of diet-induced obesity. PLoS One 2011;6:e19831
127. Deng T, Lyon CJ, Minze LJ, Lin J, Zou J, Liu JZ, Ren Y, Yin Z, Hamilton DJ, Reardon PR, Sherman V, Wang HY, Phillips KJ, Webb P, Wong ST, Wang RF, Hsueh WA: Class II Major Histocompatibility Complex Plays an Essential Role in Obesity-Induced Adipose Inflammation. Cell metabolism 2013;17:411-422
128. Morris DL, Cho KW, Delproposto JL, Oatmen KE, Geletka LM, Martinez-Santibanez G, Singer K, Lumeng CN: Adipose Tissue Macrophages Function as Antigen Presenting Cells and Regulate Adipose Tissue CD4+ T Cells in Mice. Diabetes 2013;
129. Duffaut C, Zakaroff-Girard A, Bourlier V, Decaunes P, Maumus M, Chiotasso P, Sengenes C, Lafontan M, Galitzky J, Bouloumie A: Interplay between human adipocytes and T lymphocytes in obesity: CCL20 as an adipochemokine and T lymphocytes as lipogenic modulators. Arteriosclerosis, thrombosis, and vascular biology 2009;29:1608-1614
130. Yang H, Youm YH, Vandanmagsar B, Ravussin A, Gimble JM, Greenway F, Stephens JM, Mynatt RL, Dixit VD: Obesity increases the production of proinflammatory mediators from adipose tissue T cells and compromises TCR repertoire diversity: implications for systemic inflammation and insulin resistance. J Immunol 2010;185:1836-1845
131. Winer DA, Winer S, Shen L, Wadia PP, Yantha J, Paltser G, Tsui H, Wu P, Davidson MG, Alonso MN, Leong HX, Glassford A, Caimol M, Kenkel JA, Tedder TF, McLaughlin T, Miklos DB, Dosch HM, Engleman EG: B cells promote insulin resistance through modulation of T cells and production of pathogenic IgG antibodies. Nature medicine 2011;17:610-617
132. Cancello R, Henegar C, Viguerie N, Taleb S, Poitou C, Rouault C, Coupaye M, Pelloux V, Hugol D, Bouillot JL, Bouloumie A, Barbatelli G, Cinti S, Svensson PA, Barsh GS, Zucker JD, Basdevant A, Langin D, Clement K: Reduction of macrophage infiltration and chemoattractant gene expression changes in white adipose tissue of morbidly obese subjects after surgery-induced weight loss. Diabetes 2005;54:2277-2286
133. Wing RR, Hill JO: Successful weight loss maintenance. Annu Rev Nutr 2001;21:323-341
134. Waring ME, Eaton CB, Lasater TM, Lapane KL: Incident diabetes in relation to weight patterns during middle age. Am J Epidemiol 2010;171:550-556
135. Hamm P, Shekelle RB, Stamler J: Large fluctuations in body weight during young adulthood and twenty-five-year risk of coronary death in men. Am J Epidemiol 1989;129:312-318
136. Olson MB, Kelsey SF, Bittner V, Reis SE, Reichek N, Handberg EM, Merz CN: Weight cycling and high-density lipoprotein cholesterol in women: evidence of an adverse effect: a report from the NHLBI-sponsored WISE study. Women's Ischemia Syndrome Evaluation Study Group. J Am Coll Cardiol 2000;36:1565-1571

137. Blair SN, Shaten J, Brownell K, Collins G, Lissner L: Body weight change, all-cause mortality, and cause-specific mortality in the Multiple Risk Factor Intervention Trial. Ann Intern Med 1993;119:749-757
138. Folsom AR, French SA, Zheng W, Baxter JE, Jeffery RW: Weight variability and mortality: the Iowa Women's Health Study. Int J Obes Relat Metab Disord 1996;20:704-709
139. Ron D, Walter P: Signal integration in the endoplasmic reticulum unfolded protein response. Nat Rev Mol Cell Biol 2007;8:519-529
140. Rutkowski DT, Arnold SM, Miller CN, Wu J, Li J, Gunnison KM, Mori K, Sadighi Akha AA, Raden D, Kaufman RJ: Adaptation to ER stress is mediated by differential stabilities of pro-survival and pro-apoptotic mRNAs and proteins. PLoS Biol 2006;4:e374
141. Zinszner H, Kuroda M, Wang X, Batchvarova N, Lightfoot RT, Remotti H, Stevens JL, Ron D: CHOP is implicated in programmed cell death in response to impaired function of the endoplasmic reticulum. Genes Dev 1998;12:982-995
142. Brown MK, Naidoo N: The endoplasmic reticulum stress response in aging and age-related diseases. Front Physiol 2012;3:263
143. Kerr JF, Wyllie AH, Currie AR: Apoptosis: a basic biological phenomenon with wide-ranging implications in tissue kinetics. Br J Cancer 1972;26:239-257
144. Curtin JF, Cotter TG: Apoptosis: Historical perspectives. Essays Biochem 2003;39:1-10
145. Lamkanfi M, Dixit VM: Manipulation of host cell death pathways during microbial infections. Cell Host Microbe 2010;8:44-54
146. Pfaffl MW: A new mathematical model for relative quantification in real-time RT-PCR. Nucleic Acids Res 2001;29:e45
147. Grubbs F: Procedures for detecting outlying observations in samples. Technometrics 1969;11:1-21
148. Lumeng CN, Bodzin JL, Saltiel AR: Obesity induces a phenotypic switch in adipose tissue macrophage polarization. The Journal of clinical investigation 2007;117:175-184
149. Kiki I, Altunkaynak BZ, Altunkaynak ME, Vuraler O, Unal D, Kaplan S: Effect of high fat diet on the volume of liver and quantitative feature of Kupffer cells in the female rat: a stereological and ultrastructural study. Obes Surg 2007;17:1381-1388
150. Ball RY, Stowers EC, Burton JH, Cary NR, Skepper JN, Mitchinson MJ: Evidence that the death of macrophage foam cells contributes to the lipid core of atheroma. Atherosclerosis 1995;114:45-54
151. Smith JD, Trogan E, Ginsberg M, Grigaux C, Tian J, Miyata M: Decreased atherosclerosis in mice deficient in both macrophage colony-stimulating factor (op) and apolipoprotein E. Proc Natl Acad Sci U S A 1995;92:8264-8268
152. Shi H, Kokoeva MV, Inouye K, Tzameli I, Yin H, Flier JS: TLR4 links innate immunity and fatty acid-induced insulin resistance. J Clin Invest 2006;116:3015-3025
153. Seimon TA, Nadolski MJ, Liao X, Magallon J, Nguyen M, Feric NT, Koschinsky ML, Harkewicz R, Witztum JL, Tsimikas S, Golenbock D, Moore KJ, Tabas I: Atherogenic lipids and lipoproteins trigger CD36-TLR2-dependent

apoptosis in macrophages undergoing endoplasmic reticulum stress. Cell metabolism 2010;12:467-482
154. Wong BX, Kyle RA, Myhill PC, Croft KD, Quinn CM, Jessup W, Yeap BB: Dyslipidemic diabetic serum increases lipid accumulation and expression of stearoyl-CoA desaturase in human macrophages. Lipids 2011;46:931-941
155. Wong BX, Kyle RA, Croft KD, Quinn CM, Jessup W, Yeap BB: Modulation of macrophage fatty acid content and composition by exposure to dyslipidemic serum in vitro. Lipids 2011;46:371-380
156. Mas S, Martinez-Pinna R, Martin-Ventura JL, Perez R, Gomez-Garre D, Ortiz A, Fernandez-Cruz A, Vivanco F, Egido J: Local non-esterified fatty acids correlate with inflammation in atheroma plaques of patients with type 2 diabetes. Diabetes 2010;59:1292-1301
157. Feng B, Yao PM, Li Y, Devlin CM, Zhang D, Harding HP, Sweeney M, Rong JX, Kuriakose G, Fisher EA, Marks AR, Ron D, Tabas I: The endoplasmic reticulum is the site of cholesterol-induced cytotoxicity in macrophages. Nat Cell Biol 2003;5:781-792
158. Karaskov E, Scott C, Zhang L, Teodoro T, Ravazzola M, Volchuk A: Chronic palmitate but not oleate exposure induces endoplasmic reticulum stress, which may contribute to INS-1 pancreatic beta-cell apoptosis. Endocrinology 2006;147:3398-3407
159. Pfaffenbach KT, Gentile CL, Nivala AM, Wang D, Wei Y, Pagliassotti MJ: Linking endoplasmic reticulum stress to cell death in hepatocytes: roles of C/EBP homologous protein and chemical chaperones in palmitate-mediated cell death. Am J Physiol Endocrinol Metab 2010;298:E1027-1035
160. Alhusaini S, McGee K, Schisano B, Harte A, McTernan P, Kumar S, Tripathi G: Lipopolysaccharide, high glucose and saturated fatty acids induce endoplasmic reticulum stress in cultured primary human adipocytes: Salicylate alleviates this stress. Biochemical and biophysical research communications 2010;397:472-478
161. Urano F, Wang X, Bertolotti A, Zhang Y, Chung P, Harding HP, Ron D: Coupling of stress in the ER to activation of JNK protein kinases by transmembrane protein kinase IRE1. Science 2000;287:664-666
162. Hu P, Han Z, Couvillon AD, Kaufman RJ, Exton JH: Autocrine tumor necrosis factor alpha links endoplasmic reticulum stress to the membrane death receptor pathway through IRE1alpha-mediated NF-kappaB activation and down-regulation of TRAF2 expression. Mol Cell Biol 2006;26:3071-3084
163. Zinszner H, Kuroda M, Wang X, Batchvarova N, Lightfoot RT, Remotti H, Stevens JL, Ron D: CHOP is implicated in programmed cell death in response to impaired function of the endoplasmic reticulum. Genes Dev 1998;12:982-995
164. Ozcan U, Cao Q, Yilmaz E, Lee AH, Iwakoshi NN, Ozdelen E, Tuncman G, Gorgun C, Glimcher LH, Hotamisligil GS: Endoplasmic reticulum stress links obesity, insulin action, and type 2 diabetes. Science 2004;306:457-461
165. Sharma NK, Das SK, Mondal AK, Hackney OG, Chu WS, Kern PA, Rasouli N, Spencer HJ, Yao-Borengasser A, Elbein SC: Endoplasmic reticulum stress markers are associated with obesity in nondiabetic subjects. The Journal of clinical endocrinology and metabolism 2008;93:4532-4541

166. Myoishi M, Hao H, Minamino T, Watanabe K, Nishihira K, Hatakeyama K, Asada Y, Okada K, Ishibashi-Ueda H, Gabbiani G, Bochaton-Piallat ML, Mochizuki N, Kitakaze M: Increased endoplasmic reticulum stress in atherosclerotic plaques associated with acute coronary syndrome. Circulation 2007;116:1226-1233
167. Ozcan U, Yilmaz E, Ozcan L, Furuhashi M, Vaillancourt E, Smith RO, Gorgun CZ, Hotamisligil GS: Chemical chaperones reduce ER stress and restore glucose homeostasis in a mouse model of type 2 diabetes. Science 2006;313:1137-1140
168. Erbay E, Babaev VR, Mayers JR, Makowski L, Charles KN, Snitow ME, Fazio S, Wiest MM, Watkins SM, Linton MF, Hotamisligil GS: Reducing endoplasmic reticulum stress through a macrophage lipid chaperone alleviates atherosclerosis. Nature medicine 2009;15:1383-1391
169. Saraswathi V, Hasty AH: Inhibition of long-chain acyl coenzyme A synthetases during fatty acid loading induces lipotoxicity in macrophages. Arterioscler Thromb Vasc Biol 2009;29:1937-1943
170. Kopp E, Ghosh S: Inhibition of NF-kappa B by sodium salicylate and aspirin. Science 1994;265:956-959
171. Yuan M, Konstantopoulos N, Lee J, Hansen L, Li ZW, Karin M, Shoelson SE: Reversal of obesity- and diet-induced insulin resistance with salicylates or targeted disruption of Ikkbeta. Science 2001;293:1673-1677
172. Koliwad SK, Streeper RS, Monetti M, Cornelissen I, Chan L, Terayama K, Naylor S, Rao M, Hubbard B, Farese RV, Jr.: DGAT1-dependent triacylglycerol storage by macrophages protects mice from diet-induced insulin resistance and inflammation. The Journal of clinical investigation 2010;120:756-767
173. Phillips CM, Goumidi L, Bertrais S, Field MR, Cupples LA, Ordovas JM, Defoort C, Lovegrove JA, Drevon CA, Gibney MJ, Blaak EE, Kiec-Wilk B, Karlstrom B, Lopez-Miranda J, McManus R, Hercberg S, Lairon D, Planells R, Roche HM: Gene-nutrient interactions with dietary fat modulate the association between genetic variation of the ACSL1 gene and metabolic syndrome. Journal of lipid research 2010;51:1793-1800
174. Lindner I, Rubin D, Helwig U, Nitz I, Hampe J, Schreiber S, Schrezenmeir J, Doring F: The L513S polymorphism in medium-chain acyl-CoA synthetase 2 (MACS2) is associated with risk factors of the metabolic syndrome in a Caucasian study population. Mol Nutr Food Res 2006;50:270-274
175. Martin G, Schoonjans K, Lefebvre AM, Staels B, Auwerx J: Coordinate regulation of the expression of the fatty acid transport protein and acyl-CoA synthetase genes by PPARalpha and PPARgamma activators. The Journal of biological chemistry 1997;272:28210-28217
176. Clemenz M, Frost N, Schupp M, Caron S, Foryst-Ludwig A, Bohm C, Hartge M, Gust R, Staels B, Unger T, Kintscher U: Liver-specific peroxisome proliferator-activated receptor alpha target gene regulation by the angiotensin type 1 receptor blocker telmisartan. Diabetes 2008;57:1405-1413
177. Fu S, Yang L, Li P, Hofmann O, Dicker L, Hide W, Lin X, Watkins SM, Ivanov AR, Hotamisligil GS: Aberrant lipid metabolism disrupts calcium

homeostasis causing liver endoplasmic reticulum stress in obesity. Nature 2011;473:528-531
178. Holzer RG, Park EJ, Li N, Tran H, Chen M, Choi C, Solinas G, Karin M: Saturated fatty acids induce c-Src clustering within membrane subdomains, leading to JNK activation. Cell 2011;147:173-184
179. Al-Khalili O, Duke BJ, Zeltwanger S, Eaton DC, Spier B, Stockand JD: Cloning of the proto-oncogene c-src from rat testis. DNA Seq 2001;12:425-429
180. Weisberg SP, McCann D, Desai M, Rosenbaum M, Leibel RL, Ferrante AW, Jr.: Obesity is associated with macrophage accumulation in adipose tissue. J Clin Invest 2003;112:1796-1808
181. Xu H, Barnes GT, Yang Q, Tan G, Yang D, Chou CJ, Sole J, Nichols A, Ross JS, Tartaglia LA, Chen H: Chronic inflammation in fat plays a crucial role in the development of obesity-related insulin resistance. J Clin Invest 2003;112:1821-1830
182. Woo CW, Cui D, Arellano J, Dorweiler B, Harding H, Fitzgerald KA, Ron D, Tabas I: Adaptive suppression of the ATF4-CHOP branch of the unfolded protein response by toll-like receptor signalling. Nat Cell Biol 2009;11:1473-1480
183. Woo CW, Kutzler L, Kimball SR, Tabas I: Toll-like receptor activation suppresses ER stress factor CHOP and translation inhibition through activation of eIF2B. Nat Cell Biol 2012;
184. Coenen KR, Gruen ML, Chait A, Hasty AH: Diet-induced increases in adiposity, but not plasma lipids, promote macrophage infiltration into white adipose tissue. Diabetes 2007;56:564-573
185. Zeyda M, Huber J, Prager G, Stulnig TM: Inflammation correlates with markers of T-cell subsets including regulatory T cells in adipose tissue from obese patients. Obesity 2011;19:743-748
186. Kirk EA, Sagawa ZK, McDonald TO, O'Brien KD, Heinecke JW: Monocyte chemoattractant protein deficiency fails to restrain macrophage infiltration into adipose tissue [corrected]. Diabetes 2008;57:1254-1261
187. Kanda H, Tateya S, Tamori Y, Kotani K, Hiasa K, Kitazawa R, Kitazawa S, Miyachi H, Maeda S, Egashira K, Kasuga M: MCP-1 contributes to macrophage infiltration into adipose tissue, insulin resistance, and hepatic steatosis in obesity. The Journal of clinical investigation 2006;116:1494-1505
188. Nara N, Nakayama Y, Okamoto S, Tamura H, Kiyono M, Muraoka M, Tanaka K, Taya C, Shitara H, Ishii R, Yonekawa H, Minokoshi Y, Hara T: Disruption of CXC motif chemokine ligand-14 in mice ameliorates obesity-induced insulin resistance. J Biol Chem 2007;282:30794-30803
189. Weisberg SP, Hunter D, Huber R, Lemieux J, Slaymaker S, Vaddi K, Charo I, Leibel RL, Ferrante AW, Jr.: CCR2 modulates inflammatory and metabolic effects of high-fat feeding. The Journal of clinical investigation 2006;116:115-124
190. Tamura Y, Sugimoto M, Murayama T, Ueda Y, Kanamori H, Ono K, Ariyasu H, Akamizu T, Kita T, Yokode M, Arai H: Inhibition of CCR2 ameliorates insulin resistance and hepatic steatosis in db/db mice. Arteriosclerosis, thrombosis, and vascular biology 2008;28:2195-2201
191. Ito A, Suganami T, Yamauchi A, Degawa-Yamauchi M, Tanaka M, Kouyama R, Kobayashi Y, Nitta N, Yasuda K, Hirata Y, Kuziel WA, Takeya M,

Kanegasaki S, Kamei Y, Ogawa Y: Role of CC chemokine receptor 2 in bone marrow cells in the recruitment of macrophages into obese adipose tissue. J Biol Chem 2008;283:35715-35723
192. Elmore S: Apoptosis: a review of programmed cell death. Toxicol Pathol 2007;35:495-516
193. Bodles AM, Varma V, Yao-Borengasser A, Phanavanh B, Peterson CA, McGehee RE, Jr., Rasouli N, Wabitsch M, Kern PA: Pioglitazone induces apoptosis of macrophages in human adipose tissue. J Lipid Res 2006;47:2080-2088
194. Di Gregorio GB, Yao-Borengasser A, Rasouli N, Varma V, Lu T, Miles LM, Ranganathan G, Peterson CA, McGehee RE, Kern PA: Expression of CD68 and macrophage chemoattractant protein-1 genes in human adipose and muscle tissues: association with cytokine expression, insulin resistance, and reduction by pioglitazone. Diabetes 2005;54:2305-2313
195. Feng B, Jiao P, Nie Y, Kim T, Jun D, van Rooijen N, Yang Z, Xu H: Clodronate liposomes improve metabolic profile and reduce visceral adipose macrophage content in diet-induced obese mice. PLoS One 2011;6:e24358
196. Altintas MM, Rossetti MA, Nayer B, Puig A, Zagallo P, Ortega LM, Johnson KB, McNamara G, Reiser J, Mendez AJ, Nayer A: Apoptosis, mastocytosis, and diminished adipocytokine gene expression accompany reduced epididymal fat mass in long-standing diet-induced obese mice. Lipids Health Dis 2011;10:198
197. Wang CY, Mayo MW, Korneluk RG, Goeddel DV, Baldwin AS, Jr.: NF-kappaB antiapoptosis: induction of TRAF1 and TRAF2 and c-IAP1 and c-IAP2 to suppress caspase-8 activation. Science 1998;281:1680-1683
198. Chiang SH, Bazuine M, Lumeng CN, Geletka LM, Mowers J, White NM, Ma JT, Zhou J, Qi N, Westcott D, Delproposto JB, Blackwell TS, Yull FE, Saltiel AR: The protein kinase IKKepsilon regulates energy balance in obese mice. Cell 2009;138:961-975
199. Hawiger J: Innate immunity and inflammation: a transcriptional paradigm. Immunol Res 2001;23:99-109
200. TINSAL-T2D: Salsalate lowered glucose in patients with type 2 diabetes. Endocrine Today 2012;
201. Boden G, Duan X, Homko C, Molina EJ, Song W, Perez O, Cheung P, Merali S: Increase in endoplasmic reticulum stress-related proteins and genes in adipose tissue of obese, insulin-resistant individuals. Diabetes 2008;57:2438-2444
202. Sharma NK, Das SK, Mondal AK, Hackney OG, Chu WS, Kern PA, Rasouli N, Spencer HJ, Yao-Borengasser A, Elbein SC: Endoplasmic reticulum stress markers are associated with obesity in nondiabetic subjects. J Clin Endocrinol Metab 2008;93:4532-4541
203. Ron D, Walter P: Signal integration in the endoplasmic reticulum unfolded protein response. Nature reviews Molecular cell biology 2007;8:519-529
204. Oh J, Riek AE, Weng S, Petty M, Kim D, Colonna M, Cella M, Bernal-Mizrachi C: Endoplasmic reticulum stress controls M2 macrophage differentiation and foam cell formation. The Journal of biological chemistry 2012;287:11629-11641

205. Feuerer M, Herrero L, Cipolletta D, Naaz A, Wong J, Nayer A, Lee J, Goldfine AB, Benoist C, Shoelson S, Mathis D: Lean, but not obese, fat is enriched for a unique population of regulatory T cells that affect metabolic parameters. Nat Med 2009;15:930-939
206. Winer S, Chan Y, Paltser G, Truong D, Tsui H, Bahrami J, Dorfman R, Wang Y, Zielenski J, Mastronardi F, Maezawa Y, Drucker DJ, Engleman E, Winer D, Dosch HM: Normalization of obesity-associated insulin resistance through immunotherapy. Nat Med 2009;15:921-929
207. Ohmura K, Ishimori N, Ohmura Y, Tokuhara S, Nozawa A, Horii S, Andoh Y, Fujii S, Iwabuchi K, Onoe K, Tsutsui H: Natural killer T cells are involved in adipose tissues inflammation and glucose intolerance in diet-induced obese mice. Arteriosclerosis, thrombosis, and vascular biology 2010;30:193-199
208. Rausch ME, Weisberg S, Vardhana P, Tortoriello DV: Obesity in C57BL/6J mice is characterized by adipose tissue hypoxia and cytotoxic T-cell infiltration. Int J Obes (Lond) 2008;32:451-463
209. Stevens VL, Jacobs EJ, Sun J, Patel AV, McCullough ML, Teras LR, Gapstur SM: Weight cycling and mortality in a large prospective US study. Am J Epidemiol 2012;175:785-792
210. Schotte DE, Cohen E, Singh SP: Effects of weight cycling on metabolic control in male outpatients with non-insulin-dependent diabetes mellitus. Health Psychol 1990;9:599-605
211. Jeffery RW, Wing RR, French SA: Weight cycling and cardiovascular risk factors in obese men and women. Am J Clin Nutr 1992;55:641-644
212. Li Z, Hong K, Wong E, Maxwell M, Heber D: Weight cycling in a very low-calorie diet programme has no effect on weight loss velocity, blood pressure and serum lipid profile. Diabetes Obes Metab 2007;9:379-385
213. Eden E, Edstrom S, Bennegard K, Schersten T, Lundholm K: Glucose flux in relation to energy expenditure in malnourished patients with and without cancer during periods of fasting and feeding. Cancer Res 1984;44:1718-1724
214. Deopurkar R, Ghanim H, Friedman J, Abuaysheh S, Sia CL, Mohanty P, Viswanathan P, Chaudhuri A, Dandona P: Differential effects of cream, glucose, and orange juice on inflammation, endotoxin, and the expression of Toll-like receptor-4 and suppressor of cytokine signaling-3. Diabetes Care 2010;33:991-997
215. Fujisaka S, Usui I, Bukhari A, Ikutani M, Oya T, Kanatani Y, Tsuneyama K, Nagai Y, Takatsu K, Urakaze M, Kobayashi M, Tobe K: Regulatory mechanisms for adipose tissue M1 and M2 macrophages in diet-induced obese mice. Diabetes 2009;58:2574-2582
216. Schoenborn JR, Wilson CB: Regulation of interferon-gamma during innate and adaptive immune responses. Adv Immunol 2007;96:41-101
217. Gately MK, Renzetti LM, Magram J, Stern AS, Adorini L, Gubler U, Presky DH: The interleukin-12/interleukin-12-receptor system: role in normal and pathologic immune responses. Annu Rev Immunol 1998;16:495-521
218. Kim HP, Imbert J, Leonard WJ: Both integrated and differential regulation of components of the IL-2/IL-2 receptor system. Cytokine Growth Factor Rev 2006;17:349-366

219. Woodland DL, Kohlmeier JE: Migration, maintenance and recall of memory T cells in peripheral tissues. Nat Rev Immunol 2009;9:153-161
220. Stein LJ: Repeated weight fluctuation increases plasma insulin in the obese Wistar fatty diabetic rat. Physiol Behav 1992;52:345-350
221. Lu H, Buison A, Uhley V, Jen KL: Long-term weight cycling in female Wistar rats: effects on metabolism. Obes Res 1995;3:521-530
222. Rocha VZ, Folco EJ, Sukhova G, Shimizu K, Gotsman I, Vernon AH, Libby P: Interferon-gamma, a Th1 cytokine, regulates fat inflammation: a role for adaptive immunity in obesity. Circ Res 2008;103:467-476
223. McGillicuddy FC, Chiquoine EH, Hinkle CC, Kim RJ, Shah R, Roche HM, Smyth EM, Reilly MP: Interferon gamma attenuates insulin signaling, lipid storage, and differentiation in human adipocytes via activation of the JAK/STAT pathway. The Journal of biological chemistry 2009;284:31936-31944
224. Ojdana D, Safiejko K, Lipska A, Radziwon P, Dadan J, Tryniszewska E: Effector and memory CD4+ and CD8+ T cells in the chronic infection process. Folia Histochem Cytobiol 2008;46:413-417
225. Moore KJ, Tabas I: Macrophages in the pathogenesis of atherosclerosis. Cell 2011;145:341-355
226. Leibel RL, Hirsch J, Berry EM, Gruen RK: Alterations in adipocyte free fatty acid re-esterification associated with obesity and weight reduction in man. Am J Clin Nutr 1985;42:198-206
227. Roth Flach RJ, Matevossian A, Akie TE, Negrin KA, Paul MT, Czech MP: beta3-Adrenergic Receptor Stimulation Induces E-Selectin-mediated Adipose Tissue Inflammation. The Journal of biological chemistry 2013;288:2882-2892
228. Kito H, Yamazaki D, Ohya S, Yamamura H, Asai K, Imaizumi Y: Up-regulation of K(ir)2.1 by ER stress facilitates cell death of brain capillary endothelial cells. Biochemical and biophysical research communications 2011;411:293-298
229. Albu J, Reed G: Weight cycling: more questions than answers. Endocr Pract 1995;1:346-352
230. Beeson V, Ray C, Coxon A, Kreitzman S: The myth of the yo-yo: consistent rate of weight loss with successive dieting by VLCD. Int J Obes 1989;13 Suppl 2:135-139
231. Brownell KD, Greenwood MR, Stellar E, Shrager EE: The effects of repeated cycles of weight loss and regain in rats. Physiology & behavior 1986;38:459-464
232. Gray DS, Fisler JS, Bray GA: Effects of repeated weight loss and regain on body composition in obese rats. Am J Clin Nutr 1988;47:393-399
233. Jebb SA, Goldberg GR, Coward WA, Murgatroyd PR, Prentice AM: Effects of weight cycling caused by intermittent dieting on metabolic rate and body composition in obese women. Int J Obes 1991;15:367-374
234. Leibel RL, Hirsch J: Diminished energy requirements in reduced-obese patients. Metabolism 1984;33:164-170
235. Simpson JA, Wainwright PE, Hoffman-Goetz L, Levesque S: Effects of different weight loss treatments on weight cycling and metabolic measures in male mice. Physiology & behavior 1994;56:197-201

236. Seok J, Warren HS, Cuenca AG, Mindrinos MN, Baker HV, Xu W, Richards DR, McDonald-Smith GP, Gao H, Hennessy L, Finnerty CC, Lopez CM, Honari S, Moore EE, Minei JP, Cuschieri J, Bankey PE, Johnson JL, Sperry J, Nathens AB, Billiar TR, West MA, Jeschke MG, Klein MB, Gamelli RL, Gibran NS, Brownstein BH, Miller-Graziano C, Calvano SE, Mason PH, Cobb JP, Rahme LG, Lowry SF, Maier RV, Moldawer LL, Herndon DN, Davis RW, Xiao W, Tompkins RG: Genomic responses in mouse models poorly mimic human inflammatory diseases. Proc Natl Acad Sci U S A 2013;110:3507-3512
237. Parks BW, Nam E, Org E, Kostem E, Norheim F, Hui ST, Pan C, Civelek M, Rau CD, Bennett BJ, Mehrabian M, Ursell LK, He A, Castellani LW, Zinker B, Kirby M, Drake TA, Drevon CA, Knight R, Gargalovic P, Kirchgessner T, Eskin E, Lusis AJ: Genetic control of obesity and gut microbiota composition in response to high-fat, high-sucrose diet in mice. Cell metabolism 2013;17:141-152
238. Ye J, McGuinness OP: Inflammation during obesity is not all bad: evidence from animal and human studies. Am J Physiol Endocrinol Metab 2013;304:E466-477